

Aus der Abteilung Neuroradiologie am Institut für Klinische Radiologie der
Ludwig-Maximilians-Universität München

Direktor: Prof. Dr. Hartmut Brückmann

**Diffusion- and perfusion-weighted magnetic resonance imaging in patients with acute
ischemic stroke: can diffusion/perfusion mismatch predict outcome?**

Dissertation zum Erwerb des Doktorgrades der Medizin an der Medizinischen Fakultät der
Ludwig-Maximilians-Universität zu München

Vorgelegt von
Jun Ma
aus
Dalian, VR China
2004

Mit Genehmigung der medizinischen Fakultät der Universität München

Berichterstatter: PD Dr. Roland Brüning

Mitberichterstatter: Prof. Dr. K. J. Pfeifer

Dekan: Prof. Dr. med. Dr. hc. K. Peter

Tag der mündlichen Prüfung: 25.11.2004

Table of Contents

1 INTRODUCTION.....	4
1.1 Definition and epidemiology of stroke.....	4
1.2 Basic consideration of ischemic stroke.....	6
1.2.1 Arteries of the brain.....	6
1.2.2 Pathogenesis of ischemic stroke.....	8
1.2.3 Pathophysiology of ischemic stroke at macro tissue level.....	9
1.3 Magnetic resonance imaging (MRI) in stroke.....	12
1.4 Acute stroke management.....	15
1.5 Rational and purpose of the current study.....	16
2 MATERIALS AND METHODS.....	19
2.1 Patients.....	19
2.2 Neurological assessment.....	22
2.3 Technical consideration.....	23
2.3.1 Diffusion weighted imaging (DWI).....	23
2.3.2 Perfusion weighted imaging (PWI).....	27
2.4 MRI protocol.....	32
2.5 Data processing.....	34
2.6 Statistics.....	37
3 RESULTS.....	38
3.1 General.....	38
3.2 MRI hemodynamic parameters evaluation.....	40
3.3 Hemodynamic parameters in relation with assessment of stroke severity (NIHSS) and outcome (MRS).....	45
3.3.1 Hemodynamic parameters in relation to NIHSS.....	45
3.3.2 Hemodynamic parameters in relation to MRS.....	49
3.3.3 NIHSS and MRS in relation to other factors.....	54
4 DISCUSSION.....	57
4.1 Finding and impact of the present study.....	57
4.2 Penumbra and Mismatch.....	61
4.3 Other methods of neuroimaging to assess acute stroke.....	64
5 SUMMARY.....	68
6 ABBREVIATIONS.....	72
7 APPENDIX.....	74
8 REFERENCES.....	78
9 CURRICULUM VITAE.....	88
10 ACKNOWLEDGEMENTS.....	89

1 INTRODUCTION

1.1 Definition and epidemiology of stroke

The World Health Organization (WHO) standard definition of stroke is “a focal (or global) neurological impairment of sudden onset, and lasting more than 24 hours (unless interrupted by surgery or death), and with no apparent nonvascular cause”¹. Transient cerebral ischemia or stroke events in cases of blood disease or brain tumors and secondary strokes caused by trauma were not included by this definition².

Stroke was estimated to result in 5.5 million deaths each year worldwide, approximately 10% of all deaths. In addition to its being the third leading cause of death, stroke is the major cause of disabilities among adult^{3, 4}. Report on the US region indicated that the economic cost of stroke reached to billions of dollars in US each year⁵. Projections to the year 2020 indicate that the number of people suffering from stroke will substantially increase each year⁶. Stroke incidence also increases as life expectancy is increasing in most parts of the world. By 2025 there will be more than 800 million people over 65 years of age in the world⁷. The majority of the stroke burden will be in developing countries, largely due to the adoption of "western" lifestyles and their accompanying risk factors - smoking, high-fat diet, and lack of exercises^{7,8}.

Stroke death rates have shown a steady decline since early 1990s⁹⁻¹¹. The reason for the accelerated decline of stroke mortality is uncertain, but it may have resulted from improved antihypertensive therapy, management of risk factors, decrease in stroke incidence or case fatality, or some other factors¹². It was proposed that a possible explanation of decline of death rate that the increased use of neuroimaging over time detected more mild strokes that would not have been recognized previously^{13,14}.

Stroke may result from different causes such as cerebral arterial ischemia, intracerebral hemorrhage, subarachnoid hemorrhage or venous sinus thrombosis. If the stroke etiology is ischemia, it may be caused by cardiac emboli, arterial thromboemboli, vasculopathies,

iatrogenic insult and pregnancy, etc. Clinically, more than 80% of all stroke result from arterial occlusion^{15, 16}.

The knowledge of the cerebral vascular anatomy and pathogenesis of ischemic stroke is the basis for understanding and studying ischemic stroke; therefore it will be briefly reviewed in the following sections.

1.2 Basic consideration of ischemic stroke

1.2.1 Arteries of the brain

The brain is supplied by a dense network of blood vessels, which transport adequate oxygen and nutrients for brain's normal function. The internal carotid arteries (ICAs) usually split into the anterior cerebral artery (ACA) and the middle cerebral artery (MCA), and supply blood to the anterior three-fifths of cerebrum, except for parts of the temporal and occipital lobes. The vertebrobasilar arteries supply the posterior two-fifths of the cerebrum, part of the cerebellum, and the brain stem.

ACA and its branches supply most of the medial surface of the cerebral cortex (anterior three fourths), frontal pole (via cortical branches), and anterior portions of the corpus callosum. Its perforating branches (including the recurrent artery of Heubner and Medial Lenticulostriate Arteries) supply the anterior limb of the internal capsule, the inferior portions of head of the caudate and anterior globus pallidus (figure 1).

1. A. Carotis interna
2. Äste der A. Cerebri media
3. A. Cerebri anterior
4. A. frontobasalis medialis
5. A. callosomarginalis (A. cingulomarginalis)
6. A. frontopolaris
7. A. frontalis anteromedialis (A. frontalis interna anterior)
8. A. frontalis mediomedialis (A. frontalis interna media)
9. A. pericallosa
10. A. frontalis posteromedialis (A. frontalis interna posterior)
11. A. paracentralis
12. A. precunealis superior (A. parietalis interna superior)
13. A. precunealis inferior (A. parietalis interna inferior)



Fig. 1. ACA of the brain. Adapted from Hans-Joachim Kretschmann and Wolfgang Weinrich ¹⁷

The MCA supplies most of the temporal lobe, anterolateral frontal lobe, and parietal lobe. Its perforating branches supply the posterior limb of the internal capsule, part of the head and

body of the caudate and globus pallidus. (figure 2).

1. A. carotis interna
2. A. cerebri media, orthograd verlaufend
3. Abgang der A. cerebri anterior
4. A. frontobasalis lateralis
5. Aa. Insulares
6. Aa. Prefrontales
7. A. sulci precentralis (A. praerolandica)
8. A. sulci centralis (A. rolandica)
9. A. parietalis anterior
10. A. parietalis posterior
11. A. gyri angularis
12. A. temporooccipitalis (A. occipitotemporalis)
13. A. temporalis posterior
14. A. temporalis intermedia (A. temporalis media)
15. A. temporalis anterior
16. A. temporopolaris

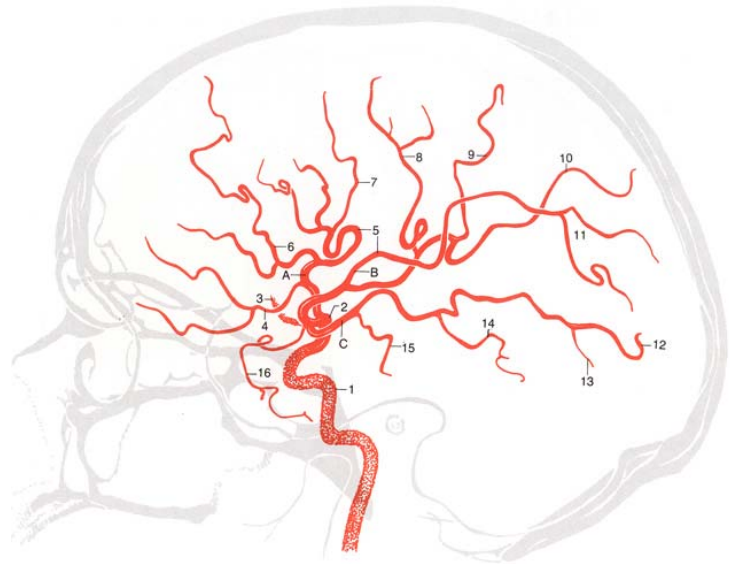


Fig. 2. MCA of the brain. Adapted from Hans-Joachim Kretschmann and Wolfgang Weinrich¹⁷

The two vertebral arteries continue in the basilar artery that splits into arteries supplying the posterior fossa and the two posterior cerebral arteries (PCAs). The PCA supplies parts of the midbrain, the subthalamic nucleus, the basal nucleus, the thalamus, the mesial inferior temporal lobe, and the occipital and occipitoparietal cortices. In addition, the PCAs, via the posterior communicating arteries, may become important sources of collateral circulation for the MCA territory. (figure 3).

1. A. vertebralis
2. Abgang der A. cerebelli inferior posterior
3. A. basilaris
4. Abgang der A. cerebelli inferior anterior
5. Abgang der A. cerebelli superior
6. A. cerebri posterior
7. Aa. centrales posteromedialis und posterolateralis (Aa. thalamoperforantes anteriores und posteriors)
8. Aa. choroideae posteriors medialis und lateralis
9. A. occipitalis medialis (A. occipitalis interna)
10. A. parietooccipitalis
11. A. calcarina
12. A. occipitalis lateralis (A. temporooccipitalis, A. occipitotemporalis)
13. Aa. temporales
14. A. communicans posterior
15. A. carotis interna

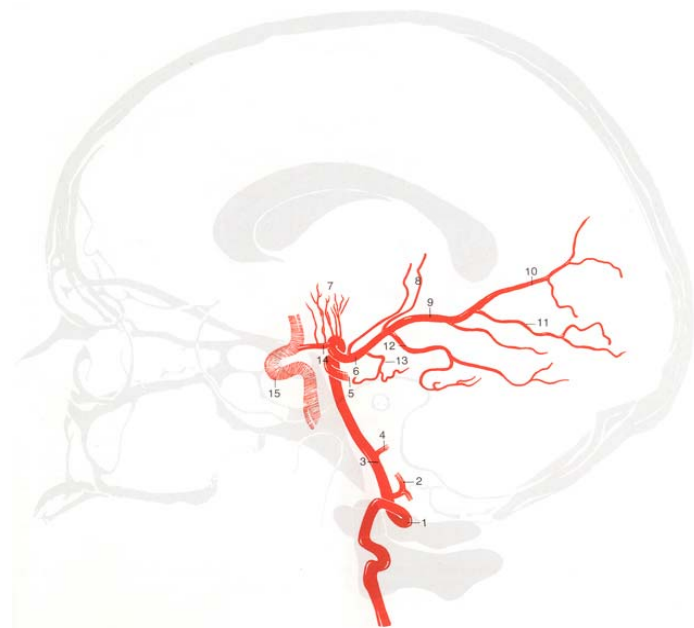


Fig. 3. Posterior circulation. Adapted from Hans-Joachim Kretschmann and Wolfgang Weinrich¹⁷

Anastomoses and collaterals

During an acute ischemic onset, the occlusion of a large vessel (such as MCA) is rarely complete because of not only the incomplete obstruction but also the collateral circulation. Common and important anastomoses can occur between (1) external carotid and internal carotid via branches of the facial-, angular- and especially the ophthalmic arteries; (2) the major intracranial vessels (e.g. PCAs, ICAs and ACAs) via the circle of Willis; (3) muscular branches of cervical arteries and the extracranial vertebral or external carotid arteries; (4) small cortical branches of ACA, MCA, and PCA, (e.g. the posterior choroidal artery or the posterior pericallosal artery) or branches of the major cerebellar arteries.

Many smaller penetrating brain vessels such as the lenticulostriate branches of MCA that supply the basal ganglia and internal capsule, as well as the penetrating branches from vessels on the brain surface that supply deep white matter, are terminal arteries. This means that they form few if any connections (anastomoses) with other arteries. When they are occluded, the brain regions they supply will therefore become ischemic.

The occlusion of the MCA or its branches is the most common type of anterior circulation infarct, accounting for approximately 90% of infarcts and two thirds of all first strokes¹⁸. For this reason and for group homogeneity, this work will concentrate on ischemic stroke on MCA territory only.

1.2.2 Pathogenesis of ischemic stroke

The main mechanisms causing ischemic strokes are: (1) cardiogenic embolism, (2) arteriosclerosis causing arterial embolism. Hypotensive ischemia, venous occlusion, hemorrhagic stroke and other causes such as vasospasm and arteritis stand out among the infrequent causes of stroke, and will not be reviewed here.

(1) Cardiogenic embolism. Cardiogenic embolic stroke can result from mobilization of an embolus in the central circulation from a variety of sources. Besides clot, fibrin, pieces of athermanous plaque, materials known to embolize into the central circulation include fat, air,

tumor or metastasis, bacterial clumps, and foreign bodies. Superficial branches of cerebral arteries are the most frequent targets of emboli, most emboli lodge in the middle cerebral artery distribution. The two most common sources of emboli are the left sided cardiac atrium and large arteries. Many embolic strokes become “hemorrhagic” due to reperfusion.

(2) Arterial thromboembolism. Arteriosclerosis is the most common pathological feature of vascular obstruction resulting in arterial thromboembolism stroke. Arteriosclerotic plaques can undergo pathological changes such as ulceration, thrombosis, calcification, and intra-plaque hemorrhage, which in turn might lead to disruption of endothelium. The endothelium disruption might cause further platelet adherence and inflammatory response. The plaque gradually narrows the diameter of the artery reducing the flow of blood. Typical sites for arterial thromboembolism to migrate from are the arteriosclerotic plaque of the carotid bifurcation and the proximal portion of the internal carotid artery.

The various vascular territories affected in cerebral infarcts usually correlate to the different etiologies¹⁹. MCA territory infarction is most likely to be caused by emboli. The deep penetrating end-arteries of MCA and PCA can be occluded individually leading to lacunar infarcts. These lacunar defects are due to local lipohyalinosis induced by hypertension or arterial thromboembolism caused by arteriosclerosis and are not further discussed here.

1.2.3 Pathophysiology of ischemic stroke at macro tissue level

Perfusion metabolism - coupling and uncoupling²⁰

Under physiological conditions, a coupling exists between the demand for oxygen and glucose by the cells and the regional cerebral perfusion. During cerebral ischemia, the supply of blood and therefore the supply of oxygen and glucose are decreased and energy demands may not be met. The uncoupling process of the regional cerebral perfusion and metabolism has been examined by positron emission tomography (PET) in several animal and human studies²⁰. The threshold principle of regional cerebral perfusion and metabolism in ischemia are reviewed in the following.

Cerebral blood flow (CBF) and ischemic thresholds

An embolus or a thrombus can occlude a cerebral artery and cause ischemia in the affected vascular territory. No matter what the ischemia cause is, they eventually lead to a focal or general reduction of perfusion in the brain and reduce supply of oxygen and glucose.

The normal CBF is approximately 50 to 60 ml/100g/min and varies in different parts of the brain in monkey. When the CBF is reduced around 22 ml/100g/min, hypoperfusion appears; while when the CBF drops to 8 ml/100g/min irreversible damage occurs^{21, 22}. (Figure 4)

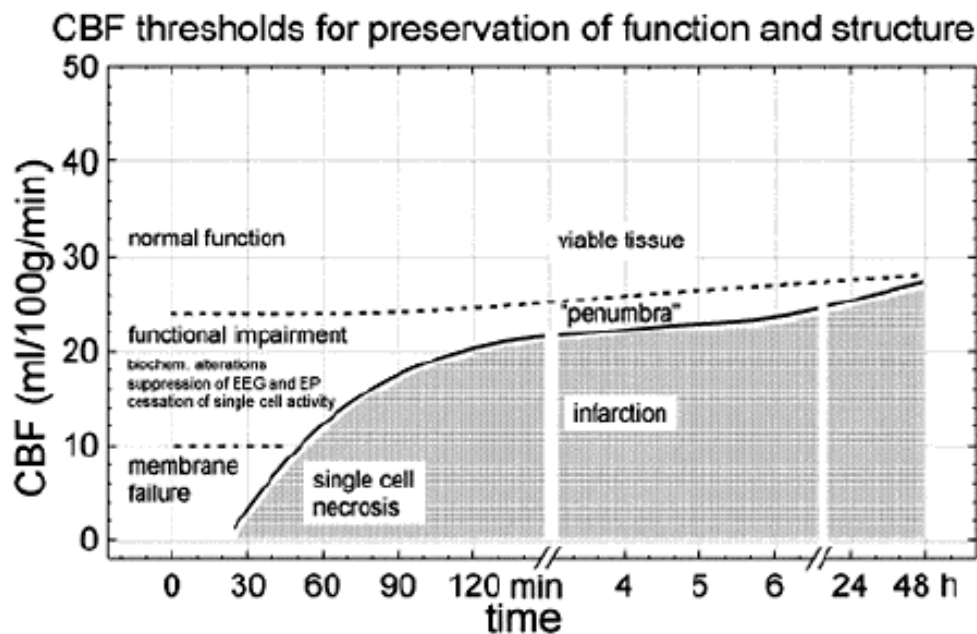


Fig. 4: Diagram of CBF thresholds required for the preservation of function and morphology of brain tissue. The development of single cell necrosis and infarction is dependent on the duration of time for which CBF is impaired below a certain level. The solid line separates structurally damaged from functionally impaired but morphologically intact tissue (the "penumbra"), and the dashed line distinguishes viable from functionally impaired tissue.²³

The viable tissue (i.e. with CBF between 22 and 8 ml/100g/min), in contrary to the core of the ischemia (i.e. with CBF <8 ml/100 g/min), was termed "*ischemic penumbra*" to describe the geographic configuration of an ischemic area²¹. The mild hypoperfusion tissue (i.e. from the normal range down to 22 ml/100 g/min) was well tolerated by the tissue and did not induce neuronal dysfunction was termed *oligemia*. In contrast to the penumbra, the oligemic tissue is not at risk of infarction under uncomplicated conditions²⁴. In the studies of man, different imaging techniques concur very well in suggesting a penumbra threshold around 20 ml/100

g/min, and an infarction threshold around 8 ml/100 g/min for stroke duration in the 3-24 h interval. Between 22 and 8 ml/100g/min, there was a well-defined “perfusion window of opportunity” for tissue salvage²⁴. Figure 5 illustrates the proposed CBF thresholds in man.

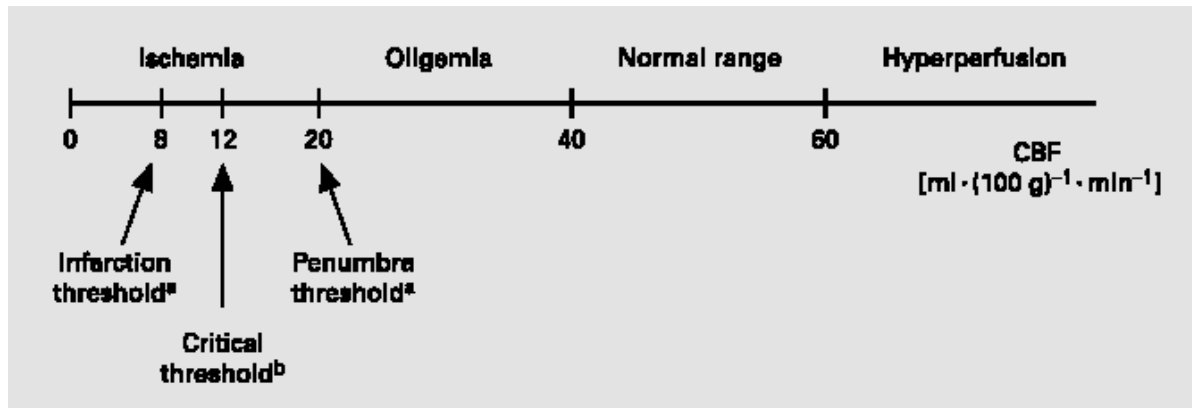


Fig. 5. Schematic drawing of the different CBF thresholds in man, based on the literature. a Marchal et al^{25, 26} and Furlan et al.²⁷; b Heiss et al^{28, 29}.

1.3 Magnetic resonance imaging (MRI) in stroke

MRI provides excellent anatomic detail; has the ability to differentiate between ischemic and infarcted brain tissue; and potentially provides angiographic, spectroscopic, and perfusion weighted information of the cerebral vessels and of the tissue bed. MRI also has higher sensitivity and specificity than computed tomography (CT) in the detection of other brain diseases that can mimic stroke clinically such as cerebral edema, vascular malformations, neoplasms, infections, inflammatory diseases, and toxicometabolic disorders³⁰. MRI has the added advantage of lack of exposure to ionizing radiation but the disadvantage of higher cost.

The value of conventional MRI in stroke examination is limited during the hyperacute stage (<6 hrs). At acute stage (6-24 hrs after ictus) the tissue ischemia is well developed on fast-fluid-attenuated inversion recovery (FLAIR) images and begins to show on T2 weighted imaging (T2WI) (hyperintensity) and T1 weighted imaging (T1WI) (hypointensity). After the first 24 hours, conventional MRI is most useful since the focus now shifts from identifying the presence and extent of infarct and ischemic penumbra to identifying the underlying pathophysiology and to provide follow-up data. Edema is generally maximal at 48 to 72 hours beyond ictus; mass effect is best appreciated on T1WI; gyriform parenchymal enhancement is typically seen approximately 5 to 7 days and might remain for a few weeks during the subacute stage; both petechial hemorrhage and frank hematomas may be seen, especially at 24 to 48 hours after stroke onset; and petechial hemorrhage within infarctions may give rise to a "fogging" phenomenon in which hemoglobin degradation products, extravasated proteins, or both generate signal changes within infarcted tissue, which mask the infarction on T1WI and T2WI.

In hyperacute stroke, the contribution of functional MRI is important. In the past decade, diffusion weighted imaging (DWI) and perfusion weighted imaging (PWI) techniques have revolutionized the role of MRI in the evaluation of patients with acute stroke³¹. DWI provides a measure of cell swelling, as the interstitial space is compromised and then the Brownian motion of water molecules is shifting from the extra- to the intracellular space due to the failure of the Na/K pumps in the absence of O₂. PWI is a measure of hemodynamic compromise, as it

measures the delay of arrival time at the brain and allows to calculate cerebral blood volume (CBV), CBF and other hemodynamic parameters. The combined data from these two modalities can delineate the pathophysiological state of ischemia and may provide a practical means to rapidly identify the ischemic penumbra in the acute stroke setting³². Thus, MR imaging can now fully assess the brain in cases of acute stroke and a full vascular imaging protocol is thus usually possible in less than 30 minutes. (Table 1).

Table 1. MRI findings in acute ischemic changes

Time	MRI finding	Etiology
2-3 min	DWI - Reduced ADC	Decreased motion of protons
2-3 min	PWI - Reduced CBF, CBV, MTT	Decreased CBF
0-2 hr	T2WI - Absent flow void signal	Slow flow or occlusion
0-2 hr	T1WI - Arterial enhancement	Slow flow
2-4 hr	T1WI - Subtle sulcal effacement	Cytotoxic edema
2-4 hr	T1WI - Parenchymal enhancement	Incomplete infarction
8 hr	T2WI - Hyperintense signal	Vasogenic and cytotoxic edema
16-24 hr	T1WI - Hypointense signal	Vasogenic and cytotoxic edema
5-7 days	Parenchymal enhancement	Complete infarction

The specific role of MRI in detecting ischemic stroke is from its three main advantages relative to other techniques: (1) Its ability to image not only cerebral perfusion but also the status of tissue (diffusion), the patency of the vasculature (MR angiography [MRA]), and the anatomical substrate during the same imaging session; (2) The potential for differentiating reversibly and irreversibly ischemic tissue by defining the diffusion/perfusion mismatch; (3) The rapidity of imaging the entire brain during the perfusion study, rather than a limited volume of brain tissue.

There are, however, limitations of the DWI and PWI that need to be emphasized. (1) The absolute values of the parameters are dependent on variety of factors, such as time and spread of the injected bolus during the passage of the lung. It is necessary for PWI reconstruction to utilize the deconvolution method and requires knowledge of arterial input function (AIF), thus

makes the post-processing complex and is dependent on experienced user. Also the determination of AIF is dependent on acquisition and bolus injection, it is difficult to make the accuracy of the quantification of perfusion imaging; (2) The DWI lesion potentially overestimates the volume of the irreversibly ischemic tissue early after the onset of ischemia, and the mean transit time (MTT) map appears to overestimate the size of the reversible tissue. Hence, the diffusion/perfusion mismatch area might only be an index of the ischemic penumbra. (3) Motion artefact is one of the limitations of DWI. DWI is highly sensitive in detecting tissue damage in cerebral ischemia, but it is also highly sensitive to macroscopic motion either by patient motion or by tissue motion due to cerebro-spinal fluid (CSF) pulsation. This problem can be avoided through pulse sequence design and image post-processing techniques. For this reason, echo-planar imaging (EPI) is the most frequently used sequence. It requires a higher gradient strength specification.

1.4 Acute stroke management

According to European Stroke Initiative (EUSI) recommendation for stroke³³, there are 5 main areas in the treatment of acute stroke:

- (1) General therapy. Treatment of general conditions that need to be stabilized.
- (2) Specific therapy directed against particular aspects of stroke pathogenesis, either recanalization of a vessel occlusion or prevention of mechanisms leading to neuronal death in the ischemic brain (neuroprotection).
- (3) Prophylaxis and treatment of complications which may be either neurological (such as secondary hemorrhage, space-occupying edema or seizures) or medical (such as aspiration, infections, decubital ulcers, deep venous thrombosis or pulmonary embolism).
- (4) Early secondary prevention, which is aimed at reducing the incidence of early stroke recurrence.
- (5) Early rehabilitation.

Thrombolytic therapy is among the main specific treatment options³⁴ for stroke. By intravenous *recombinant tissue plasminogen activator (rt-PA)* given within 3 hours after onset, it significantly improves outcome. This thrombolytic therapy is suggested to be given only if the diagnosis is established since serious complications may occur. Intravenous *streptokinase* has been shown to be associated with an unacceptable risk of hemorrhage and associated with death. Aspirin and other therapies such as defibrinogenating enzymes, early anticoagulation, hemodilution and neuroprotection has shown improved outcome or reduced the mortality after stroke.

1.5 Rational and purpose of the current study

When an acute ischemic stroke patient arrives at a hospital, it is important to obtain timely information about the likely outcome and to make a treatment decision. Though it is well accepted that infarct size as detected on neuroimaging studies constitutes a strong predictor of clinical outcome³⁵, and the severity of the clinical deficit on admission is considered to be the major determinant of functional outcome^{36, 37}, however, the recognition of the ischemia in the hyperacute stage using both clinical assessment and routine neuroimaging technique implies some uncertainties, which in turn makes it difficult to clinically predict an outcome of an ischemia that likely to improve or reverse spontaneously from that likely to persist or worsen.

Among neuroimaging techniques, MRI with its excellent anatomic detail and the ability to differentiate between ischemic and infarcted brain tissue; and to provide angiographic, perfusion information of the cerebral vessels and tissue bed, is recognized as the major technique in stroke evaluation. Soon after DWI being introduced to stroke evaluation, research began to focus on the correlation of acute ischemic volume with outcome. There is a strong positive correlation of neurologic deficit with volume of the initial DWI lesion, as well as with the severity of the initial apparent diffusion coefficient (ADC) abnormality³⁸. Combined evaluation of lesion volume at early DWI, the National Institutes of Health Stroke Scale (NIHSS) and time from stroke onset to MRI shows that the volume of ischemic brain tissue on MRI DWI give the best prediction of stroke outcome³⁹. While DWI provides a measure of the ischemic tissue swelling, a PWI provides information about the hemodynamic status of brain tissue and detects regions with impaired cerebral perfusion^{40, 41}.

During the first hours of stroke evolution, regions with abnormal perfusion are typically larger than the DWI lesions^{42, 43}. This is referred to as a diffusion/perfusion mismatch, and is often associated with large vessel (such as proximal MCA) occlusion. It has been postulated that this mismatch region reflects the ischemic penumbra⁴⁴, i.e., the functionally impaired “tissue at risk” surrounding the irreversibly damaged ischemic core (figure 6).

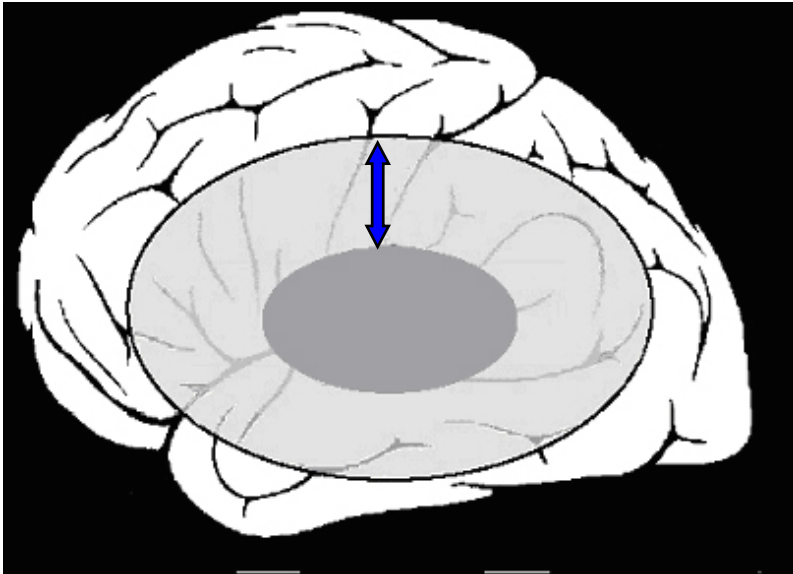
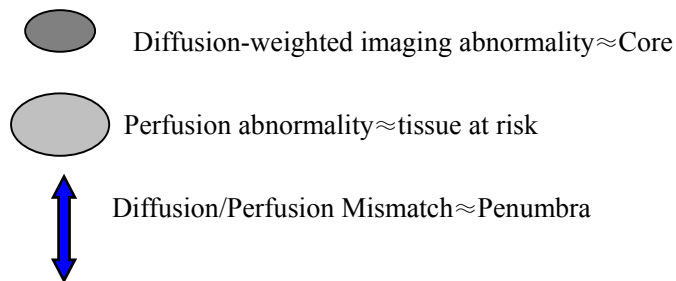


Fig. 6. Schematic of the mismatch model for defining the ischemic penumbra.



Clinical reports have demonstrated that the impaired perfusion region is typically larger than the lesion detected by DWI early after stroke onset, and this diffusion/perfusion mismatch volume correlated with growth in DWI lesion volume on follow-up studies⁴⁵. Derived from perfusion MR imaging the hemodynamic parameters (such as CBV, CBF, and MTT) has been proved to be useful adding information estimating ischemia stroke⁴⁶⁻⁴⁸. It is might also be useful to quantify the perfusion deficit within the diffusion/perfusion mismatch region to distinguish the real area at risk for infarction from the oligemic tissue in which blood flow is greater than the critical viability threshold. Since both ischemic core and the diffusion/perfusion mismatch region may have perfusion abnormalities, correlations of perfusion abnormalities with clinical severity and outcome might exist in those two corresponding regions.

The diffusion/perfusion mismatch was recognized as a simple and feasible means to identify the ischemic penumbra³². Therefore, we evaluated the hemodynamic parameters in both ischemic core and diffusion/perfusion mismatch region in acute stroke patients. It was our hypothesis that the hemodynamic parameters, such as rCBF,

rCBV, MTT, TTP and T0, exhibited correlation with the NIHSS score and the outcome measured by modified Rankin scale (MRS). To our knowledge, no previous study concerning prediction of outcome of ischemic stroke by MRI derived hemodynamic parameters was reported.

2 MATERIALS AND METHODS

2.1 Patients

All patients who presented to the neurological department of Klinikum Großhadern with symptoms of acute stroke between October 2000 and April 2004 were reviewed. Approximately 140 patients underwent both DWI and PW imaging. Of these, 62 were imaged within 72 hours. 35 acute stroke patients (male:female=20:15, age: 61.3±15.2 years) who met the study inclusion and exclusion criteria were then selected on the basis of the following criteria.

The inclusion criteria were as follows:

- (1) Imaging within 72 hours of stroke onset;
- (2) Availability of conventional MRI images and DWI and PWI image data sets;
- (3) Abnormalities shown on both time to peak (TTP) images and the DWI image;

The exclusion criteria were as follows:

- (1) With any contraindication to MRI scanning as: a) Central nervous system aneurysm clips; b) Implanted neural stimulator; c) Implanted cardiac pacemaker or defibrillator; d) Cochlear implant; e) Ocular foreign body (e.g. metal shavings); f) Insulin pump; g) Metal shrapnel or bullet; h) Any implanted device that is incompatible with MRI.
- (2) Patients with recent ischemic stroke within prior 30 days or rapidly resolving deficit.
- (3) Patients with ischemia at infratentorial region, lacunar ischemia and ischemia at thalamus or pons.
- (4) Any intracranial surgery, intraspinal surgery, or serious head trauma (any head injury that required hospitalization) within the past 3 months.
- (5) PWI not obtained or uninterpretable.

(6) No TTP defect corresponding to acute stroke deficit.

(7) Remarkable artifact on MRI images which were not workable for further analysis.

Significant cerebro-vascular risk factors such as arterial hypertension, hypercholesterolemia, diabetes mellitus and nicotine were recorded in 27 patients. Patient characteristics (including age, sex, clinical symptoms, risk factors, time to scan, occlusion type, patency of the artery in MRA, NIHSS scale, means of treatment, MRS outcome score and volume ratio were recorded and summarized in table 2.

Table 2. Patients' clinical information

No.	Age	Sex	Symptoms	Risk factor	Time to Occlusion scan (h)	to Occlusion type	Patency of artery in MRA	NIHSS	Treatment	MRS	Vd/Vp ratio
1	58	F	rt hemip	hypercholest., art. hypert	1.7	MCA, lt	0	4	(-)	2	<1/3
2	68	F	aphasia, weakness of rt hand	art. hypert	3.4	MCA, lt	0	13	i.v. Lysis	3	<1/3
3	77	F	aphasia, weakness of rt arm	art. hypert	14	MCA, lt	0	19	i.a.	6	<1/3
4	47	F	lt hemip	none	6	MCA, rt	0	9	(-)	4	<1/3
5	49	M	aphasia	hypercholest., art. hypert	4.5	MCA, lt	60	9	i.v. Lysis	4	<1/3
6	67	M	aphasia, rt hemip	art. hypert, hypercholest.	2.5	MCA, lt	0	12	i.v.+i.a.	4	<1/3
7	41	M	weakness of lt leg	none	2.4	MCA, rt	0	11	i.v.	3	<1/3
8	26	F	hemip rechts,aphasia	nicotine	2.5	MCA, lt	0	19	i.v.+i.a.	2	1/3<ratio<1/2
9	39	M	aphasia, weakness of rt hand	art. hypert	0.9	MCA, rt	(-)	16	i.v.+i.a.	3	<1/3
10	72	M	rt hemip, aphasia	DM, art. hypert	4.1	MCA, lt	(-)	11	i.a.	3	<1/3
11	62	M	aphasia, lt arm weakness	hypercholest., art. hypert	48	MCA, rt	0	14	i.v.	4	1/2<ratio<1
12	73	M	aphasia	art. hypert	48	MCA, rt	0	4	(-)	2	<1/3
13	72	M	aphasia, weakness of rt side	hypercholest., art. hypert	15	MCA, lt	100	7	(-)	0	<1/3
14	40	F	hemip rt, aphasia	hypercholest., art. hypert	1.9	MCA, lt	0	8	i.a.	2	1/2<ratio<1
15	74	M	hemip rt, aphasia	hypercholest.	5	MCA, lt	0	12	i.a.	5	<1/3
16	77	F	aphasia, weakness of rt side	not available	12	MCA, lt	(-)	12	(-)	3	<1/3
17	78	M	aphasia, weakness of rt side	diabetes mellitus	18	MCA, lt	100	11	i.v.	4	<1/3
18	75	M	hemip rt, aphasia	not available	72	MCA, lt	20	4	(-)	3	1/2<ratio<1
19	86	F	aphasia, righ hemip	hypercholest., art. hypert	45	MCA, lt	100	8	(-)	2	1/2<ratio<1
20	56	F	rt hemip, aphasia	CHD, art. hypert, nicotine	4.6	MCA, lt	(-)	9	i.a.	3	<1/3
21	56	M	weakness of lt arm	nicotine	7.7	MCA, rt	(-)	8	(-)	3	<1/3
22	40	M	hemip rt, aphasia	art. hypert	66	ICA lt	0	16	i.a.	1	<1/3
23	40	F	hemip rt, aphasia	none	5	ICA lt	0	13	i.a.	6	<1/3
24	61	M	hemip lt	not available	3.9	MCA, rt	(-)	12	i.a.	6	<1/3
25	70	M	hemip rt, aphasia	not available	5	MCA, lt	0	10	i.v.	3	<1/3
26	64	F	aphasia, weakness of lt side	hypercholest., art. hypert,	23.8	MCA, rt	(-)	4	(-)	4	<1/3
27	65	F	aphasia	art. hypert	5.4	MCA, lt	(-)	8	(-)	3	<1/3
28	73	F	hemip lt	hypercholest., art. hypert	12	ICA rt	(-)	0	(-)	0	<1/3
29	92	M	hemip, lt	art. hypert	7	MCA, rt	0	11	(-)	6	<1/3
30	48	M	hemip, lt	DM, art. hypert,	22	ICA, rt	(-)	12	(-)	4	<1/3
31	63	M	hemip lt, aphasia	arrythmia	3	MCA+ICA, lt	0	13	(-)	4	<1/3
32	61	F	hemip lt, Dysarthrie	hypercholest.	3.7	MCA, rt	20	13	(-)	4	<1/3
33	72	F	aphasia	art. hypert	5.4	MCA, lt	30	6	i.a.	4	<1/3
34	46	M	hemip lt	hypercholest., Adipositas	16	MCA, rt	10	3	(-)	2	<1/3
35	56	M	hemip rt, aphasia	none	5.9	ICA, lt	50	15	(-)	5	<1/3

Note: rt = right, lt =left, hemip=hemiparesis, hypercholest = hypercholesterolemia, art. hypert= arterial hypertension, DM= Diabetes mellitus, Vd=volume on DWI, Vp =volume on PWI. (-)= no lysis treatment, with secondary stroke prophylaxis; i.a.= intraarterial treatment (anjojet, clot-retriever, intraarterial lysis)

2.2 Neurological assessment

The NIHSS^{49, 50} assessment was immediately performed at the patients' admission by a certified and trained neurologist. The NIHSS contains several categories on (1) level of consciousness, (2) best visual, (3) best gaze, (4) facial weakness, (5)/(6) motor arm and leg, (7) limb ataxia, (8)sensory, (9) best language, (10) dysarthria, and (11) extinction and inattention with various level of scores. (Please refer to the detail of NIHSS scale in appendix 1.)

Functional outcome was measured on the day of hospital discharge according to MRS outcome scale^{51, 52}. From scale 0 to 6, the outcome ranges from no symptoms at all to more severely disability, and death. (Table 3)

Table 3: Content of MRS ⁵²

Scale	Outcome
0	No symptoms at all
1	No significant disability despite symptoms; able to carry out all usual duties and activities
2	Slight disability; unable to carry out all previous activities, but able to look after own affairs without assistance
3	Moderate disability; requiring some help, but able to walk without assistance
4	Moderately severe disability; unable to walk without assistance and unable to attend to own bodily needs without assistance
5	Severe disability; bedridden, incontinent and requiring constant nursing care and attention
6	Dead

The NIHSS and MRS of all the patients were evaluated by an experienced neurologist.

All the recruited patients were hospitalized at a dedicated stroke unit (G7B), and received hemodilatation, antihypotensive measures and had their body temperature and blood glucose level controlled. In case of elevated temperature, up to 3 grams of Paracetamole were given, and the glucose level was controlled by insulin. Depending on the individually clinical, neurological and neuroradiological situation the patients were also selectively treated by intravenous thrombolysis, intraarterial thrombolysis, intraarterial mechanical thrombus extraction.

2.3 Technical consideration

Routine MRI sequences and DWI and PWI were employed in our patients study. Since DWI and PWI technique is the basis of the study, a general review is necessary. Although diffusion weighted imaging and perfusion weighted imaging are distinctly different techniques, they are interrelated physiological parameters, and are usually performed during the same imaging examination.

2.3.1 Diffusion weighted imaging (DWI)

That water molecules are in constant random motion is called diffusion. Water diffusion in the intracellular space is much more restricted than in the extracellular space and thus does not contribute to imaging. In acute brain ischemia, water shifts from the extra- to the intracellular space with subsequent reduction of water motion in the extracellular space. This in turn inhibits the dephasing normally present in a DWI image, making this area bright. Thus the bright spots in DWI masks areas of acute cell ballooning due to Na/K pump failure⁵³. DWI visualizes the motion of ischemia-induced changes in water protons within minutes after an insult^{54, 55}.

DWI offers the unique opportunity to address noninvasively fundamental issues regarding the response of the brain tissue to ischemia at different stages. In order to do this, a pair of strong gradients pulses symmetrically placed around the 180° refocusing radiofrequency (RF) pulse is added to dephase and rephrase static water protons to separate fast and slow moving water molecules⁵⁶. The first gradient dephases the spins, while the second gradient, which is applied after a distinct time interval (diffusion time Δ), rephases the spins. (Figure 7).

Since the random molecular motion exists in all tissues, there is a certain loss of phase coherence that produces a signal loss in normal tissue. On the contrary, with less water movement, less dephasing occurs while the diffusion gradient are resulting in a higher signal intensity, as occurs with ischemic cell depolarization^{55, 57}.

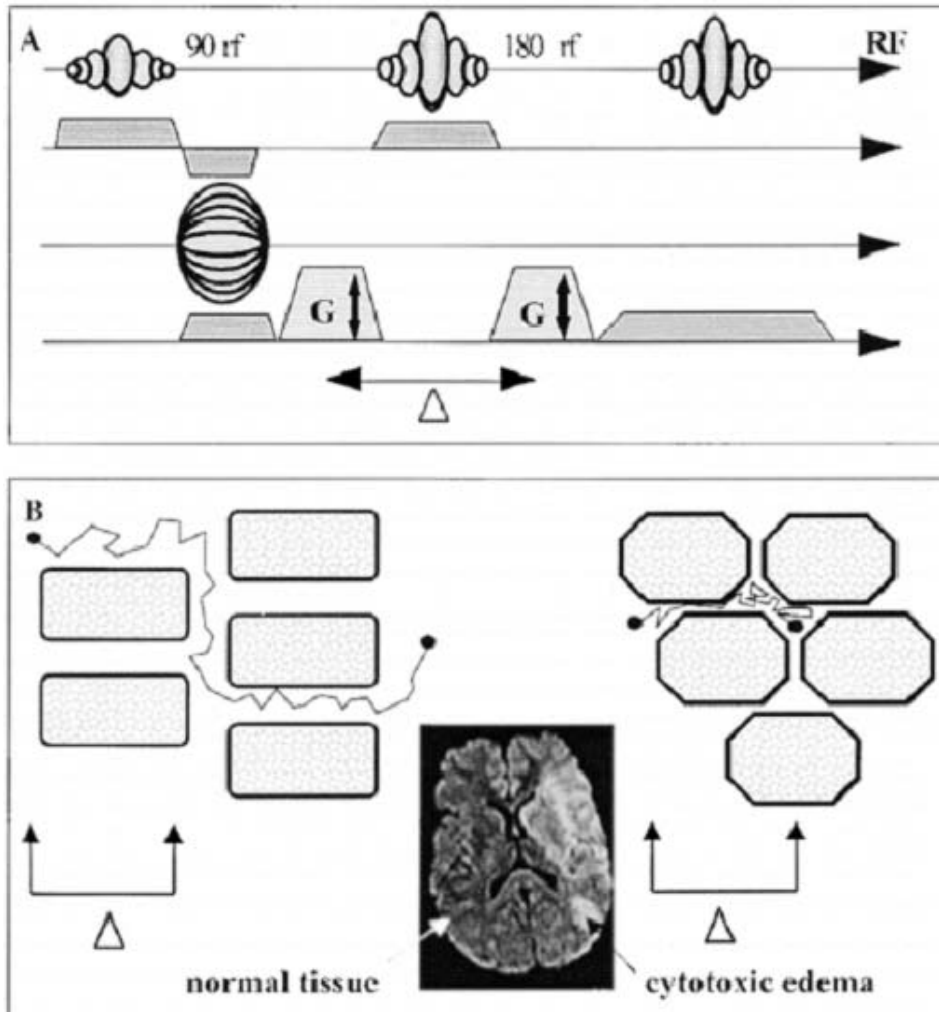


Fig. 7. DWI utilizes a pair of magnetic field gradient pulses placed symmetrically around the 180° refocusing RF pulse to dephase and rephase static water protons. Randomly moving water protons in normal brain tissue will experience incomplete spin rephasing resulting in a signal loss. Restricted diffusion as occurs with ischemic cell depolarization results in spin rephasing and retained MR signal with hyperintensity in DWI (Adapted from Hamann).

This signal variation depends on two parameters: (1) the tissue parameter, apparent diffusion coefficient (ADC), reflecting the mobility of the water molecules. ADC is a quantitative value, which can show the amount of water movement. A low ADC value indicates less water movement. (2) The sequence parameters, b-value⁵⁸, reflecting the degree of diffusion-weighting (Figure 8). Quotation 1 reflect the relation among the signal variation, ADC and b-value:

$$\frac{S}{S_0} = e^{-b \cdot ADC}$$

1

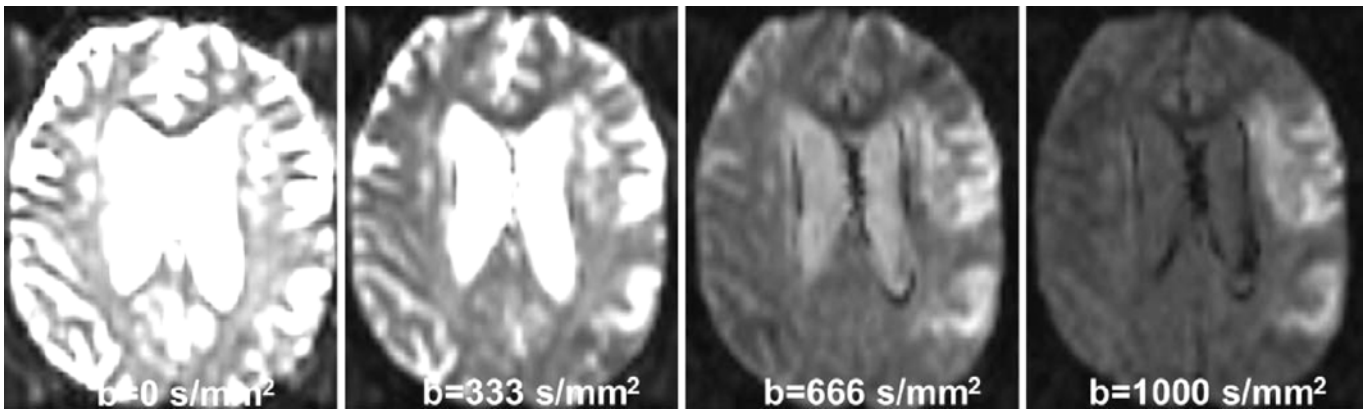


Fig. 8. Within an ischemic lesion where the diffusion is reduced. The contrast between ischemic and nonischemic tissue increases (on the left side) with the diffusion weighting (b -value). (Adapted from Heiland⁵⁹)

ADC value changes parallel with T2 in the ischemic development, from cellular energy failure, brain edema, till cellular necrosis. Based on experimental and clinical data, the MRI of ischemia evolving to infarction may be characterized by the following sequence of scenarios as illustrated in figure 9 and shown in table 4.

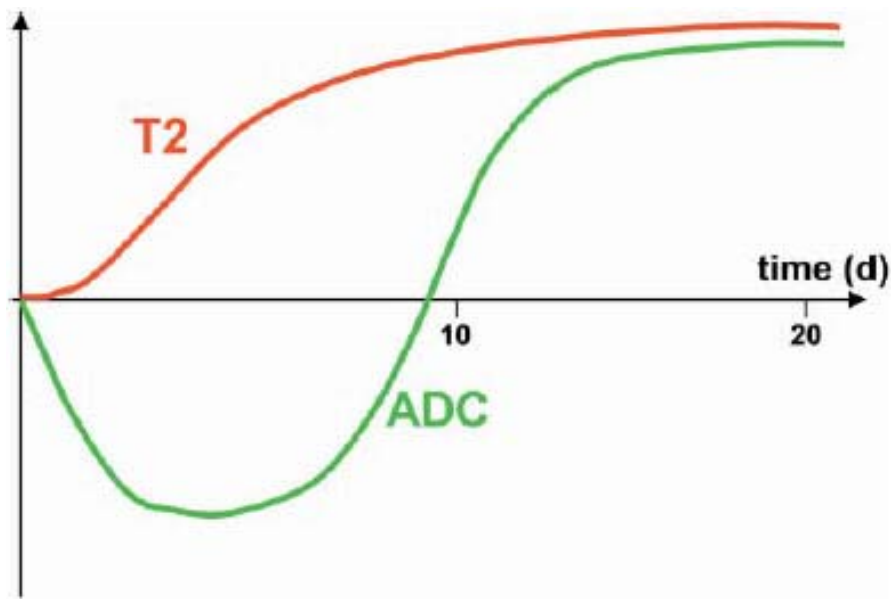


Fig. 9. Diagram of the time course of ADC and T2 after artery occlusion. In hyperacute cerebral ischemia the ADC decreases, whereas there is no change in T2. A minimum ADC is reached at day 2 to 3, then ADC increases again. In the subacute stage of ischemia, ADC is still decreased, whereas there is a distinct T2 increase. In chronic cerebral ischemia both ADC and T2 are increased. Adapted from S Heiland⁵⁹.

Table 4. The characteristic appearance of acute ischemic infarction on ADC map, diffusion-weighted imaging and T2WI

	Acute stage (minutes)	Subacute stage (hours – days)	9-10 days	Complete infarction
ADC	Decrease, hypointense	Decrease, hypointense	Isointense (pseudonormalization)	Increase, hyperintense
DWI	Hyperintense	hyperintense	hyperintense	Hyperintense or isointense
T2WI	Isointense (not detectable)	Hyperintense from 24 hrs	Hyperintense	Hyperintense

At these early time points, a low ADC and a hyperintensity on DWI would suggest membrane depolarization with water shift from extra- to intracellular space (cytotoxic edema). Without immediate reperfusion, regions with low ADC will most likely get infarcted.

In the later stages (hours to days), low ADC values are still seen in regions exhibiting signal intensity increase in T2WI MRI. This can occur when cytotoxic cellular swelling (within intact cells) exists in regions of increased water content (vasogenic edema).

In regions of complete infarction, both T2 and ADC are observed to be higher than normal within similar regional distributions. The corresponding histopathology of these regions indicates cellular necrosis, in which cell lysis breaks down water diffusion barriers leading to an increase in ADC. However, the “recovery” of ADC and hyperintensity on DWI to normal exhibits a high variety in the later steps, depending on type, size of infarction.

DWI has been shown to be very accurate in the diagnosis of acute cerebral infarction, with reported sensitivities of 88% to 100% and specificities of 86% to 100% in clinical studies⁶⁰⁻⁶⁴.

ADC change does not uniquely occur in ischemia. There are number of pathologies that might cause ischemia-mimic, such as multisclerosis plaques, status epileptics, herpes encephalitis, abscess and etc⁵³. Other MRI sequences including T1 and T2 change might help to distinguish ischemia from these entities. Consideration of vascular territories and clinical presentation will play an extremely important role in the differential diagnosis.

DWI mechanism is complex but its performance is quite convenient. In most hospitals it takes less than half minute scan time to get a series diffusion images and the ADC maps.

2.3.2 Perfusion weighted imaging (PWI)

There are two types of perfusion MRI, the first pass bolus tracking technique (also called dynamic susceptibility contrast-enhanced [DSC] imaging) and the arterial spin-labeling (ASL) method. Since the DSC method is more frequently used and is the clinical established method^{31, 65-69}, it is also used in our study. This technique will be reviewed in the following.

The DSC method was first proposed by Villringer and Rosen^{40, 70}. For this method, a bolus of paramagnetic contrast agent is used to visualize the blood perfusing the capillary network in the brain; the signal change caused by the contrast agent molecules passing through the capillaries in a voxel is monitored by a repetitive MRI measures in the same region. (Figure 10).

The presence of contrast agent molecules causes changes in both T1 and T2* relaxation. T1 effects, however, are small as the contrast agent does not cross the blood-brain barrier⁷¹. The T1 interaction is only strong for a very short distance and therefore it only affects protons within the capillaries, i.e. about 3–5% of the protons in brain tissue⁷². A stronger signal change is caused in T2*-weighted sequences by the unequal distribution of the contrast agent in the intravascular and the extracellular fluid space. This creates local field gradients, resulting in T2* shortening of the proton spin relaxation times. The radius of the T2* interaction is much larger than that of T1 as the surrounding tissue is also affected. The signal change is strong enough to monitor a contrast agent bolus passing through the brain.

If a paramagnetic contrast agent is injected and the susceptibility effect of the bolus in the brain is followed with a rapid series of T2*-weighted images, a drop in signal that fades away after a few seconds can be measured. Normally, there is no difference between the two hemispheres (figure 10). Regions with little or no perfusion (e.g., ischemic tissue) allow passage of only a small amount of contrast agent and therefore remain bright. (figure 11). Thus, ischemic areas

can be detected on the original contrast-enhanced MRI series by means of the signal decrease. A low signal decrease indicates that the tissue is less well or not perfused.

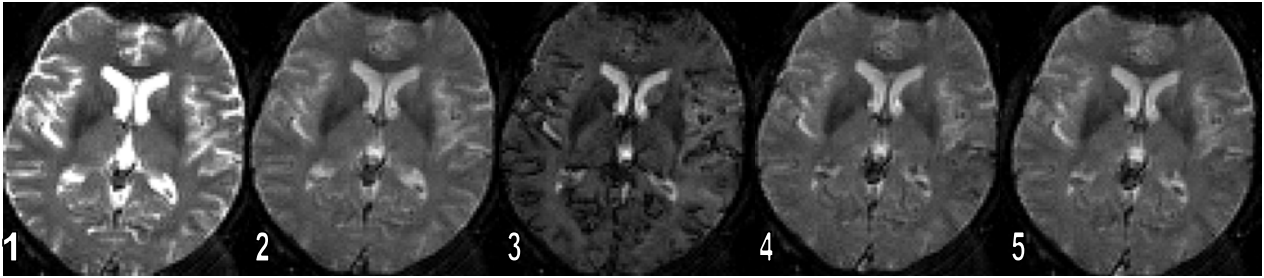


Fig. 10. Series of source images obtained at intervals during the perfusion imaging sequence. The initial gradient echo, EPI image (1) shows normal appearances before arrival of the bolus. The bolus arrives at image (2) and the concentration increases to a peak at image (3) where marked loss of signal is seen within the cortical vessels and brain parenchyma. The signal loss declines rapidly (4). The final image (5) shows appearances similar to those pre-contrast. The relatively low spatial and contrast resolution of the source images is apparent.

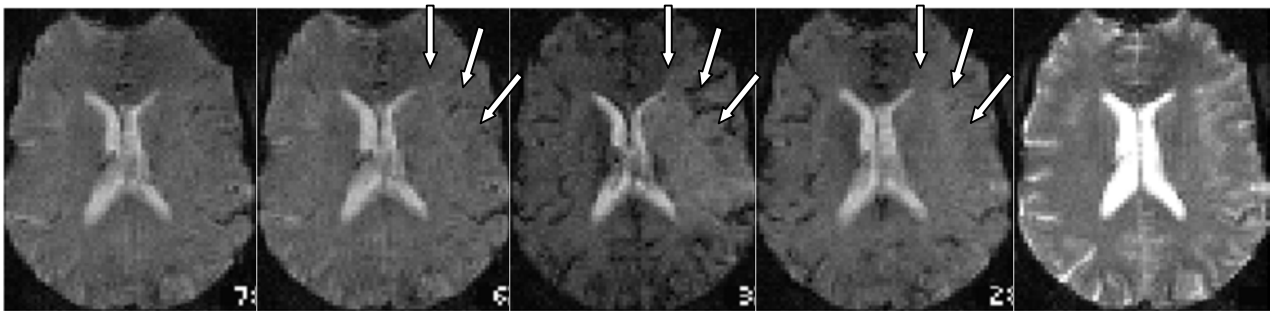


Fig. 11. Source images of a dynamic susceptibility contrast enhanced MRI series in a patient with focal cerebral ischemia. Within the ischemic territory the signal decreases much less than in the normal tissue.

The maximum signal decrease, however, does not correlate to any physiological parameter. For quantitative assessment of the hemodynamics, the signal time curve must first be transformed into a concentration-time curve. This can be done either in user-defined regions of interest (ROI) or on a pixel-by-pixel basis using the equation 2:

$$C(t) \propto \ln \frac{S(t)}{S_0} \quad 2$$

where $C(t)$ is the concentration-time curve, $S(t)$ is the signal-time curve, and S_0 is the baseline signal determined by averaging the signal intensities before bolus arrival.

The relative concentration of the contrast agent does not return to baseline after the bolus passage, but remains slightly increased; often a second passage of the bolus is visible (Figure

12).

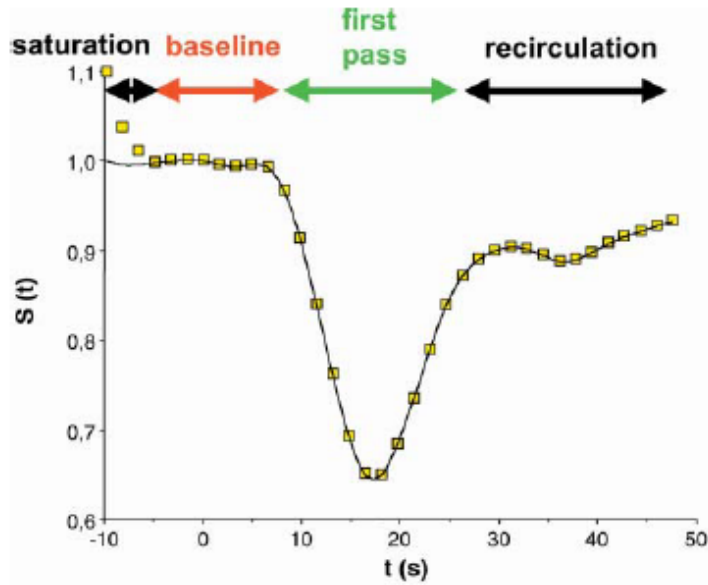


Fig. 12. Signal-time course in normally perfused tissue. The baseline is determined from the signal before bolus arrival. During first pass, there is a sharp signal decrease. The first pass is often followed by a second pass, with a signal decrease that is less steep than in the first pass.⁵⁹

For calculation of the cerebrovascular parameter, only the first pass of contrast agent through the brain tissue can be considered. Therefore, recirculation effects have to be excluded. This can be accomplished either by interactive truncation of the second pass or by fitting a gamma variate function to the measured concentration-time curve (Figure 13):

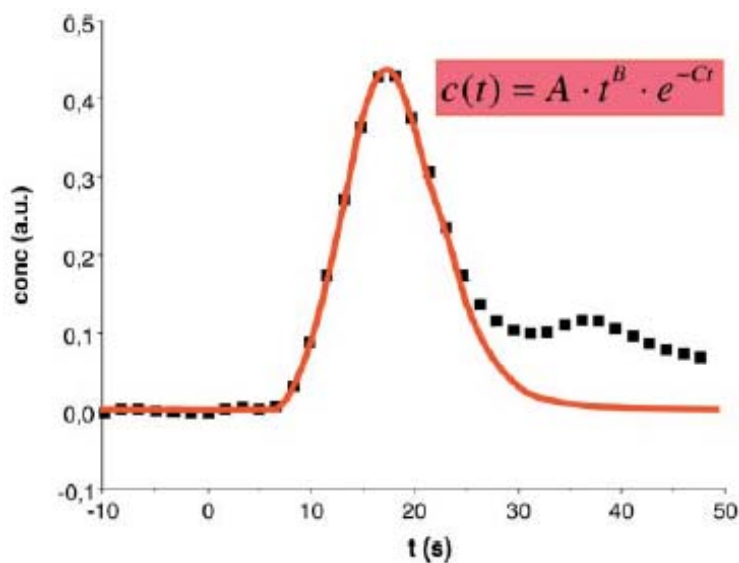


Fig. 13 Concentration-time course in normally perfused tissue. A gamma variate function is fitted to the curve to avoid effects of persistent contrast agent and of the second pass.⁵⁹

The parameters A, B, D, and bolus arrival time (T0) are then determined by an iterative fitting algorithm using the least-squares method⁷³. According to the indicator-dilution theory⁷⁴ the *relative regional blood volume* (rrCBV) can be calculated as the area under the concentration-time curve, the *relative mean transit time* (rMTT) is approximately the width at half maximum of the concentration-time curve, and the *time to arrival* (TTA) as the time between bolus injection and appearance of the first contrast agent molecules in the capillaries (Figure. 14)^{73, 75, 76}. TTA corresponds to the parameter T0 of the gamma variate function already mentioned. Some manufacturers calculate the TTP instead of rMTT. TTP and rMTT are inversely correlated with the CBF, i.e., low regional CBF results in high TTP and rMTT⁷⁷.

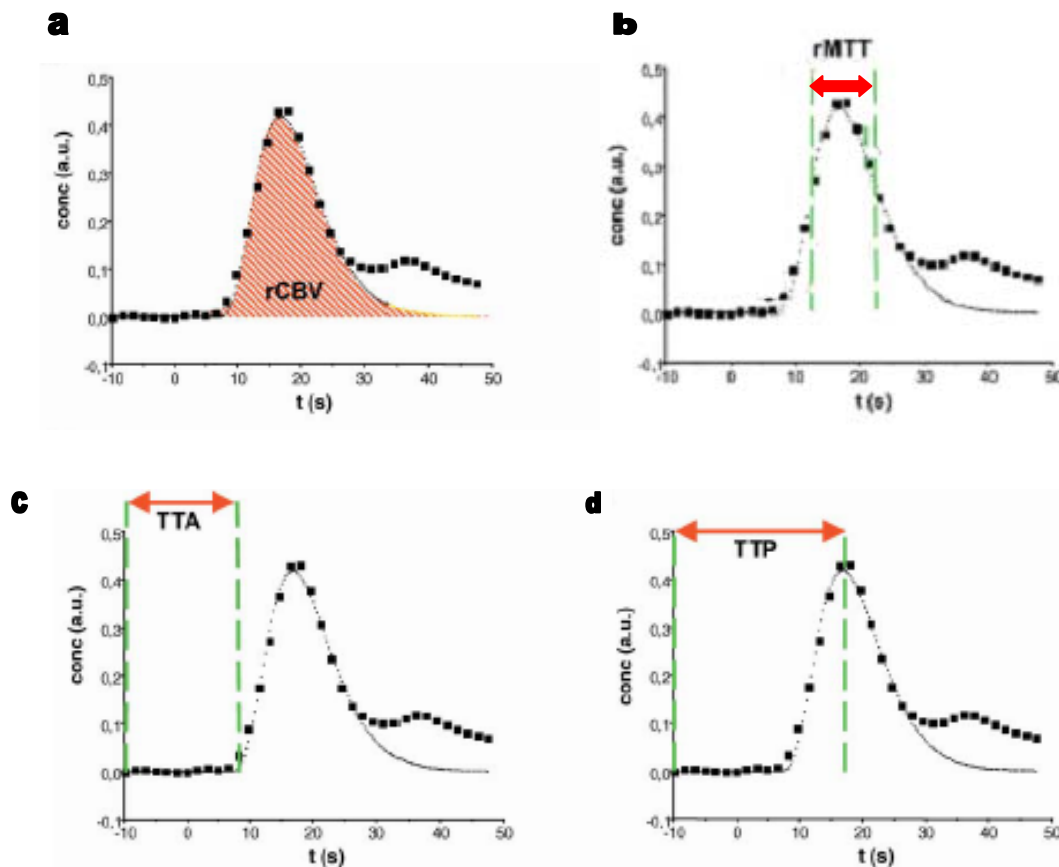


Fig. 14. Various cerebrovascular parameters can be calculated from the concentration-time curve: (a) rrCBV is defined as area under the concentration-time curve, (b) rMTT is the width at half maximum of the curve, (c) TTA is the time between contrast agent injection and arrival of the first contrast agent molecules within the region of interest, and (d) TTP is the time between contrast agent injection and the maximum contrast agent concentration within the region of interest.⁵⁹

Although these are relative parameters, they are sufficient for examining a focal disease. Hemodynamic parameters calculated in diseased area can be compared with the parameters of normal tissue⁵⁹. In diseases affecting hemodynamics of the whole brain, however, the

quantitative parameters must be calculated. This can be achieved by measuring the AIF and deconvolution of the tissue concentration-time curve⁷⁸⁻⁸⁰.

2.4 MRI protocol

All MR imaging was performed on a 1.5-T whole body system (Magnetom Vision; Siemens, Erlangen, Germany), using the standard head coil for radiofrequency (RF) transmission and detection. After a localizer, T2- and T1-weighted spin-echo sequences with 19 sections were acquired, covering the whole brain (T2: 2210/85 ms, 14/1 [TR/TE/number of excitations]; T1: 665/14/1 ms, 5-mm section thickness, 210-mm field of view). The gap between slices in both T1- and T2-weighted sequences was 1.5 mm. DWI and PWI were also performed with the following protocol.

DWI

DWI was performed using a multislice, single-shot, spin-echo EPI sequence. The diffusion gradient was applied in three dimensions, with three b values ranging from 50, 500 to 1,000 sec/mm^2 . Typical imaging parameters were an echo time (TE) of 137 msec, matrix size of 128 x 128, field of view (FOV) of 250 mm, slice thickness of 5 mm (gap between slices 1.5 mm), and a set of 19 axial slices. To minimize the effects of diffusion anisotropy, an average of all three diffusion directions was calculated to give the trace of the diffusion tensor. Only the DWI map when $b=1000 \text{ sec}/\text{mm}^2$ were chosen as the map to measure the abnormalities volume, and the hyperintensive abnormality was recognized as the ischemic core. (Figure 15).

PWI

PWI was performed before, during, and after bolus injection of a standard dosage⁷¹ of 0.2 mmol/kg contrast material (Ominiscan, Nycomed Imaging AS, Oslo, Norway; Magnevist, Schering, Berlin, Germany) injected by a power injector (Spectris; Medrad, Volkach, Germany) at a rate of 5 cc/s. Echo-planar sequence was performed with the following parameters: echo time (TE) 60.7 msec, repetition time (TR) 2 seconds, FOV 240 mm, acquisition matrix 128 x 128, and the slice thickness was 5 mm with the gap between slices of 1.5 mm. The perfusion sequence had 12 slices, which were positioned to cover the region suspected to be ischemic based on the extent of abnormal signal intensity on the DWI. (Figure 15).

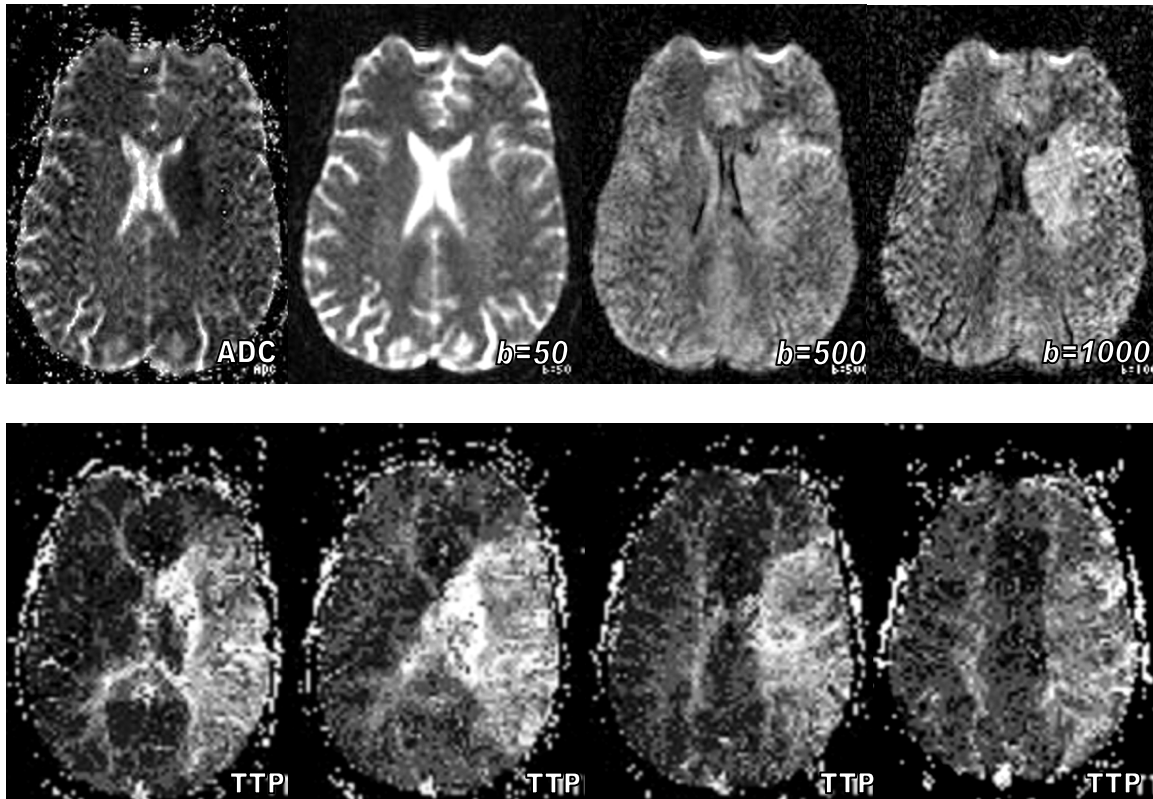


Fig. 15. The upper row is the DW images. The lower row is the TTP images of PWI.

On DWI, the ADC map the ischemia is hypointense, while the ischemia contrast to nonischemic tissue increased when b value increased. On PWI, TE=60.7 msec, TR=2 seconds, FOV 240 mm, matrix 128 x 128. Notice the diffusion/perfusion mismatch. Only the hyperintense abnormality on DWI when $b=1000\text{sec/mm}^2$ were used to compare the hyperintense abnormality on corresponding PWI TTP images.

The raw images of DWI and MR angiography were interpreted in consensus by two experienced radiologists (RB, JM) without the knowledge of the clinical information of the patients.

2.5 Data processing

The raw perfusion scanning data were transferred to a Linux Red Hat workstation for further processing. All the post-processing was done with MEDx 3.4.1® (Sensor Systems, Virginia, US). Image processing of all dynamic data was performed on a pixel-by-pixel basis calculating a gamma fit. AIF was determined using both time curves and anatomic overlay. The first pass arterial response was based on fitting a gamma-variate function to the arterial data. Analysis of the PWI included calculation of territorial CBV, CBF, MTT, T0 and TTP.

The following analysis or measurement was performed without knowledge of the patients' symptoms.

On the perfusion MRI map, ROIs were manually drawn contoured in ischemic core (hyperintensive area on DWI map when $b=1000$ s/mm²) and the diffusion/perfusion mismatch area (the area normal on DWI, but abnormal on TTP), and in both normal mirror area. The apparent TTP maps were chosen to delineate perfusion abnormalities. To minimize errors related to imprecise coregistration and contouring, the perfusion parameters were calculated only in ROIs that were larger than 30 mm² in ischemic core and in ROIs that were larger than 60 mm² in diffusion/perfusion mismatch areas. Finally there were two sets of ROIs were established and were copied and pasted to all the maps as CBV, CBF, MTT, TTP and T0 for each case. (Figure 16). With MEDx, the original values of the hemodynamic parameters were automatically calculated and displayed.

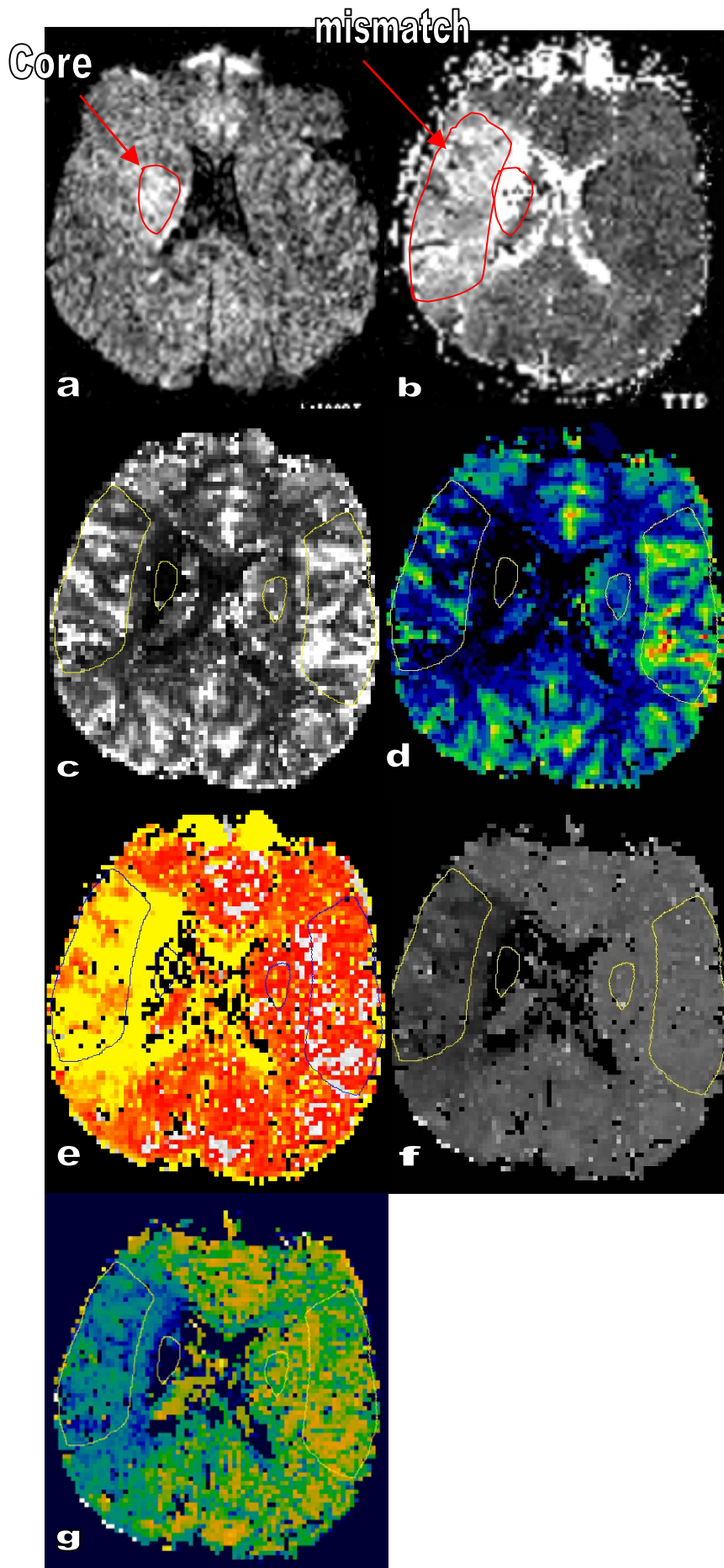


Fig. 16. On *a*. DWI the hyperintensity was recognized as ischemic core; and on *b*. TTP, the area normal on DWI but abnormal on MTT map was recognized as mismatch; On *c*. CBV; *d*. CBF; *e*. MTT; *f*. TTP and *g*. T0 maps, the ROIs were manually drawn in the ischemic core and the mismatch region on the perfusion maps, and were rotated to the mirror region on each map.

Calculation of perfusion parameters. The original value of the CBV, CBF, MTT, T0 and TTP of each territory was obtained in ischemic core, mismatch region and the contralateral mirror regions. The relative perfusion values (rCBV and rCBF) were then calculated as ratio of value in diseased area and the contralateral mirror area (equation 3), while the time parameters (MTT, T0 and TTP) were the difference between the diseased area and the mirror area:

$$\text{relative value of parameter} = (P_{\text{disease}} - P_{\text{mirror}}) / P_{\text{mirror}} \times 100\% \quad 3$$

where P_{disease} means the parameters in disease area, and P_{mirror} means the parameters in normal mirror area.

Measurement and calculation of the volume in both DWI and PWI. On MEDx, drawing of the ROIs manually along the contour of the hyperintensive abnormalities on DWI and PWI images (figure 17) on each slice was used to derive the quantitative area values. With the area values timed the slice thickness and gap, and then added, the volume (in cm^3) value was achieved. The diffusion/perfusion volume ratio was calculated according to the following formula 4:

$$\text{Ratio} = \text{Volume on DWI} / \text{Volume on PWI} \quad 4$$

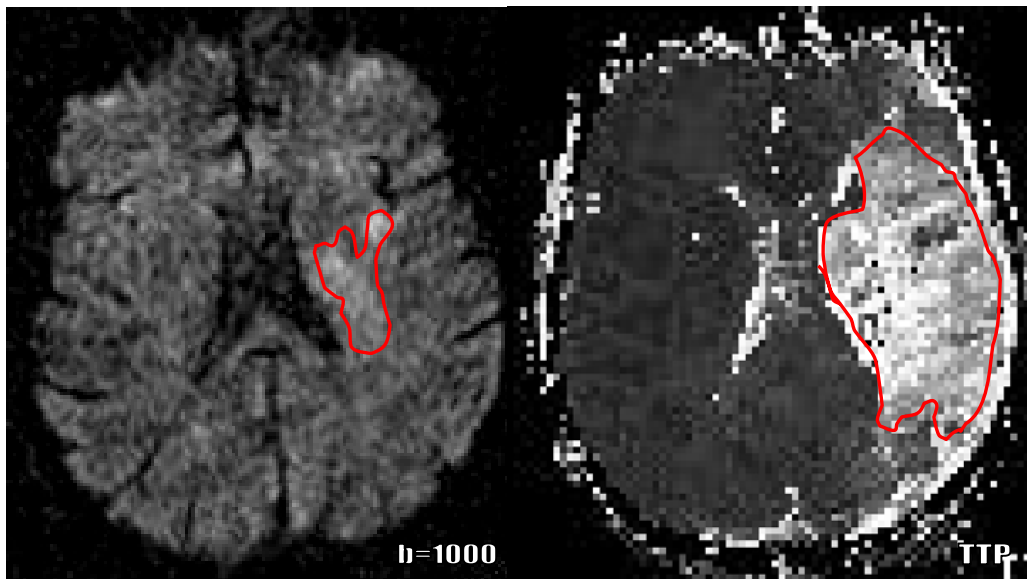


Fig. 17. DWI and PWI images. The ROIs were drawn contouring the hyperintensive abnormalities on the images. The volume equals to area x (slice thickness+gap). The diffusion/perfusion volume ratio is $<1/3$ in this patient.

2.6 Statistics

Statistical analysis was performed using the SPSS software package, version 11.0 (SPSS, Inc, Chicago, USA). One way analysis of variance was used to determine whether significant differences existed between the time to scan, age, sex, NIHSS and MRS between groups of good outcome and poor outcome. This one way analysis of variance was also used in analysis of age, sex, NIHSS and MRS between groups of volume ratio greater than 1/3 and less than 1/3. Linear regression was used to evaluate the relation between rCBV, rCBF, MTT, TTP and T0 values, and NIHSS and MRS in both the infarcted core and mismatch regions. Mean value plus standard deviation (SD) was used to give the average value of rCBV, rCBF, MTT, TTP and T0 in both infarcted core and mismatch region. Paired-samples T test was used for evaluation of the relation between NIHSS and MRS.

3 RESULTS

3.1 General

In the patients group (n=35), time between ictus to MRI scan ranged from 0.9 to 72 hours. There were 21 patients examined by MRI within 6 hours, and 14 patients between 6 and 72 hours. The average volume of the hyperintensive abnormalities on DWI was 22.5 (range: 5.2 to 122.4) cm³, and the average volume of hyperintensive abnormalities on PWI was 124.3 (range: 23.4 to 465.8) cm³. The volume ratio of diffusion/perfusion was less than 1/3 in 30 patients (85.7), and ratio greater than 1/3 in 5 patients (14.3%).

MRA was available in 25 patients (71.4%). Patency of the artery on the basis of MRA at the time of MRI scan was shown as follows: 0% patency (occluded, n=16), 10-60% patency (partially open, n=6), and 100% patency (totally open, n=3).

In this patients group, 6 (17%) patients received intravenous thrombolysis (within 3 hours at the standard dose), 9 (25%) patients received intraarterial treatment as exclusion criteria for the intravenous thrombolysis existed, 3 (9%) patients received both intravenous and intraarterial treatment. All of the above patients were managed in combination to intensive care treatment. 17 (49%) patients received intensive care treatment only including secondary stroke prophylaxis treatment.

The NIHSS score of the patients at initial examination ranged from 0 to 19 (10.2±4.4). The outcome MRS scale ranged from 0 to 6 (mean: 3.23). A good outcome (MRS 0 to 3) was observed in 19 patients (54.3%), whereas 16 patients (45.7%) had a poor outcome (MRS 4 to 6). In the latter group, MRS showed that 10 patients had scale 4, 2 patients had scale 5 and 4 patients had scale 6 (death).

Between the good and poor outcome groups, time to scan (17.1±22.1 versus 11.1±12 hours), DW/PW volume ratio (0.40±0.15 versus 0.36±0.11), age (59.6±16.7 versus 63.2±13.5 years) and female/male ratio (9/10 versus 6/10) did not show significant differences. (Table 5)

The mean NIHSS score was 9±5.3 in the group with good outcome, and 11.6±3.5 in the group

with poor outcome; Although there was a trend that lower NIHSS score had good outcome and high NIHSS had poor outcome, it did not reach statistical significance in our group.

Table 5. Relationship Between Stroke Outcome, time to scan, NIHSS, volume ratio, age and sex ratio.

	Outcome		<i>p</i>
	Good* (n=19)	Poor* (n=16)	
Time to scan (h)	17.1±22.1	11.1±12	.346
NIHSS	9±5.3	11.6±3.5	.089
Volume ratio (DW/PW)	0.4±0.2	0.4±0.1	.322
Age (y)	59.6±16.7	63.2±13.5	.498
Female/male ratio	9/10	6/10	.570

*Good outcome indicated the MRS ranged from 0 to 3, and a poor outcome indicated that MRS ranged from 4 to 6.

3.2 MRI hemodynamic parameters evaluation

Ischemic core

rCBF showed a remarkable decrease in all patients on average by $59.3 \pm 33.7\%$ (range: 23.2 - 97.4%). rCBV decreased in 29 patients by $41.7 \pm 23.7\%$ (range 19.6 - 55.6%), while 6 patients showed an increase of rCBV by $60.4 \pm 57.1\%$ (range 0.7 -139%). The mean rCBV change of the entire group was $26.3 \pm 52.5\%$. MTT, TTP and T0 prolonged for 4.7 (SD=15.1), 2.8 (SD=12.9) and 0.5 (SD=10.4) seconds, respectively.

Mismatch region

The evaluation of rCBF showed two controversial trends in the patients group, as rCBF decreased in 15 patients by $26.2 \pm 19.9\%$ (range: 5.3-58.4%) while increased in 20 patients by $35 \pm 23.2\%$ (range: 6.8–74.4%). As a result, the change of the rCBF of the whole patients group was on average $5.8 \pm 38.4\%$. rCBV decreased in 7 patients by $14.7 \pm 16.5\%$ (range: 0.8-44.5%) and increased in 28 patients by $39.5 \pm 36\%$ (range: 2.2-91.1%). The mean change of the rCBV of the whole group was $19.9 \pm 31.2\%$. The mean value of MTT, TTP and T0 prolonged for 2.7 (SD=8.5), 3.2 (SD=5.2) and 1.3 (SD=4.2) seconds respectively.

Figure 18 to 21 show four examples of MCA territory ischemia.

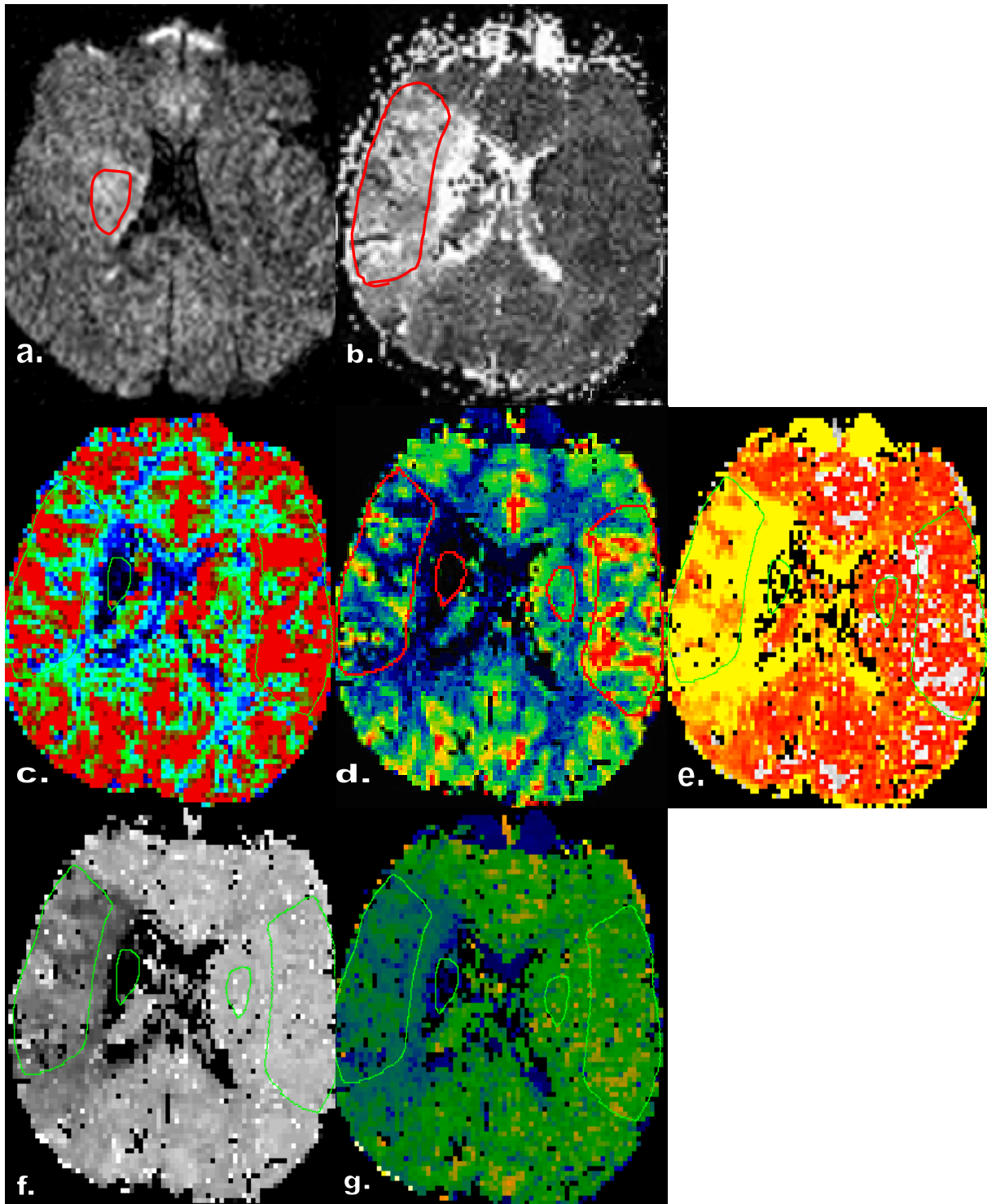


Fig. 18. K. R. Male, 61. Left hemiparesis. Ischemia on right MCA territory. NIHSS score was 12. The immediate study (4 hours after onset) showed an ischemia with a large DWI-PWI mismatch in the right MCA territory. Volume ratio was greater than 1/3. The ROIs for the hemodynamic parameters were drawn on ischemic core and the mismatch region, and on the normal mirror region. Patient received systemic thrombolysis and mechanical recanalization. Patient deceased in the course of the disease (MRS=6). a. DWI showed relative small hyperintensive abnormality, while b. PWI showed larger hypertensive abnormality. c. CBV map, rCBV decreased by 89.4% in core and 44.5% in mismatch. d.CBF map. rCBF decreased by 97.4% in core and 63.3% in mismatch region; e. MTT map. MTT prolonged 24.1s in core and 12.3s in mismatch region; f. TTP map. and g. T0 map. TTP shortened 32.2 s and 7.6 s in core and mismatch region, T0 shortened 22.6 s and 6.4 s in core and mismatch region correspondingly.

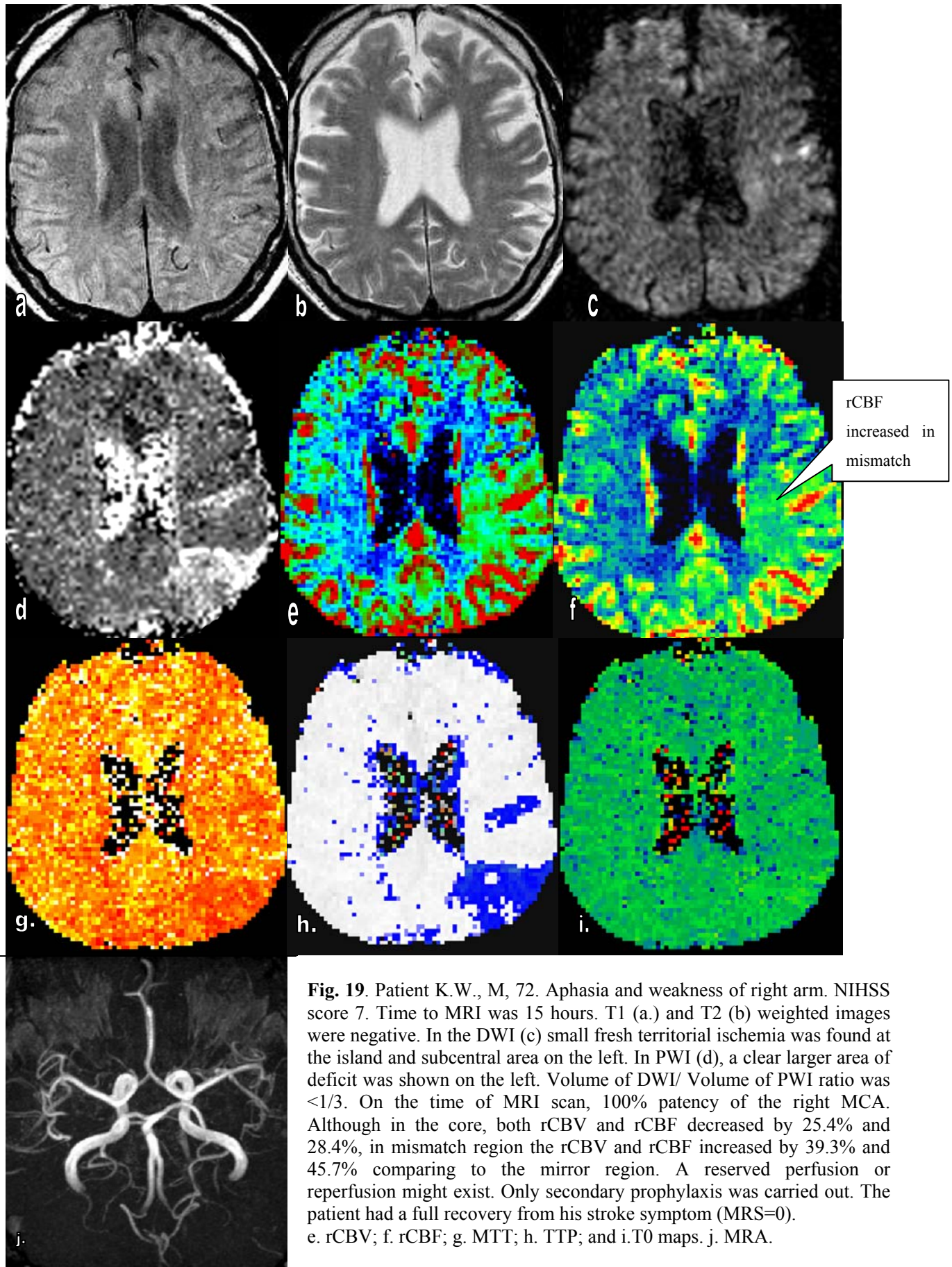


Fig. 19. Patient K.W., M, 72. Aphasia and weakness of right arm. NIHSS score 7. Time to MRI was 15 hours. T1 (a.) and T2 (b) weighted images were negative. In the DWI (c) small fresh territorial ischemia was found at the island and subcentral area on the left. In PWI (d), a clear larger area of deficit was shown on the left. Volume of DWI/ Volume of PWI ratio was $<1/3$. On the time of MRI scan, 100% patency of the right MCA. Although in the core, both rCBV and rCBF decreased by 25.4% and 28.4%, in mismatch region the rCBV and rCBF increased by 39.3% and 45.7% comparing to the mirror region. A reserved perfusion or reperfusion might exist. Only secondary prophylaxis was carried out. The patient had a full recovery from his stroke symptom (MRS=0). e. rCBV; f. rCBF; g. MTT; h. TTP; and i. T0 maps. j. MRA.

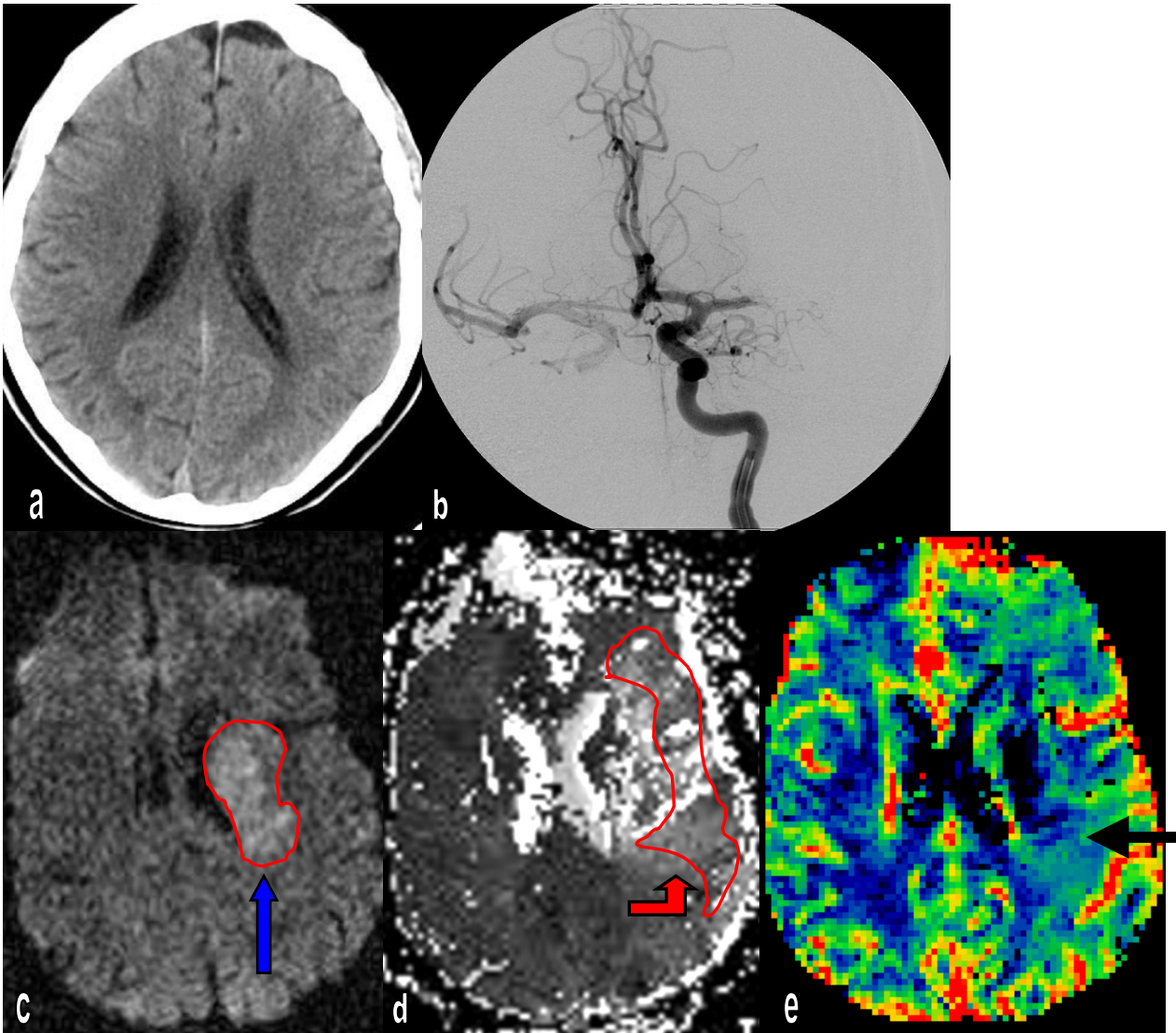




Fig. 20 L. F. M/67. The patient could not speak and his right side could not move. The initial NIHSS was 12. CT (a) found a dubious hypodense on the lens. Both DWI and PWI (c and d) showed a hyperintense deficit on left MCA territory. DSA (b) showed occlusion was in the proximal M1 segment. A spontaneous reperfusion was established at the time of MRI within 2.5 hours after onset. After the systemic thrombolysis, a mechanical aspiration by means of Angiojet was successfully performed. His mRS outcome score was 4.

↑ The arrow points the core region on DWI.

The red arrow  points the mismatch on TTP map.

Notice the green up region pointed by arrow , where the rCBF is 1.91, almost twice of that of the mirror region. This might be interpreted as spontaneous reperfusion.

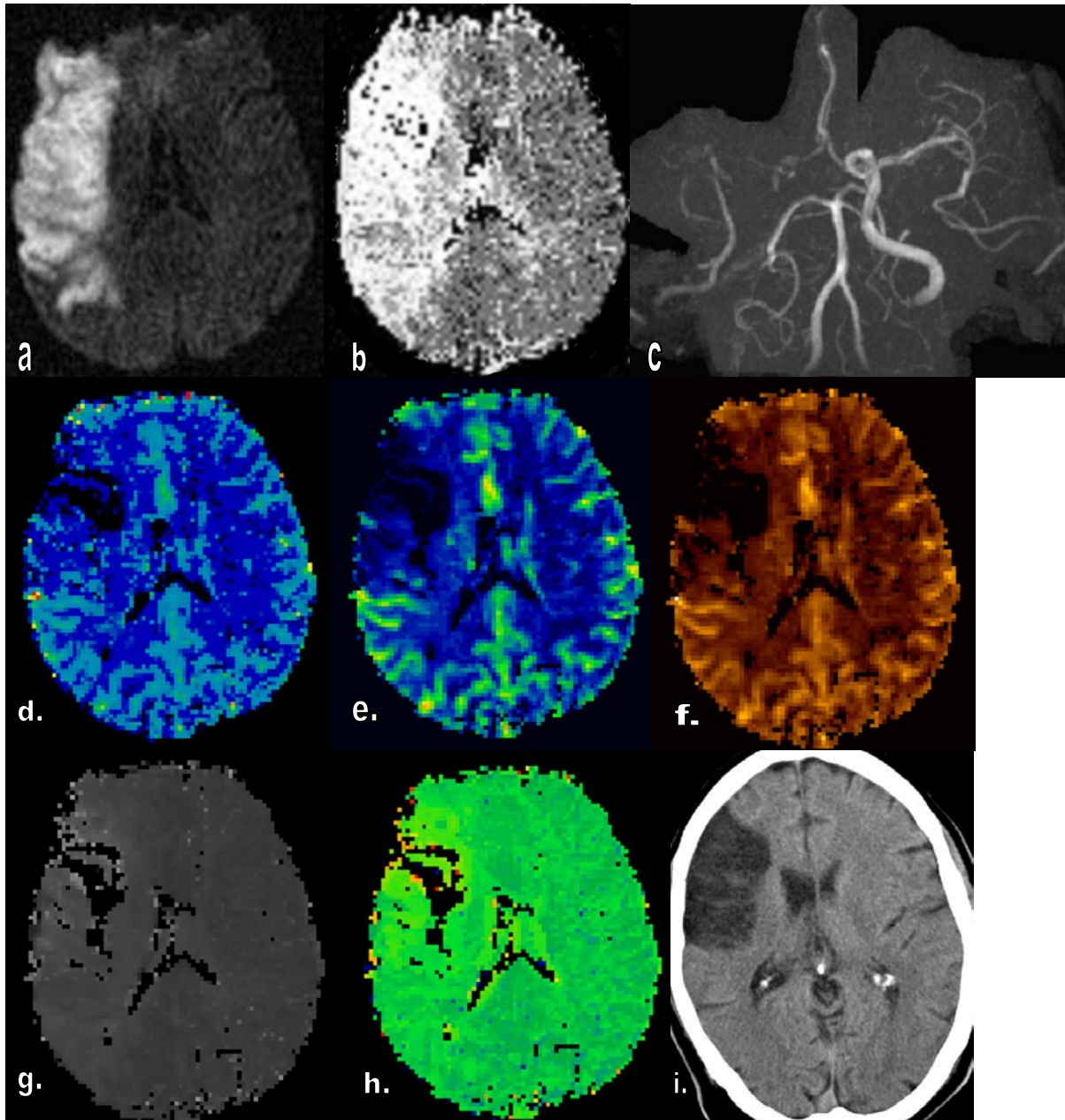


Fig. 21. Patient M/62, aphasia and hemiparesis left. NIHSS score 14. Time to MRI scan 48 hours. a and b: DWI and PWI, both DWI and PWI showed an ischemic deficit on the right. A mismatch exists, with $1/2 < \text{volume of DWI} / \text{volume of PWI} < 1$. c. MRA showed a right carotid artery and MCA occlusion. d- h. rCBV, rCBF, MTT, TTP and T0 maps. In the ischemic core, rCBV and rCBF decreased by 55.6% and 67.1%, while in mismatch region rCBV and rCBF increased by 27.4% and 74.4% in comparison to the mirror region correspondingly. i. Follow-up (58days) CT confirmed that the size of the infarction was smaller than that on both DWI and PWI. The patient presented a clear recovery from hemiparesis and could move within the rolling-chair. MRS 4.

3.3 Hemodynamic parameters in relation with assessment of stroke severity (NIHSS) and outcome (MRS)

3.3.1 Hemodynamic parameters in relation to NIHSS

Ischemic core

There was no statistic significance ($p>0.05$) between each hemodynamic parameters derived from ischemic core (figure 22-26) with the stroke severity (NIHSS) score.

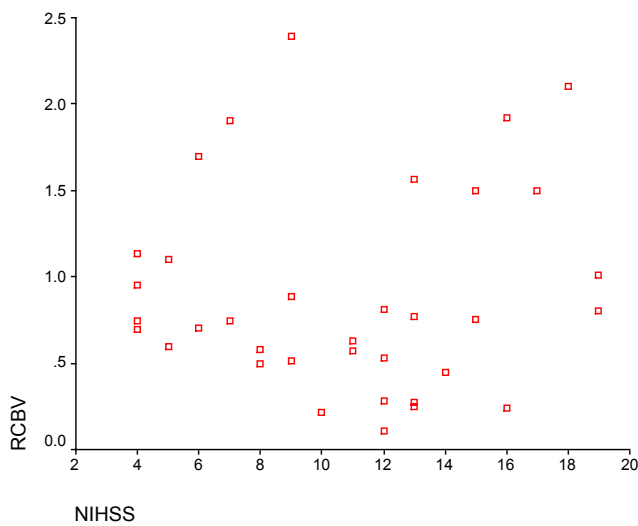


Fig. 22. Graphic demonstration of the relation of rCBV with NIHSS in ischemic core region. ($p=.894$)

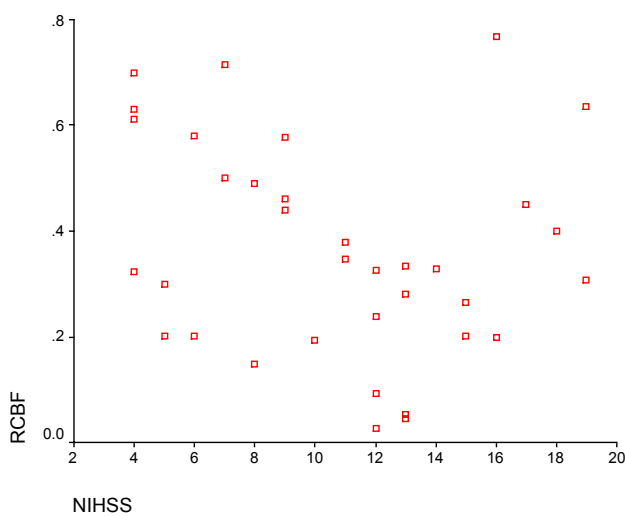


Fig. 23. Graphic demonstration of the relation of rCBF with NIHSS in ischemic core region. Notice there was a trend that the more the rCBF decrease the higher the NIHSS (the severe the symptom was) although there was no statistic significance shown ($p=.122$)

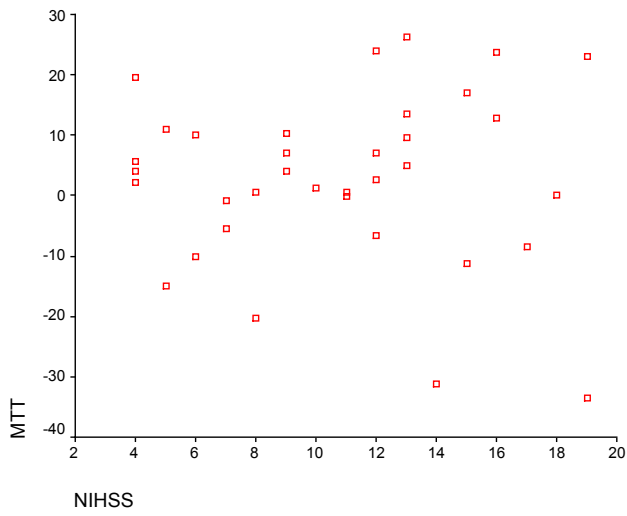


Fig. 24. Graphic demonstration of the relation of MTT with NIHSS in ischemic core region. ($p=.134$).

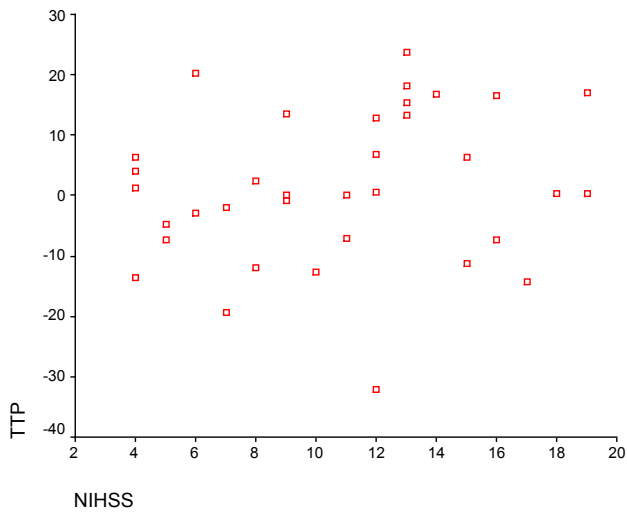


Fig. 25. Graphic demonstration of the relation of TTP with NIHSS in ischemic core region. ($p=.147$).

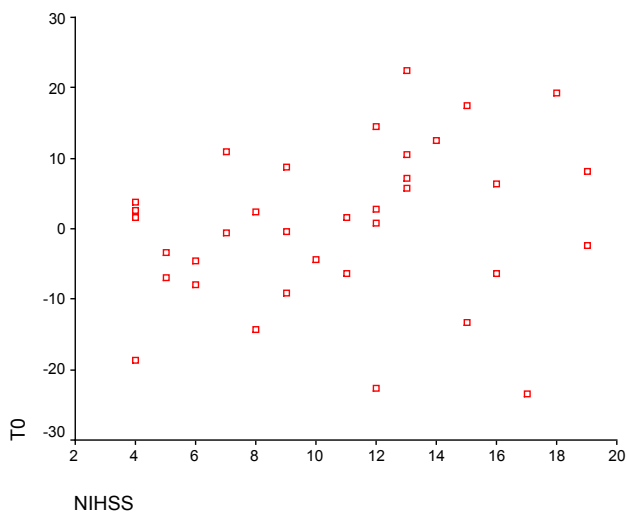


Fig. 26. Graphic demonstration of the relation of T0 with NIHSS in ischemic core region. ($p=.549$).

Mismatch region

There was no statistic significance ($p>0.05$) between each hemodynamic parameters derived from mismatch region (figure 27-31) with the stroke severity (NIHSS) score, with the exception of TTP which showed a strong statistic correlation with NIHSS ($p=0.001$). Prolongation or delay of TTP therefore was related to more severe stroke symptoms.

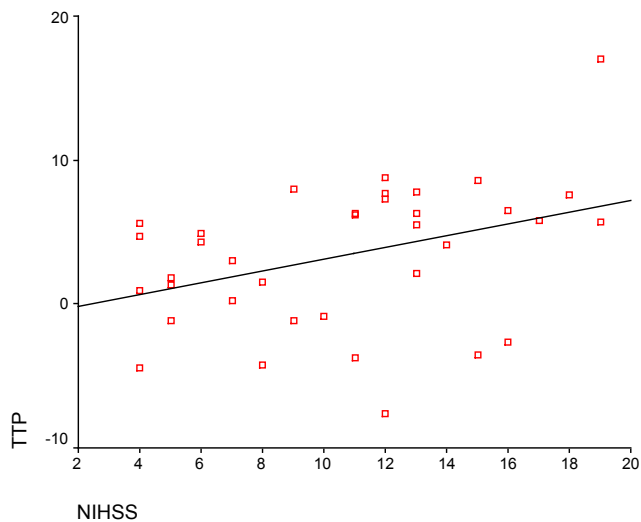


Fig. 27. Graphic demonstration of the relation of TTP with NIHSS in mismatch region, ($p=.001$), without including constant in equation. Delay of TTP in mismatch region was related to NIHSS: the longer the delay, the severe the symptoms were.

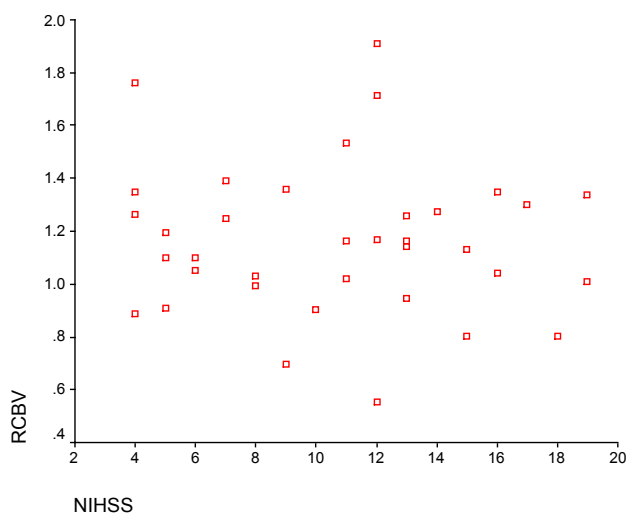


Fig. 28. Graphic demonstration of the relation of rCBV with NIHSS in mismatch region, ($p=.715$).

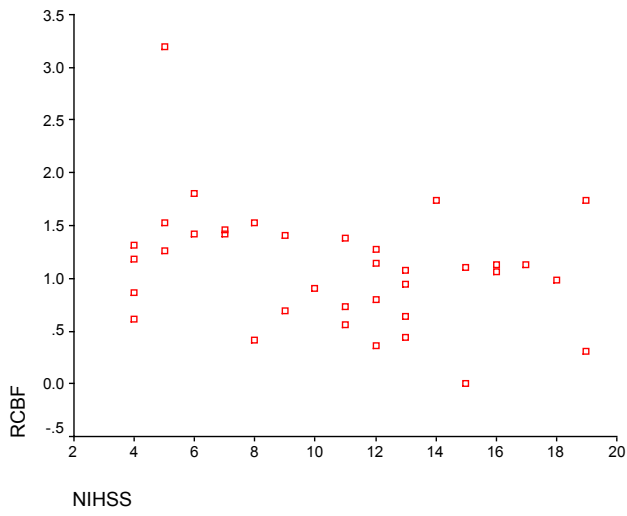


Fig. 29. Graphic demonstration of the relation of rCBF with NIHSS in mismatch region, ($p=.556$).

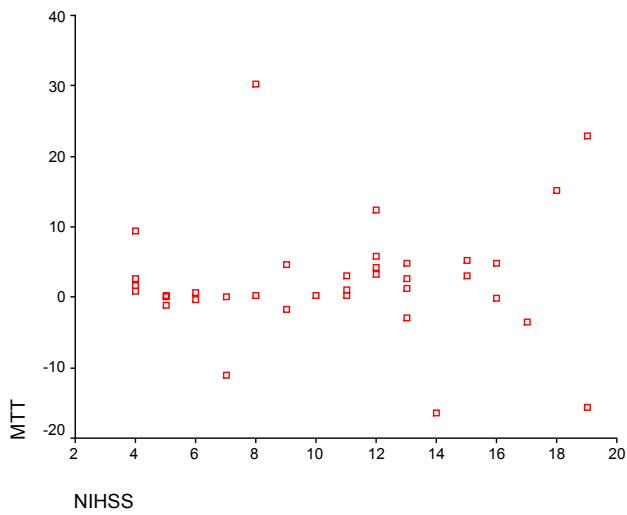


Fig. 30. Graphic demonstration of the relation of MTT with NIHSS in mismatch region, ($p=.660$).

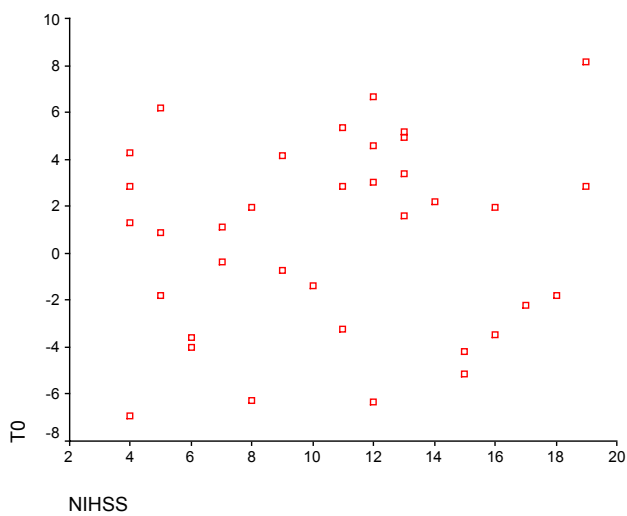


Fig. 31. Graphic demonstration of the relation of T0 with NIHSS in mismatch region, ($p=.064$).

3.3.2 Hemodynamic parameters in relation to MRS

Ischemic core

rCBF regressed statistically significant with MRS ($P=.0003$). It showed the trend that higher rCBF in the core related to less MRS (better outcome), and vice versa. (Figure 32). MTT also showed statistic significance of regression with MRS. Prolongation or delay of MTT related to higher MRS (worse outcome). (Figure 33). No statistic significance between other parameters with the MRS outcome scale. (Figure 34-36)

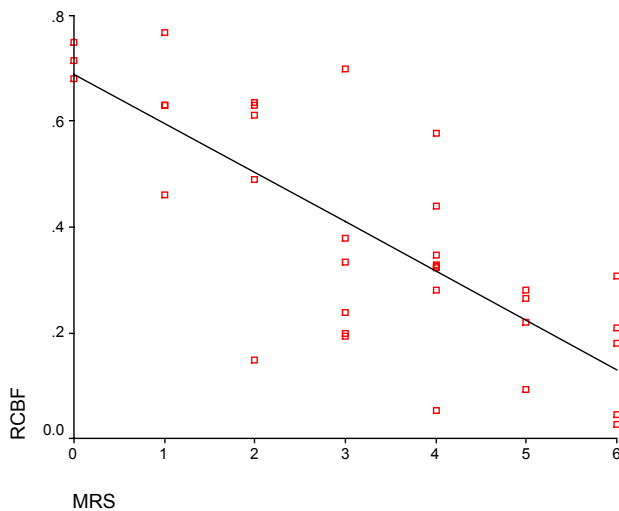


Fig. 32. The relation of rCBF with the MRS outcome scale on ischemia core region. Notice the tendency that decreased rCBF correlated with high MRS (worse outcome), and increased rCBF had lower MRS (better outcome) ($p=.0003$).

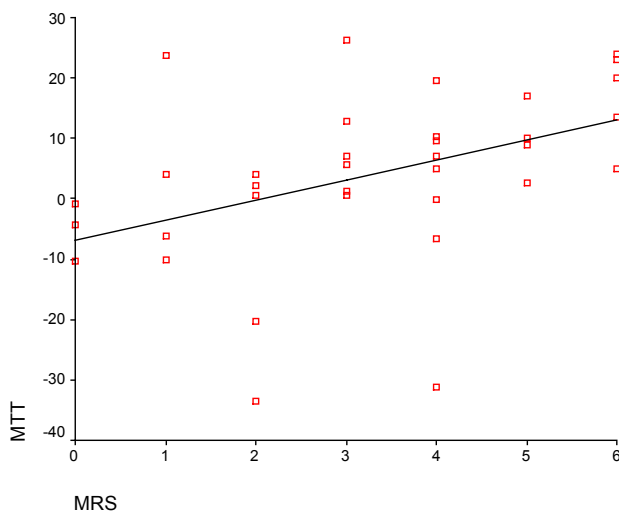


Fig. 33. On ischemic core region, the graphic relation between MTT and MRS outcome scale, ($p=.033$). Notice that the delay of MTT was related to higher MRS (worse outcome).

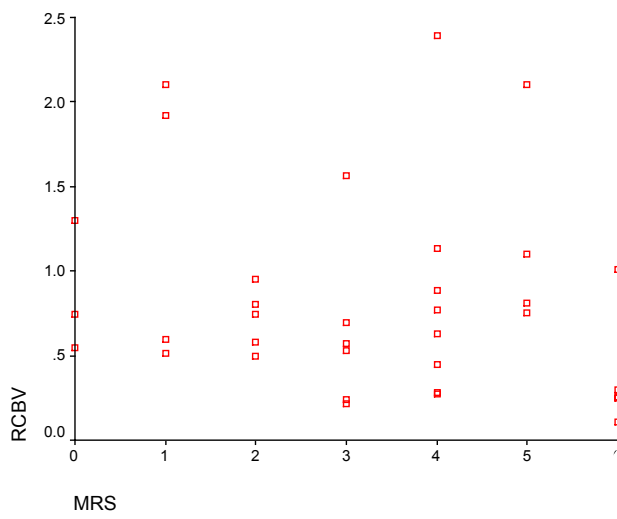


Fig. 34. On ischemic core region, the graphic relation between rCBV and MRS outcome scale, ($p=.415$).

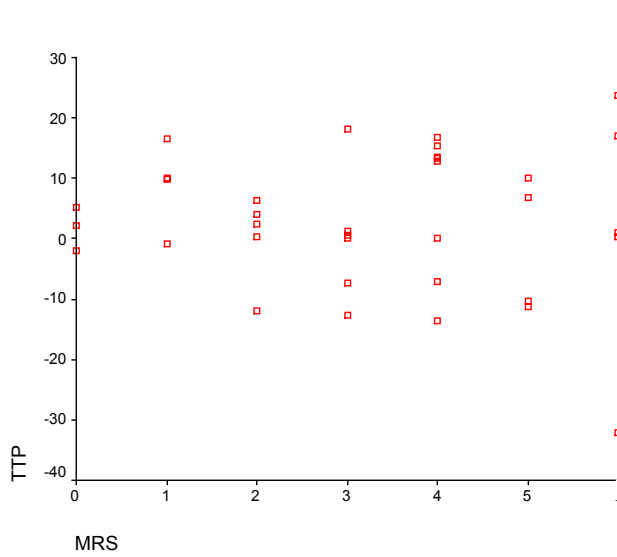


Fig. 35. On ischemic core region, the graphic relation between TTP and MRS outcome scale, ($p=.301$).

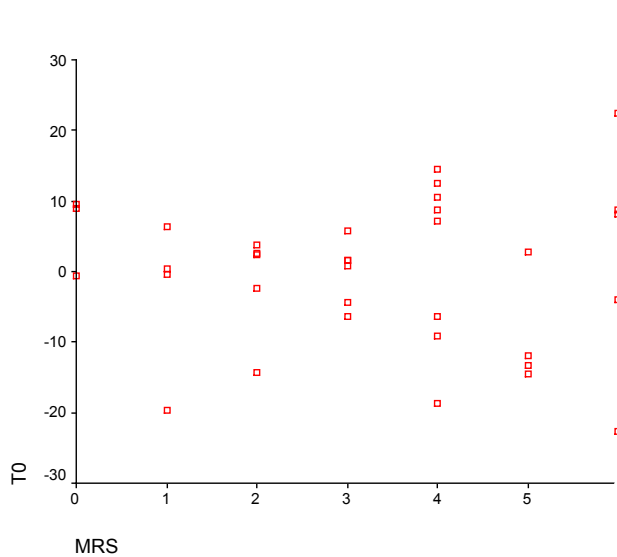


Fig. 36. On ischemic core region, the graphic relation between T0 and MRS outcome scale, ($p=.769$).

Mismatch region

rCBF was elevated in 22 patients (72%), possibly representing preserved perfusion or reperfusion establishment at the time of MRI. The rCBF value correlated significantly to MRS ($P=0.004$) (figure 37). There was a tendency that the higher the rCBF, the better the outcome. TTP was also regressed significantly with the MRS outcome scale ($p=0.006$). It showed the trend that delay of TTP might have higher MRS scale or worse outcome (figure 38). The rest of the parameters did not regress significantly with the MRS outcome scale (figure 39-41).

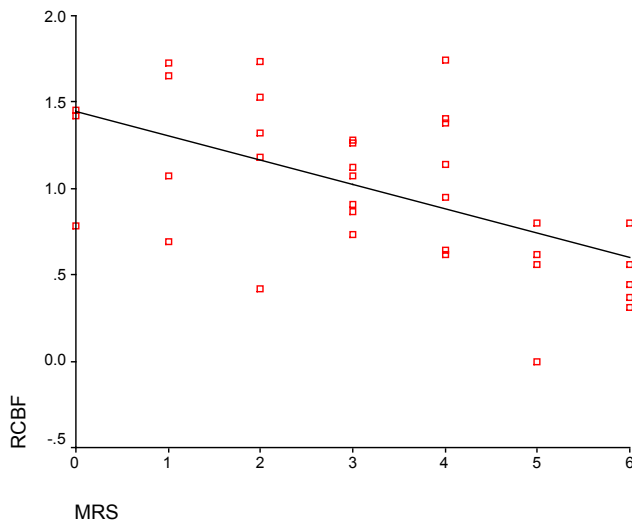


Fig. 37. The relation of rCBF with the MRS outcome scale on mismatch region. ($p=.004$). The lower rCBF correlated with worse outcome (high MRS) and the higher rCBF with better outcome (low MRS).

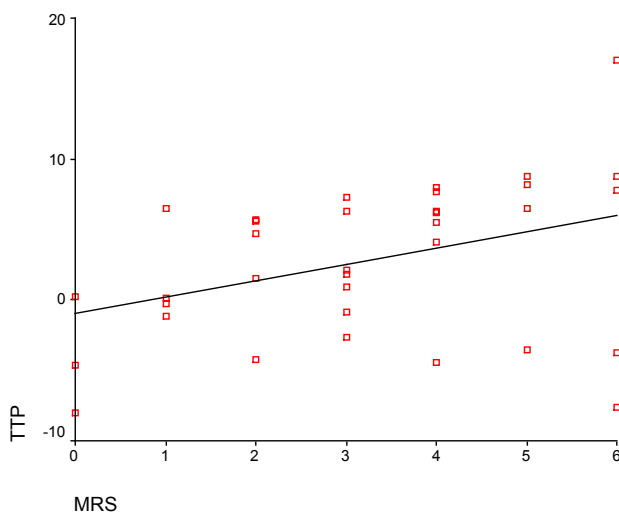


Fig. 38. The relation of TTP with the MRS outcome scale on mismatch region. ($p=.006$). The delay of TTP might have higher MRS scale or worse outcome.

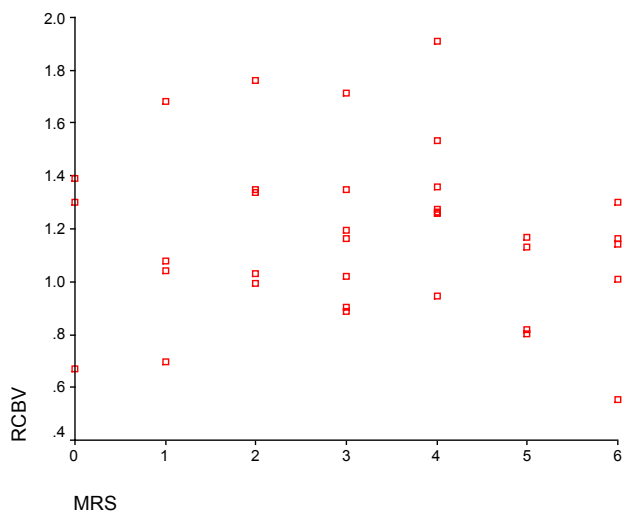


Fig. 39. In mismatch region, the graphic relation between rCBV and MRS, ($p=.539$).

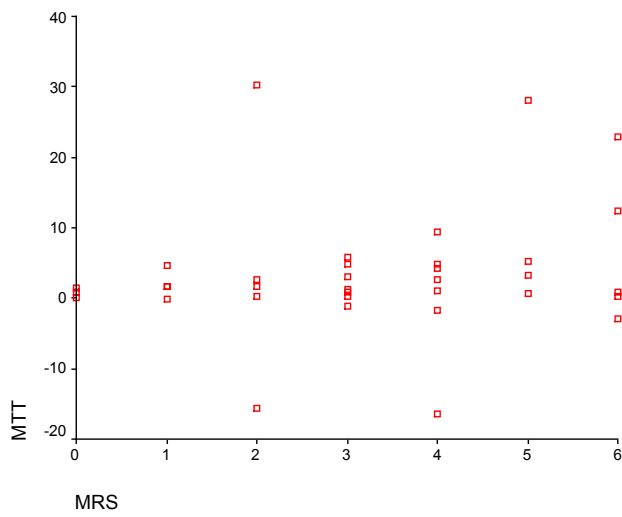


Fig. 40. In mismatch region, the graphic relation between MTT and MRS, ($p=.060$).

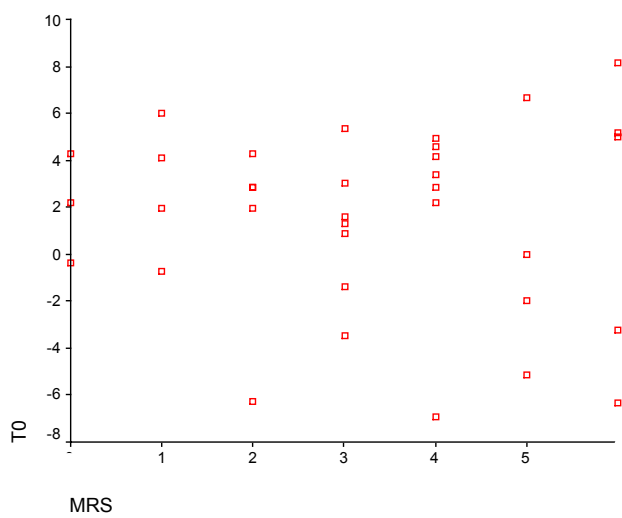


Fig. 41. In mismatch region, the graphic relation between T0 and MRS, ($p=.131$).

Table 6 provides the summary of statistic p value between hemodynamic parameters and NIHSS and MRS in both core and mismatch region.

Table 6. Summary of the statistic p value between hemodynamic parameters and NIHSS and MRS in both core and mismatch region

	core		mismatch	
	p (NIHSS)	p (MRS)	p (NIHSS)	p (MRS)
rCBV	.894	.415	.715	.539
rCBF	.122	.0003*	.556	.004*
MTT	.134	.033*	.154	.060
TTP	.147	.301	.001*	.006*
T0	.549	.769	.064	.131

*statistically significant

3.3.3 NIHSS and MRS in relation to other factors

Statistic significance was found between NIHSS and MRS ($p=0.008$). (figure 42).

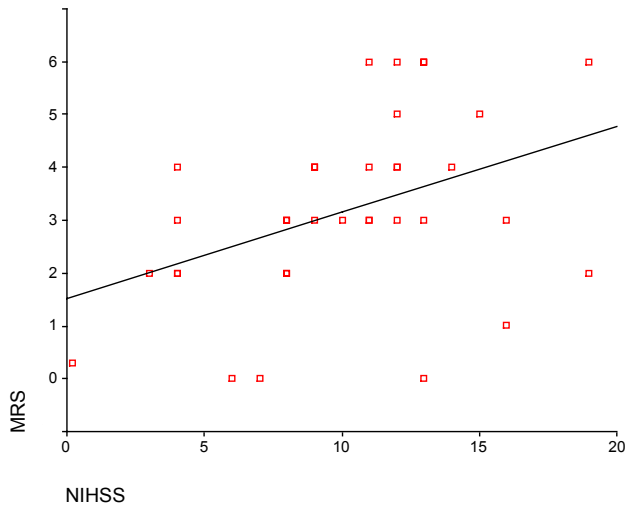


Fig. 42. Graphic demonstration of the relation between NIHSS and MRS. Statistic significance was found ($p=.008$).

No statistic significance was found between age and sex with NIHSS (figure 43-44), and between age and sex with MRS (figure 45-46).

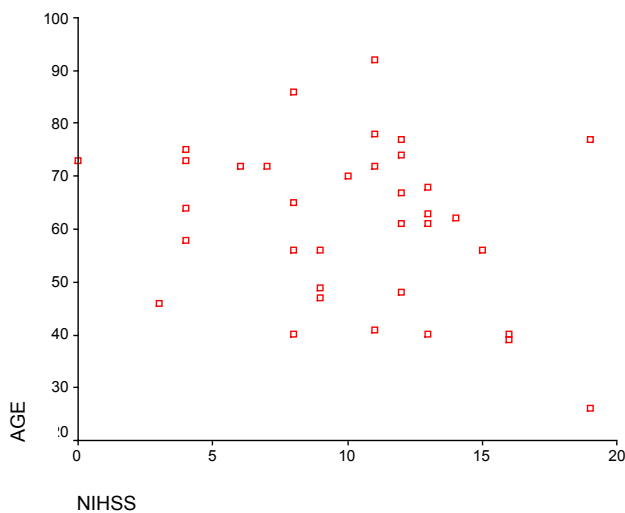


Fig. 43. Graphic relation between age and NIHSS, ($p=.112$).

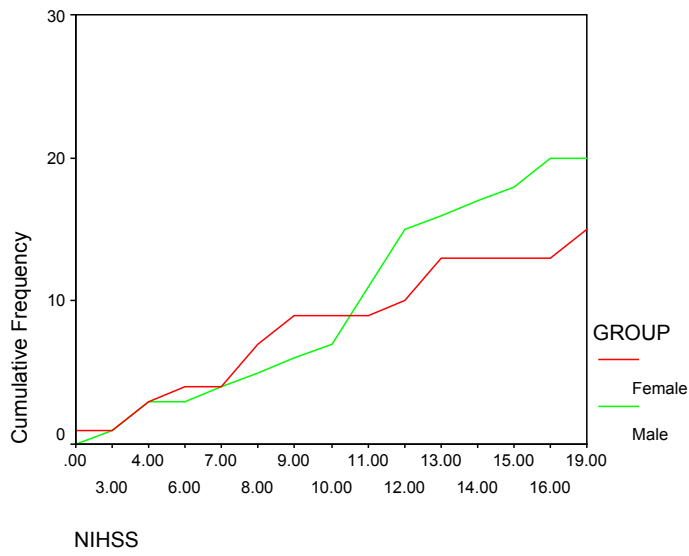


Fig. 44. Graphic relation of sex with NIHSS ($p=.568$)

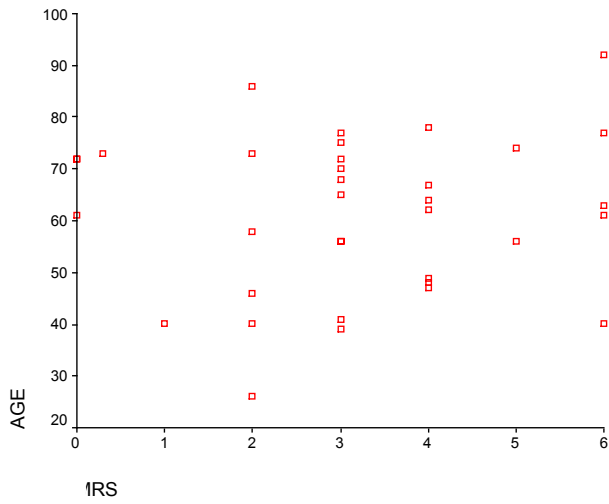


Fig. 45. Graphic relation between age and MRS, ($p=.455$)

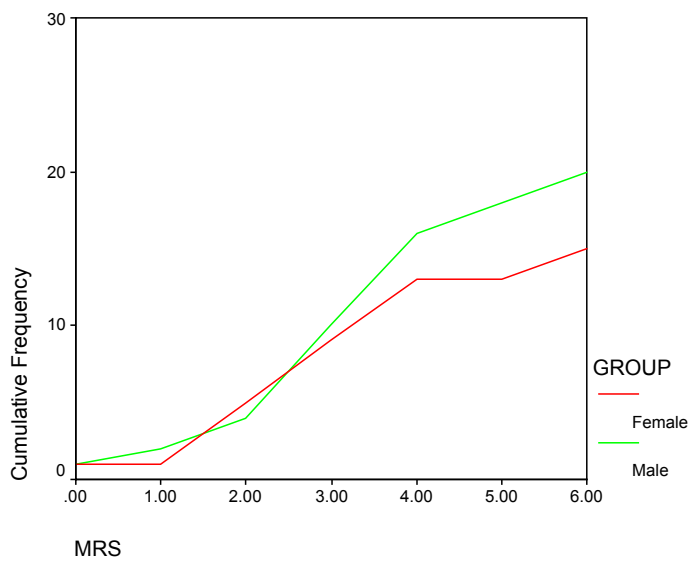


Fig. 46. Graphic relation of sex with MRS ($p=.636$).

No statistic significance was found between patency of the occluded artery at the time of MRA with NIHSS (figure 47), and with MRS (figure 48).

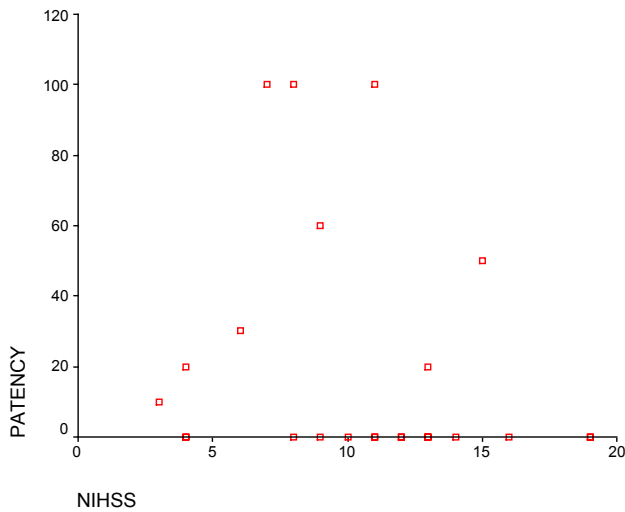


Fig. 47. Graphic relation between the percentage of patency of the occluded artery and NIHSS, ($p=.334$).

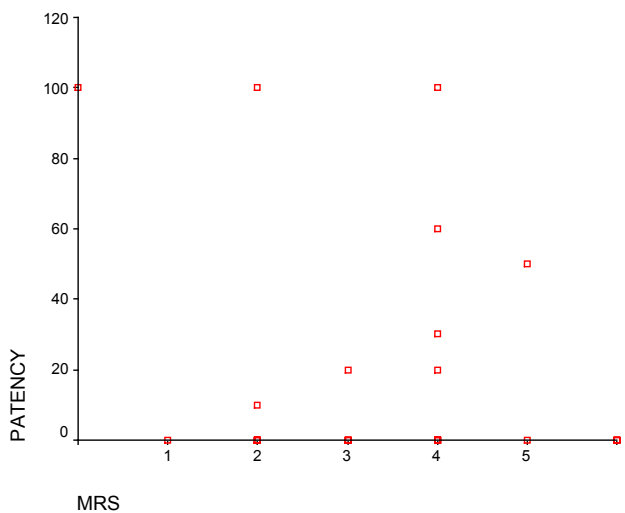


Fig. 48. Graphic relation between the percentage of patency of the occluded artery and MRS, ($p=.266$).

Between groups of volume ratio less than 1/3 and volume ratio greater than 1/3, there was no statistic difference in: age (61.83 ± 13.57 vs 57.8 ± 24.68 years) ($p=.590$); NIHSS score (10.1 ± 4.28 vs 10.6 ± 5.9) ($p=.820$) and MRS outcome scale (3.47 ± 1.57 vs 2.6 ± 0.89) ($p=.241$).

4 DISCUSSION

4.1 Finding and impact of the present study

The outcome of ischemic stroke is influenced by a variety of factors including site and size of the ischemia, and other combined factors^{81, 82}. Our intention was to evaluate the hemodynamic parameters in mismatch regions as well as in ischemia core, to find out if the parameters could be useful to predict clinical severity and outcome of acute stroke.

In the present study, data showed that rCBF value were useful in prediction of the stroke outcome. rCBF decreased in the ischemic core region in all the patients, while in the mismatch region the rCBF measurement was shown to be either decreased or increased. The decrease of rCBF in both core and mismatch region was interpreted to be due to the occlusion of the supplying artery and the reduction of perfusion before autoregulation mechanisms were able to compensate. The more the rCBF was decreased in both regions, the worse the outcome was (figure 32, 37). The interesting findings in mismatch region were that the more increase of the rCBF the better outcome would be, and vice versa. The findings of increased rCBF in the mismatch region (in 28/35 patients) might be due to either a preserved perfusion or establishment of reperfusion occurred in the tissue at risk--*penumbra*. Heiss et al.²⁸ used [¹⁵O]-H₂O PET to investigate the penumbra before and after thrombolysis in a group (12 patients), and found out that the penumbra could be preserved by reperfusion. Baird et al.⁸³ studied a group (22 patients) with ^{99m}Tc-hexamethylpropyleneamine oxime single photon emission computed tomography (SPECT), and found that those with no reperfusion after streptokinase administration had higher mortality rate, less neurological improvement and more disability than those who had reperfusion. In his later SPECT studies, Baird et al.⁸⁴ concluded that changes in cerebral tissue perfusion during the first 48 hours of ischemic stroke are significant outcome predictors. Our study added to previous researches by emphasizing the importance of quantifying the rCBF in both core and mismatch region, and especially by identifying the probable “reperfusion” in mismatch region to predict the outcome in acute stage with the tool of MR imaging.

In the acute period of a ischemic stroke, the rate of spontaneous reperfusion relevant for

induced thrombolysis appears to be less than 20%⁸⁵. Thrombolysis is more effective to occlusions caused by an embolus rather than a thrombus, although there is an exception that if the embolus is well organized as seen in rheumatic heart disease⁸⁶. It has been shown that spontaneous reperfusion is associated with better clinical outcome and smaller size of the infarction^{81, 87}. For a positive treatment decision, the reopening of the vessel (e.g.: MCA) can be detected by MRA. However, it is difficult or impossible to distinguish between a spontaneous reperfusion or embolus migration with MRA. Partial reperfusion or embolus migration is known to occur in human stroke. If a proximal thrombus causing a MCA occlusion migrates distally in the supply territory, a cortical area rescued from infarction by meningeal collateral blood supply collaterals can become infarcted when the migrated occlusion is situated distal to the collateral anastomoses. It is also known that reperfusion into the ischemically injured vessels can therefore result in blood extravasation through the damaged blood-brain barrier and cause hemorrhagic infarction. To measure the cerebral reperfusion, PET and SPECT has been well accepted as established tools^{84, 88}. Using perfusion MRI, Marks et al⁸⁹ interpreted the reperfusion as normalization on PWI on MRI in a 12 patients group, while Barber et al⁹⁰ recognized reperfusion by calculating the volume ratio according to the formula [(acute PWI-subacute PWI lesion volume)/ acute PWI lesion volume] with the idea that the PWI volume may be contracted in subacute stage than in acute stage if reperfusion established. Our study interpreted the increase of rCBF in mismatch region compared with the mirror region as reperfusion and found out that those with this reperfusion showed better outcome.

TTP was shown to be useful for prediction of both NIHSS and MRS in mismatch region in the study. The average delay of TTP was 3.2 seconds in the mismatch region on average despite a relative high standard deviation. This delay of TTP was related to severe clinical symptom and worse outcome. Neumann-Haefelin et al⁹¹ found that TTP delay correlated with European Stroke Scale (ESS). Though we used different stroke scales, the result of our study of TTP had correlation to stroke severity and was in limits matched to their study. Grandin et al⁹² studied the relation of perfusion parameters and infarct growth and found that the TTP combined with peak height had the best sensitivity (71%) and specificity (98%) to predict the

final infarct volume, which in turn was the strongest prognostic factor on stroke outcome⁹³⁻⁹⁵.

We found delay of MTT, in the ischemic core, was correlated significantly with the outcome measured with MRS. The more the MTT delay, the poorer the outcome was. However, changes of MTT in the mismatch region did not show significant correlation to NIHSS or MRS, as might have been expected. The rCBV showed no statistical significance to NIHSS or MRS in both core and mismatch region. We assume that rCBV might be influenced by compensatory mechanisms like vasoreactivity more than the other parameters discussed above. This in turn may have had an effect on parts of the patients group, resulting in an inhomogeneous correlation (figure 28 and 34). It is believed that in cerebral ischemia, MTT increases immediately after vessel occlusion^{96, 97}; parallel to the change in MTT there is a rCBV decrease, particularly in the infarction core. In small lesions, however, rCBV is not reliable⁹⁸. Furthermore, there may be an increase in rCBV in the border zone of the hypoperfused tissue related to compensatory vasodilatation⁹⁹. Because of this inhomogeneous behavior of rCBV, MTT and rCBF are considered the most important and reliable cerebrovascular parameters in acute ischemia¹⁰⁰.

The use of perfusion parameters to predict the outcome of ischemic stroke has been evaluated earlier. Barber et al⁸⁷ used ⁹⁹Tc-hexamethylpropyleneamine oxime (⁹⁹Tc-HMPAO) SPECT to examine 41 acute ischemic stroke patients, and found spontaneous reperfusion is associated with improved outcome. However, neither proportions of the perfusion nor complications such as bleeding can be determined in a single SPECT study, which makes the emergent management of acute stroke unpractical. Fiehler et al¹⁰¹, in a acute stroke patients group of 32 patients, used MRI derived CBF to predict the infarction growth and released a light for further prognostic estimation using perfusion parameters. Seidel et al¹⁰² used ultrasound perfusion imaging in a 23 patients group study, and showed bolus harmonic imaging a useful tool for analyzing cerebral perfusion deficits, and found bolus harmonic imaging data correlated with the outcome of stroke after 4 months.

The study of Warach et al¹⁰³ was the first which compared neurologic outcome with the presence or absence of DWI abnormalities in 12 patients with acute ischemia of less than 6

hours duration. DWI and PWI were found to be highly sensitive and specific in predicting persistent neurologic deficits and accurate determined outcome in 11 (91%) of 12 patients. However, no accepted stroke scales were used to quantify the severity of neurologic deficit, and stroke volumes could not be assessed because only single slice DWI and PWI images were obtained in most patients.

Other studies regarding MRI diffusion/perfusion mismatch volume with the prediction of severity of ischemic stroke were reported. Beaulieu et al⁹⁴ studied a ischemic stroke group (21 patients) and found the diffusion/perfusion mismatch volume correlated well with initial NIHSS and outcome. Uno et al¹⁰⁴ used the mismatch ratio percentage ($[(\text{initial PWI} - \text{initial DWI}) / \text{initial PWI}] \times 100$) and the rescued ratio percentage ($[(\text{initial PWI} - \text{final T2}) / \text{initial PWI}] \times 100$) for evaluation of 10 patients who received thrombolysis recanalization. He found the mismatch ratio was significantly correlated with initial NIHSS score, and the rescued ratio may be an objective indicator of the efficacy of treatment. However, these studies concentrated more on the mismatch volume rather than the perfusion parameters.

To use perfusion parameters to predict the outcome, there is a difficulty to overcome: calculation of the quantitative (or absolute) perfusion parameters. Technically, calculation of quantitative perfusion parameters requires dedicated software and some awareness of the user. On the other hand, in most clinical studies, perfusion analysis needs prompt assessment and thus only relative measurements (ratios or differences between the abnormal area and a contralateral normal area) are available. The easiest method is to calculate relative parameters on the tissue curve without any deconvolution, but this does not provide absolute or quantitative measurement of CBF and other hemodynamic parameters. However, a recent study compared relative values of six parameters (MTT, TTP, T0, CBV, Peak height, CBF index or CVF) with the corresponding quantitative value, and showed the same accuracy of both relative and absolute values to predict infarction growth⁹². Their result potentially indicated that relative value of the hemodynamic parameters may be used as absolute value equally in evaluation of ischemic stroke. According to this, we calculated the relative parameters as ratio (rCBV, rCBF) and difference (MTT, TTP and T0) between the abnormal and contralateral mirror region instead of absolute values in our study.

The advantage of relative parameter assessment is that the values are quickly and easily obtained, which is especially crucial for clinical setting when to manage a hyperacute stroke patient. The disadvantage of relative values is the difficulty to use them prospectively. They necessitate the definition of an ROI and its normal mirror ROI, but the contralateral hemisphere is not always normal, and that may bias the results. A solution for routine practice is to use small ROIs on both diseased and mirror region, but this reduces considerably the spatial resolution of the method, probably does not resolve the problem of the normality of the mirror ROI, and costs additional time⁹².

4.2 Penumbra and Mismatch

As many of the authors¹⁰⁵⁻¹⁰⁷ emphasized, the target of current neuroprotective therapy is to save the tissue at the *penumbra*, the ischemic tissue that is functionally impaired but whose damage is potentially reversible^{108, 109}. If reversible ischemic tissue is not present at the time of treatment, then neuroprotective therapy cannot be expected to be sufficient^{105, 110}.

The ischemic penumbra was defined by Astrup et al²¹ as brain tissue perfused at a level within the thresholds of functional impairment and morphologic integrity, which has the capacity to recover if perfusion is improved. Because tolerance of tissue to ischemic damage is dependent on residual flow and duration of flow disturbance¹¹¹, the ischemic penumbra is a dynamic process; it exists for a short period even in the center of ischemia, from which the conversion into irreversible necrosis propagates over time to the neighboring tissue. This also makes the time window of the various therapeutic approaches variable and ill-defined; the time interval given usually is too short for the core of ischemia and may extend to several hours in the moderately ischemic surrounding tissue. The concept of the ischemic penumbra has been developed from animal experiments. Its transfer to the clinical situation requires the definition of three critical values that can usually not be assessed easily in the acute stages of ischemic stroke: (1) the flow threshold for functional impairment—to identify functionally impaired tissue; (2) the flow threshold for morphologic damage—to identify irreversibly damaged tissue; (3) the time period a tissue tolerates flow decreased to a certain value before it becomes irreversibly damaged—to predict recovery of function with reperfusion.

In the early 1980s, PET imaging was used to define the penumbra as a mismatch between CBF and oxygen (O_2) metabolism, with oxygen metabolism relatively maintained, despite severe hypoperfusion. The penumbral signature using PET was defined by an increased oxygen extraction fraction, termed ‘misery perfusion’ by Baron et al.¹¹². Though some validated absolute thresholds for the CBF boundaries of the penumbra were reached, the notion of a specific CBF threshold is relatively meaningless if it is not integrated with temporal, therapeutic and tissue factors. With the limited availability of PET machines, radiation exposure and the necessity of catheterization constrain the use of PET as a tool for managing acute stroke patients and assessing investigational therapies⁴⁴. PET imaging, in an acute setting, was not available at our university hospital due to the reason of tracer availability at emergency condition. In contrary, the combination of PWI, DWI and MRA provides a feasible setting for acute stroke evaluation and is routinely performed in our and many other centers. Using the concept of mismatch with $PWI > DWI$, the high-intensity signal observed on DWI indicates the tissue usually destined to infarct, while the typically larger, hypoperfused region with prolonged mean transit times is regarded as the tissue at risk. The mismatch between the two images is postulated to represent the penumbra.

Recently, there have been two modifications made to the MRI-based penumbral concept. The first of these stemmed from the recognition that within the region of hypoperfused tissue, as measured using mean transit times (MTT), there are varying degrees of hypoperfusion. For example, Parsons et al⁶⁶ showed that regions of very severe hypoperfusion, with $MTT \geq 6$ s compared with the normal hemisphere, nearly always went on to infarct, whereas those with lesser degrees of hypoperfusion (MTT delay of 4-6 s) had a variable likelihood of progression to infarction. Regions with MTT delays of 2-3 s typically survived, and have been assigned as regions of benign oligoemia. More recently, Butcher et al.¹⁰⁰ showed that perfusion thresholds for infarction were time-dependent in the first 6 hours after stroke and that more severely hypoperfused tissue, usually destined to infarct, could be rescued by thrombolysis. The second modification to the original penumbral concept was the recognition that the hyperintense DWI lesion does not always go on to frank infarction.

The concept of diffusion/perfusion mismatch is facing challenge. Fiehler et al ^{113, 114} studied

the ADC maps with the infarction volume in acute stroke patients, and found that the decreased ADC at early time might normalize in stroke patients (4/15) due to reperfusion. Kidwell et al¹¹⁵ showed that a portion of the DWI core could be salvaged by intra-arterial thrombolysis. These regions are likely to correlate with less severely attenuated ADC values. This finding in human stroke replicated animal DWI studies indicating reversibility¹¹⁶. The original ischemic core volume based on DWI might not keep a constant size at different time points in acute stroke, therefore, the diffusion/perfusion mismatch might therefore overestimate the penumbra^{32, 117}.

Therefore, it seems necessary to use the concept of diffusion/perfusion mismatch with care in clinical practice. However, the importance of the predictive value as rCBF, TTP in mismatch region and rCBF and MTT in the core region could not be neglected. As a quick and feasible visual recognition of penumbra, mismatch and the hemodynamic parameters derived is informative to clinician and beneficial to stroke patients.

4.3 Other methods of neuroimaging to assess acute stroke

During the past thirty years, advances in neuroimaging technology have resulted in an imaging revolution that led to a much better understanding of cerebrovascular and tissue pathology. Advances include early and accurate detection of ischemic and infarcted tissue and also the ability to reveal hypoperfused tissue at risk. Clinicians are increasingly relying on noninvasive methods to detect embolic and atherothrombotic intravascular lesions. CT, MRI, PET ultrasound and catheter angiography, each of which plays a specific role in clinical practice and research. Since MRI was introduced previously, it will not be reviewed here.

Computed Tomography

CT images of the brain are produced by scanning a collimated beam of x-rays through the brain in thin and sequential slices. CT scanning, with its advantages of quick scanning, adaptable for emergent patients who have a pacemaker or are on a ventilator, is widely available. In addition, interpretation in the hyperacute stroke setting is fairly straightforward without the need for special training.

CT delivers two important informations to evaluation of stroke: (1) Is there intracranial hemorrhage and (2) Are there early infarct signs and what is their extent? For ischemic stroke within the first hours, CT is usually not sensitive in the identification of cerebral infarction at hyperacute stage. There are, however, some early signs of infarction such as sulcal effacement with loss of gray-white differentiation in superficial cortical infarction, hypodensity of the basal ganglia in cases of deep cerebral infarction, and hyperdense large vessel as occur in cases of MCA stroke. But these early signs of cerebral infarction have a poor conspicuity with a sensitivity that ranges between 56% and 81%¹¹⁸. Even trained observers reach only moderate interrater agreements¹¹⁹⁻¹²¹. Exclusion of hemorrhage and the early signs of ischemia are helpful for the decision upon further stroke management, especially when thrombolysis is concerned. Therefore important thrombolysis protocols as European Cooperative Acute Stroke Study (ECASS) and European and Australian Cooperative Acute Stroke Study II (ECASS II) were based on CT evaluation rather than MRI. In later

progression, the changes of ischemia become more apparent on the noncontrast CT: edema, mass effect, and if happens, hemorrhagic transformation.

The other two promising techniques are CT angiography and perfusion CT. CT angiography (CTA) is a 3-dimensional reconstruction of the cerebral vasculature from source images showing contrast material in the cerebral vessels shortly after an intravenous contrast bolus. It is a fairly sensitive technique in identifying large vessel occlusions^{122, 123}. It can be also used to track patients, who have undergone recanalization procedures, with large vessel occlusions. A normal CTA can be used to exclude patients from further aggressive recanalization procedures. However, CTA is not able to define viable ischemic tissue that is likely to benefit from recanalization. CT perfusion, like the MRI based perfusion technique, works with a rapid intravenous injection of high volume contrast and is used to construct perfusion CT images. The perfusion deficit gives an estimate of the extent of microvasculature hypoperfusion and hypometabolism. Although it is validated for cerebral infarction^{124, 125}, CT perfusion is not able to cover the entire brain and is limited to a few slices depending on the scanner used^{126, 127}. CT is much appreciated in a huge proportion of hospitals as basic stroke examination settings, since it is quick and reliable.

Positron emission tomography (PET)

In vivo measurements of metabolic rates in the brain have occupied the bulk of PET development over the last few decades. Helping to understand the biochemical basis for normal function and disease states, this in turn had vast basic research implications and some promising clinical applications. PET, mainly providing coupling between rCBF, regional cerebral metabolic rate for glucose (rCMR_{glc}), and regional cerebral metabolic rate for oxygen (rCMRO₂). In acute stage of ischemic stroke, both rCMRO₂ decrease with a compensatory rise in regional oxygen extraction ration (rOER). At the same time, rCMR_{glc} fall slightly¹²⁸. SPECT is much less expensive and much less complex than PET, while it can do many of the same investigations. In cerebral infarction, SPECT of rCBF maps show changes between rCBF and metabolic demands changes which reflect the autoregulation¹²⁹. When other methods introduced to measure physiological parameter in stroke, PET and

SPECT are always regarded as a standard¹³⁰⁻¹³⁴.

Cerebral Angiography

Cerebral angiography remains the gold standard for visualizing cerebrovascular anatomy. However, with the increasing availability and reliability of CTA and MRA, it is being used less often for purely diagnostic purposes and more often for possible interventions.

In the hyperacute stroke setting, cerebral angiography is usually performed when intra-arterial thrombolysis treatment or mechanical interventions are planned. The objective of the initial part of an angiographic evaluation in patients with ischemic stroke is to document the site of the occlusion and the presence of collateralization to the affected area. In addition to occluded vessels, abnormal vascular filling patterns, such as slow antegrade flow with prolonged contrast stasis, retrograde filling through collateral channels, arteriovenous shunting, and vascular blush secondary to luxury perfusion, also aid in the characterization of cerebral infarction¹³⁵.

Ultrasonography

Ultrasonographic investigations play an important role in identifying arterial narrowing and occlusion in the setting of cerebrovascular disease. B-mode images are built on the echo impulse principle and provide information about morphologic structures within the vascular lumen and the surrounding tissues. This mode imaging does not provide sufficient morphologic details to study deeply situated intracranial vessels. The Doppler technique can calculate blood flow velocities, and in turn arterial velocities are used to indirectly calculate the degree of stenosis in the vessel studied. Modern duplex machines combine the two techniques and are able to provide both morphologic and blood flow information¹³⁶.

In stroke, Transcranial Doppler (TCD) can demonstrate that the artery in the territory of the infarct is patent, or is early recanalised by embolus lysis, migration and fragmentation¹³⁷. To noninvasively assess extracranial and intracranial vessel status Doppler ultrasound (DU) is regarded as the most widely available tool¹³⁸, which is bedside available not only to ascertain baseline vessel status but also to monitor the process or absence of recanalization.

While it is well accepted that Doppler technique is reliable method for intracranial vessel morphology, the ultrasonic perfusion imaging using ultrasound echo contrast agents is still in an early stage. However, the potential of ultrasound perfusion technologies to compete with perfusion CT, perfusion MRI, and SPECT is evident¹³⁹. It is also thought that the widely availability and cost-effectiveness of ultrasound machines makes ultrasonic perfusion imaging techniques a supplementary perfusion techniques in acute stroke diagnosis and monitoring¹⁴⁰.

5 SUMMARY

Introduction: Stroke is the third leading cause of death, and is the leading cause of disabilities worldwide. Although stroke may result from localized cerebral ischemia, intracerebral hemorrhage, subarachnoid hemorrhage or venous sinus thrombosis, ischemic stroke is the most frequently cause of the total cases. In ischemic stroke, occlusion of the MCA or its branches accounts for more than 3/4 of infarcts and two thirds of all first strokes. The main mechanisms causing ischemic strokes are embolism and arterial thromboembolism. No matter what the mechanism an ischemic stroke is, they eventually lead to a focal reduction of perfusion in the brain.

In the hyperacute stage the recognition of the ischemia using both clinical assessment and routine neuroimaging technique implies some uncertainties, which in turn makes it difficult to predict the outcome, either to improve or to reverse spontaneously, to persist or worsen. The concept of diffusion/perfusion mismatch attracted great attention since it may represent the tissue at risk or at least an index of penumbra. Our interest was to investigate whether the hemodynamic parameters had correlation with clinical severity and if they were useful for prediction of outcome in the mismatch region. Since diffusion/perfusion mismatch was recognized as a simple and feasible means to identify the ischemic penumbra, we evaluated the hemodynamic parameters in acute stroke patients and compared these parameter to the stroke scale NIHSS and to the outcome score MRS to investigate our hypothesis.

Materials and Methods: 35 acute stroke patients (male:female=20:15, age: 61.3±15.2 years) who met the study inclusion and exclusion criteria were selected. Significant cerebrovascular risk factors were recorded in 27 patients. The NIHSS assessment was immediately performed at the patients' admission by a neurologist. Functional outcome was measured on the day of hospital discharge following MRS. Routine MRI sequences and DWI and PWI (dynamic susceptibility contrast-enhanced [DSC] imaging) were employed in our patients study. The perfusion maps were processed with MEDx® and the parameters were obtained by identifying ROIs on both ischemic core and mismatch region, and the normal mirror region. Relative values of the hemodynamic perfusion parameters were used in the evaluation.

Statistic treatment was used to test the significance of the result.

Results: The NIHSS score ranged from 0 to 19 (10.2 ± 4.4) and the outcome MRS scale ranged from 0 to 6 (mean: 3.23). Between the good outcome group (MRS 0 to 3) and the poor outcome group (MRS 4 to 6), time to scan, type of treatment, DW/PW volume ratio, and age and female/male ratio did not show significant differences.

In ischemic core: rCBF showed a remarkable decrease in all patients on average by $59.3 \pm 33.7\%$ (range: 23.2 - 97.4%). rCBV decreased in 29 patients by $41.7 \pm 23.7\%$ (range 19.6 - 55.6%), while 6 patients showed an increase of rCBV by $60.4 \pm 57.1\%$ (range 0.7 -139%). The mean rCBV change of the entire group was $26.3 \pm 52.5\%$. MTT, TTP and T0 prolonged for 4.7 (SD=15.1), 2.8 (SD=12.9) and 0.5 (SD=10.4) seconds, respectively.

In mismatch region: rCBF decreased in 15 patients by $26.2 \pm 19.9\%$ (range: 5.3-58.4%) and increased in 20 patients by $35 \pm 23.2\%$ (range: 6.8–74.4%). The change of the rCBF of the whole patients group was $5.8 \pm 38.4\%$. rCBV decreased in 7 patients by $14.7 \pm 16.5\%$ (range: 0.8-44.5%) and increased in 28 patients by $39.5 \pm 36\%$ (range: 2.2-91.1%). The mean change of the rCBV of the whole group was $19.9 \pm 31.2\%$. The mean value of MTT, TTP and T0 prolonged for 2.7 (SD=8.5), 3.2 (SD=5.2) and 1.3 (SD=4.2) seconds respectively.

In both core and mismatch region, rCBF showed statistically significant regression to MRS. The more the rCBF decreased the higher the MRS (poor outcome) was. Also, the MTT delay in the core region was significantly related to MRS. TTP delay, in both core and mismatch region, was related to both NIHSS and MRS significantly. No statistic significance was found comparing CBV and T0 in relation with NIHSS or MRS.

Conclusion: The hemodynamic parameters derived from perfusion MR imaging may be helpful adjunct to predict the outcome and severity in acute stroke patients. In mismatch region, the rCBF and TTP are predictive for the stroke outcome.

ZUSAMMENFASSUNG

Der zerebrale Schlaganfall stellt in den Industrienationen den dritthäufigste Todesursache dar, und ist die häufigste Ursache bei Behinderungen weltweit. Wenn auch zerebrale Schlaganfälle durch verschiedene Ursachen wie lokale zerebrale Ischämie, intrakranielle Blutung oder venöser Infarkierung entstehen, so ist der arterielle ischämische Schlaganfall der weitaus häufigste Grund. Von diesen Fällen sind wiederum etwa 3/4 der symptomatischen Fälle bedingt durch eine Verlegung der A. cerebri media oder ihrer Äste. Hier spielen die Embolisierung oder die Thrombose eine führende Rolle. Unabhängig von dem vorliegenden Pathomechanismus spielt die resultierende Perfusionsminderung des Parenchyms eine entscheidende Rolle.

In der Akutphase eines Schlaganfalls ist häufig trotz der klinischen Untersuchung und der üblichen bildgebenden Diagnostik nur schwer abzuschätzen, ob die Prognose entsprechend einer günstigen Form verlaufen wird, oder ob der Patient klinisch stabil bleibt oder sich sogar im Verlauf weiter verschlechtert. Das Konzept des MRT-basierten „Diffusions-Perfusions-Mismatch“ hat hier großes Interesse geweckt, da es potentiell das bereits irreversibel geschädigte Gewebe im Zentrum des Infarkts (Core) von dem noch zu rettenden Gewebe (Penumbra) unterscheiden kann. Unser Interesse war es deshalb zu untersuchen, ob die hämodynamischen Parameter des Diffusions-Perfusions-Mismatches beider Regionen zuverlässig sind für die Abschätzung der Prognose bei Patienten mit einem akuten Schlaganfall.

Methodik: Nach Anwendung der Ein- und Ausschlusskriterien der Studie wurden 35 Patienten mit einem akuten Schlaganfall selektiert. Risikofaktoren waren nachweisbar in 27/35 Patienten. Die akute Untersuchung wurde von dem aufnehmenden Neurologen durchgeführt und nach dem National Institute of Health Stroke Scale (NIHSS) bewertet. Das funktionelle Outcome wurde am Tag der Entlassung durch Anwendung des Modified Ranking Scale (MRS) dokumentiert. Die MRT -Untersuchung beinhaltete T2- und T1-gewichteten Sequenzen, Diffusions-gewichtete Sequenzen (DWI), und eine dynamische, susceptibilitäts-gewichtete Perfusionsmessung, während der eine maschinellen Bolusinjektion von 0.2 mmol/KG Gadolinium-Chelaten erfolgte. Die Nachverarbeitung dieses Datensatzes

erfolgte mittels einem kommerziell erhältlichen Programm MedX® (Sensor Systems). Die Analyse von relativen Werten erfolgte mit Regions-of-interest (ROI).

Ergebnisse: Der NIHSS Score variierte von 0 bis 19 (im Mittel 10.2 ± 4.4) und der Outcome MRS variierte zwischen 0 und 6 (im Mittel 3,2). Zwischen der Gruppe mit einem guten Outcome (MRS 0- 3) und der Gruppe mit einem schlechten Outcome (MRS 4 bis 6) gab es keine signifikanten Unterschiede bezüglich Alter, Geschlecht, Zeit von Beginn der Symptome bis zum MRT, Behandlungsprotokoll, oder Diffusion/Perfusion Volumina.

In dem ischämischen Kerngebiet (Core) war ein bemerkenswerter Abfall des rCBF zu verzeichnen ($59.3\% \pm 33.7\%$). rCBV nahm bei 29 Patienten ab (im Mittel um $41.7\% \pm 23.7\%$), während bei 6 Patienten ein Anstieg zu verzeichnen war; die mittlere Änderung des rCBV betrug $26.3\% \pm 52.5\%$. die Parameter MTT, TTP und T0 verlängerten sich im ischämischen Kerngebiet um 4.7, 2.8 und 0.5 Sekunden.

In der Zone, die ein Perfusionsdefizit aufwies, aber noch keine Diffusionsstörung (Mismatch Region) war ein Abfall von rCBF in 15 Patienten im Mittel um $26.2\% \pm 19.9\%$ und bei 20 Patienten ein Anstieg von rCBF im Mittel um $35\% \pm 23.2\%$ zu verzeichnen (Durchschnitt der Gruppe $5.8\% \pm 38.4\%$). rCBV zeigte ebenfalls ein heterogenes Verhalten mit einem Anstieg bei 7 Patienten und einem rCBV Abfall bei 28 Patienten mit einer mittlere Änderung von $19.9\% \pm 31.2\%$. Die mittleren Werte von MTT, TTP und To verlängerten sich im Mittel um 2.7, 3.2 und 1.3 Sekunden.

In beiden Zonen (Zentrum und Mismatch) Region, zeigte rCBF eine statistisch signifikante Regression zum MRS. Je geringer das regionale rCBF, desto schlechter war das Outcome. Darüber hinaus fand sich eine signifikante Korrelation von MTT- Zeitverlängerung zu einem schlechteren MRS. Eine verzögerte TTP korrelierte mit NIHSS und MRS. Dagegen konnte bezüglich der Korrelation von rCBV und T0 keine Signifikanz festgestellt werden.

Schlussfolgerung: Die hämodynamischen Parameter der Perfusions-MRT können eine gute Abschätzung der Prognose bei Patienten mit einer akuten Ischämie der MCA ermöglichen. Insbesondere rCBF und TTP zeigen eine signifikante Korrelation zum Modifed Ranking Scale bei Entlassung.

6 ABBREVIATIONS

ACA anterior cerebral artery
ADC apparent diffusion coefficient
AIF Arterial input function
CBF cerebral blood flow
CBV cerebral blood volume
CT computed tomography
CTA computed tomography angiography
DU Doppler ultrasound
DWI diffusion weighted imaging
EPI Echo-planar imaging
FLAIR fast-fluid-attenuated inversion recovery
FOV field of view
ICA internal carotid artery
MCA middle cerebral artery
MRA magnetic resonance angiography
MRI magnetic resonance imaging
MRS Modified Rankin Scale
MTT mean transit time
NIHSS National Institute of Health Stroke Scale
PCA Posterior cerebral artery
PET Positron emission tomography
PWI perfusion weighted imaging
rCBF relative cerebral blood flow
rCBV relative cerebral blood volume
rrCBV relative regional cerebral blood volume
rCMR_{glc} regional cerebral metabolic rate for glucose
rCMR_{O₂} regional cerebral metabolic rate for oxygen
RF radiofrequency

ROI Regions of interest

SD standard deviation

SPECT Single Photon Emission Computed Tomography

T1WI T1 weighted imaging

T2WI T2 weighted imaging

TCD Transcranial Doppler

TE Echo Time

TR Repetition Time

TTP time to peak

7 APPENDIX

Appendix 1

NIH STROKE SCALE

The NINDS t-PA Stroke Trial No. _____

FORM 5

Pt. Date of Birth ____/____/____

1 of 4

Hospital _____ (____-____)

Date of Exam ____/____/____

Interval: 1[] Baseline 2[] 2 hours post treatment 3[] 24 hours post onset of symptoms \pm 20 minutes 4[] 7-10 days
5[] 3 months 6[] Other _____ (____)

Time: _____:_____ 1[]am 2[]pm

Administer stroke scale items in the order listed. Record performance in each category after each subscale exam. Do not go back and change scores. Follow directions provided for each exam technique. Scores should reflect what the patient does, not what the clinician thinks the patient can do. The clinician should record answers while administering the exam and work quickly. Except where indicated, the patient should not be coached (i.e., repeated requests to patient to make a special effort).

IF ANY ITEM IS LEFT UNTESTED, A DETAILED EXPLANATION MUST BE CLEARLY WRITTEN ON THE FORM. ALL UNTESTED ITEMS WILL BE REVIEWED BY THE MEDICAL MONITOR, AND DISCUSSED WITH THE EXAMINER BY TELEPHONE.

Instructions	Scale Definition	Score
<p>1a. Level of Consciousness: The investigator must choose a response, even if a full evaluation is prevented by such obstacles as an endotracheal tube, language barrier, orotracheal trauma/bandages. A 3 is scored only if the patient makes no movement (other than reflexive posturing) in response to noxious stimulation.</p>	<p>0 = Alert; keenly responsive. 1 = Not alert, but arousable by minor stimulation to obey, answer, or respond. 2 = Not alert, requires repeated stimulation to attend, or is obtunded and requires strong or painful stimulation to make movements (not stereotyped). 3 = Responds only with reflex motor or autonomic effects or totally unresponsive, flaccid, areflexic.</p>	_____
<p>1b. LOC Questions: The patient is asked the month and his/her age. The answer must be correct - there is no partial credit for being close. Aphasic and stuporous patients who do not comprehend the questions will score 2. Patients unable to speak because of endotracheal intubation, orotracheal trauma, severe dysarthria from any cause, language barrier or any other problem not secondary to aphasia are given a 1. It is important that only the initial answer be graded and that the examiner not "help" the patient with verbal or non-verbal cues.</p>	<p>0 = Answers both questions correctly. 1 = Answers one question correctly. 2 = Answers neither question correctly.</p>	_____
<p>1c. LOC Commands: The patient is asked to open and close the eyes and then to grip and release the non-paretic hand. Substitute another one step command if the hands cannot be used. Credit is given if an unequivocal attempt is made but not completed due to weakness. If the patient does not respond to command, the task should be demonstrated to them (pantomime) and score the result (i.e., follows none, one or two commands). Patients with trauma, amputation, or other physical impediments should be given suitable one-step commands. Only the first attempt is scored.</p>	<p>0 = Performs both tasks correctly 1 = Performs one task correctly 2 = Performs neither task correctly</p>	_____
<p>2. Best Gaze: Only horizontal eye movements will be tested. Voluntary or reflexive (oculocephalic) eye movements will be scored but caloric testing is not done. If the patient has a conjugate deviation of the eyes that can be overcome by voluntary or reflexive activity, the score will be 1. If a patient has an isolated peripheral nerve paresis (CN III, IV or VI) score a 1. Gaze is testable in all aphasic patients. Patients with ocular trauma, bandages, pre-existing blindness or other disorder of visual acuity or fields should be tested with reflexive movements and a choice made by the investigator. Establishing eye contact and then moving about the patient from side to side will occasionally clarify the presence of a partial gaze palsy.</p>	<p>0 = Normal 1 = Partial gaze palsy. This score is given when gaze is abnormal in one or both eyes, but where forced deviation or total gaze paresis are not present. 2 = Forced deviation, or total gaze paresis not overcome by the oculocephalic maneuver.</p>	_____

NIH STROKE SCALE

The NINDS t-PA Stroke Trial No. _____

FORM 5

Pt. Date of Birth ____/____/____

2 of 4

Hospital _____ (____-____)

Date of Exam ____/____/____

Interval: 1[] Baseline 2[] 2 hours post treatment 3[] 24 hours post onset of symptoms ±20 minutes 4[] 7-10 days
 5[] 3 months 6[] Other _____ (_____)

<p>3. Visual: Visual fields (upper and lower quadrants) are tested by confrontation, using finger counting or visual threat as appropriate. Patient must be encouraged, but if they look at the side of the moving fingers appropriately, this can be scored as normal. If there is unilateral blindness or enucleation, visual fields in the remaining eye are scored. Score 1 only if a clear-cut asymmetry, including quadrantanopia is found. If patient is blind from any cause score 3. Double simultaneous stimulation is performed at this point. If there is extinction patient receives a 1 and the results are used to answer question 11.</p>	<p>0 = No visual loss 1 = Partial hemianopia 2 = Complete hemianopia 3 = Bilateral hemianopia (blind including cortical blindness)</p>	<p>_____</p>
<p>4. Facial Palsy: Ask, or use pantomime to encourage the patient to show teeth or raise eyebrows and close eyes. Score symmetry of grimace in response to noxious stimuli in the poorly responsive or non-comprehending patient. If facial trauma/bandages, orotracheal tube, tape or other physical barrier obscures the face, these should be removed to the extent possible.</p>	<p>0 = Normal symmetrical movement 1 = Minor paralysis (flattened nasolabial fold, asymmetry on smiling) 2 = Partial paralysis (total or near total paralysis of lower face) 3 = Complete paralysis of one or both sides (absence of facial movement in the upper and lower face)</p>	<p>_____</p>
<p>5 & 6. Motor Arm and Leg: The limb is placed in the appropriate position: extend the arms (palms down) 90 degrees (if sitting) or 45 degrees (if supine) and the leg 30 degrees (always tested supine). Drift is scored if the arm falls before 10 seconds or the leg before 5 seconds. The aphasic patient is encouraged using urgency in the voice and pantomime but not noxious stimulation. Each limb is tested in turn, beginning with the non-paretic arm. Only in the case of amputation or joint fusion at the shoulder or hip may the score be "9" and the examiner must clearly write the explanation for scoring as a "9".</p>	<p>0 = No drift, limb holds 90 (or 45) degrees for full 10 seconds. 1 = Drift, Limb holds 90 (or 45) degrees, but drifts down before full 10 seconds; does not hit bed or other support. 2 = Some effort against gravity, limb cannot get to or maintain (if cued) 90 (or 45) degrees, drifts down to bed, but has some effort against gravity. 3 = No effort against gravity, limb falls. 4 = No movement 9 = Amputation, joint fusion explain: _____</p> <p>5a. Left Arm 5b. Right Arm</p>	<p>_____ _____</p>
	<p>0 = No drift, leg holds 30 degrees position for full 5 seconds. 1 = Drift, leg falls by the end of the 5 second period but does not hit bed. 2 = Some effort against gravity, leg falls to bed by 5 seconds, but has some effort against gravity. 3 = No effort against gravity, leg falls to bed immediately. 4 = No movement 9 = Amputation, joint fusion explain: _____</p> <p>6a. Left Leg 6b. Right Leg</p>	<p>_____ _____</p>

NIH STROKE SCALE

The NINDS t-PA Stroke Trial No. _____

FORM 5

Pt. Date of Birth ____/____/____

3 of 4

Hospital _____ (____-____)

Date of Exam ____/____/____

Interval: 1[] Baseline 2[] 2 hours post treatment 3[] 24 hours post onset of symptoms \pm 20 minutes 4[] 7-10 days
5[] 3 months 6[] Other _____ (____)

<p>7. Limb Ataxia: This item is aimed at finding evidence of a unilateral cerebellar lesion. Test with eyes open. In case of visual defect, insure testing is done in intact visual field. The finger-nose-finger and heel-shin tests are performed on both sides, and ataxia is scored only if present out of proportion to weakness. Ataxia is absent in the patient who cannot understand or is paralyzed. Only in the case of amputation or joint fusion may the item be scored "9", and the examiner must clearly write the explanation for not scoring. In case of blindness test by touching nose from extended arm position.</p>	<p>0 = Absent 1 = Present in one limb 2 = Present in two limbs</p> <p>If present, is ataxia in Right arm 1 = Yes 2 = No 9 = amputation or joint fusion, explain _____ Left arm 1 = Yes 2 = No 9 = amputation or joint fusion, explain _____ Right leg 1 = Yes 2 = No 9 = amputation or joint fusion, explain _____ Left leg 1 = Yes 2 = No 9 = amputation or joint fusion, explain _____</p>	<p>-----</p>
<p>8. Sensory: Sensation or grimace to pin prick when tested, or withdrawal from noxious stimulus in the obtunded or aphasic patient. Only sensory loss attributed to stroke is scored as abnormal and the examiner should test as many body areas [arms (not hands), legs, trunk, face] as needed to accurately check for hemisensory loss. A score of 2, "severe or total," should only be given when a severe or total loss of sensation can be clearly demonstrated. Stuporous and aphasic patients will therefore probably score 1 or 0. The patient with brain stem stroke who has bilateral loss of sensation is scored 2. If the patient does not respond and is quadriplegic score 2. Patients in coma (item 1a=3) are arbitrarily given a 2 on this item.</p>	<p>0 = Normal; no sensory loss.</p> <p>1 = Mild to moderate sensory loss; patient feels pinprick is less sharp or is dull on the affected side, or there is a loss of superficial pain with pinprick but patient is aware he/she is being touched.</p> <p>2 = Severe to total sensory loss; patient is not aware of being touched in the face, arm, and leg.</p>	<p>-----</p>
<p>9. Best Language: A great deal of information about comprehension will be obtained during the preceding sections of the examination. The patient is asked to describe what is happening in the attached picture, to name the items on the attached naming sheet, and to read from the attached list of sentences. Comprehension is judged from responses here as well as to all of the commands in the preceding general neurological exam. If visual loss interferes with the tests, ask the patient to identify objects placed in the hand, repeat, and produce speech. The intubated patient should be asked to write. The patient in coma (question 1a=3) will arbitrarily score 3 on this item. The examiner must choose a score in the patient with stupor or limited cooperation but a score of 3 should be used only if the patient is mute and follows no one step commands.</p>	<p>0 = No aphasia, normal</p> <p>1 = Mild to moderate aphasia; some obvious loss of fluency or facility of comprehension, without significant limitation on ideas expressed or form of expression. Reduction of speech and/or comprehension, however, makes conversation about provided material difficult or impossible. For example in conversation about provided materials examiner can identify picture or naming card from patient's response.</p> <p>2 = Severe aphasia; all communication is through fragmentary expression; great need for inference, questioning, and guessing by the listener. Range of information that can be exchanged is limited; listener carries burden of communication. Examiner cannot identify materials provided from patient response.</p> <p>3 = Mute, global aphasia; no usable speech or auditory comprehension.</p>	<p>-----</p>
<p>10. Dysarthria: If patient is thought to be normal an adequate sample of speech must be obtained by asking patient to read or repeat words from the attached list. If the patient has severe aphasia, the clarity of articulation of spontaneous speech can be rated. Only if the patient is intubated or has other physical barrier to producing speech, may the item be scored "9", and the examiner must clearly write an explanation for not scoring. Do not tell the patient why he/she is being tested.</p>	<p>0 = Normal 1 = Mild to moderate; patient slurs at least some words and, at worst, can be understood with some difficulty. 2 = Severe; patient's speech is so slurred as to be unintelligible in the absence of or out of proportion to any dysphasia, or is mute/anarthric. 9 = Intubated or other physical barrier, explain _____</p>	<p>-----</p>

NIH STROKE SCALE

The NINDS t-PA Stroke Trial No. _____

FORM 5

Pt. Date of Birth ____/____/____

4 of 4

Hospital _____ (____-____)

Date of Exam ____/____/____

Interval: 1[] Baseline 2[] 2 hours post treatment 3[] 24 hours post onset of symptoms \pm 20 minutes 4[] 7-10 days
 5[] 3 months 6[] Other _____ (_____)

<p>11. Extinction and Inattention (formerly Neglect): Sufficient information to identify neglect may be obtained during the prior testing. If the patient has a severe visual loss preventing visual double simultaneous stimulation, and the cutaneous stimuli are normal, the score is normal. If the patient has aphasia but does appear to attend to both sides, the score is normal. The presence of visual spatial neglect or anosagnosia may also be taken as evidence of abnormality. Since the abnormality is scored only if present, the item is never untestable.</p>	<p>0 = No abnormality.</p> <p>1 = Visual, tactile, auditory, spatial, or personal inattention or extinction to bilateral simultaneous stimulation in one of the sensory modalities.</p> <p>2 = Profound hemi-inattention or hemi-inattention to more than one modality. Does not recognize own hand or orients to only one side of space.</p>	<p>_____</p>
---	---	--------------

Additional item, not a part of the NIH Stroke Scale score.

<p>A. Distal Motor Function: The patient's hand is held up at the forearm by the examiner and patient is asked to extend his/her fingers as much as possible. If the patient can't or doesn't extend the fingers the examiner places the fingers in full extension and observes for any flexion movement for 5 seconds. The patient's first attempts only are graded. Repetition of the instructions or of the testing is prohibited.</p>	<p>0 = Normal (No flexion after 5 seconds)</p> <p>1 = At least some extension after 5 seconds, but not fully extended. Any movement of the fingers which is not command is not scored.</p> <p>2 = No voluntary extension after 5 seconds. Movements of the fingers at another time are not scored.</p> <p>a. Left Arm</p> <p>b. Right Arm</p>	<p>_____</p> <p>_____</p>
--	---	---------------------------

12. _____ (____-____)
 Person Administering Scale Code

8 REFERENCES

1. Hatano S. Experience from a multi centre stroke register: a preliminary report. *Bull World Health Organ* 1976;54:541-3.
2. Asplund K, Tuomilehto J, Stegmayr B, et al. Diagnostic criteria and quality control of the registration of stroke events in the MONICA project. *Acta Med Scand Suppl* 1988;728:26-39.:26-39.
3. Nakano KK. An overview of stroke. Epidemiology, classification, risk factors, clinical aspects. *Postgrad Med* 1986 Sep 15;80(4):82-7.
4. Ingall T. Stroke--incidence, mortality, morbidity and risk. *J Insur Med* 2004;36(2):143-52.
5. Gorelick PB. Epidemiology and trials. In: Caplan LR, editor. *Brain ischemia: basic concepts and clinical relevance*. 1st ed. Springer-Verlag; 1995. p. 343-53.
6. World Health Organization. STEPwise approach to stroke surveillance. http://www.who.int/ncd_surveillance/steps/stroke/en/2004.
7. World Health Organization. *The World Health Report 1998*. Geneva: WHO 1998.
8. Truelsen T, Bonita R, Jamrozik K. Surveillance of stroke: a global perspective. *Int J Epidemiol* 2001 Oct;30 Suppl 1:S11-6.:S11-S16.
9. Wolf PA, Kannel WB, McGee DL. Epidemiology of stroke in the north America. In: Barnett HJM, Stein BM, Mohr JP, et al., editors. *Stroke: pathophysiology, diagnosis and management*. 1st ed. New York: Churchill Livingstone; 1986. p. 19-29.
10. Liu L, Ikeda K, Yamori Y. Changes in stroke mortality rates for 1950 to 1997: a great slowdown of decline trend in Japan. *Stroke* 2001 Aug;32(8):1745-9.
11. Peeters A, Bonneux L, Barendregt JJ, et al. Improvements in treatment of coronary heart disease and cessation of stroke mortality rate decline. *Stroke* 2003 Jul;34(7):1610-4.
12. Klag MJ, Whelton PK, Seidler AJ. Decline in US stroke mortality. Demographic trends and antihypertensive treatment. *Stroke* 1989 Jan;20(1):14-21.
13. Broderick JP, Phillips SJ, Whisnant JP, et al. Incidence rates of stroke in the eighties: the end of the decline in stroke? *Stroke* 1989 May;20(5):577-82.
14. Brown RD, Whisnant JP, Sicks JD, et al. Stroke incidence, prevalence, and survival: secular trends in Rochester, Minnesota, through 1989. *Stroke* 1996 Mar;27(3):373-80.
15. Kent Gledhill, Kevin R.Moore, John M.Jacobs, et al. Cerebrovascular disease. In: William W.Orrison J, editor. *Neuroimaging*. 1st ed. W.B. Saunders Company; 2000. p. 719-65.
16. Michael P.Marks. Cerebral ischemia and infarction. In: Scott W.Atlas, editor. *Magnetic Resonance*

- Imaging of the Brain and spine. 3 ed. Lippincott Williams & Wilkins; 2002. p. 919-79.
17. Hans-Joachim Kretschmann, Wolfgang Weinrich. Klinische Neuroanatomie und kraniele Bilddiagnostik Computertomographie und Magnetresonanztomographie. 2nd ed. Georg Thieme Verlag Stuttgart New York; 1991.
 18. Barnett H, Mohr JP, Stein B, et al. In: Barnett H, editor. Stroke: Pathophysiology, Diagnosis and Management. 2nd ed. Churchill Livingstone; 1992. p. 360-405.
 19. Hacke W, Hennerici M, Gelmers HJ. Epidemiology and Classification of Strokes. Cerebral Ischemia. Springer-Verlag; 1991.
 20. Heiss W.D., Fink G.R., Huber M, et al. Uncoupling of flow and metabolism in early ischemic stroke. In: Hartmann A, Yatsu F, Kuschinsky W, editors. Cerebral ischemia and basic mechanisms. Springer-Verlag; 1994. p. 9-18.
 21. Astrup J, Siesjo BK, Symon L. Thresholds in cerebral ischemia - the ischemic penumbra. Stroke 1981 Nov;12(6):723-5.
 22. Jones TH, Morawetz RB, Crowell RM, et al. Thresholds of focal cerebral ischemia in awake monkeys. J Neurosurg 1981 Jun;54(6):773-82.
 23. Heiss WD, Graf R. The ischemic penumbra. Curr Opin Neurol 1994 Feb;7(1):11-9.
 24. Lassen NA. Pathophysiology of brain ischemia as it relates to the therapy of acute ischemic stroke. Clin Neuropharmacol 1990;13 Suppl 3:S1-8.:S1-S8.
 25. Marchal G, Beaudouin V, Rioux P, et al. Prolonged persistence of substantial volumes of potentially viable brain tissue after stroke: a correlative PET-CT study with voxel-based data analysis. Stroke 1996 Apr;27(4):599-606.
 26. Marchal G, Benali K, Iglesias S, et al. Voxel-based mapping of irreversible ischaemic damage with PET in acute stroke. Brain 1999 Dec;122(Pt 12):2387-400.
 27. Furlan M, Marchal G, Viader F, et al. Spontaneous neurological recovery after stroke and the fate of the ischemic penumbra. Ann Neurol 1996 Aug;40(2):216-26.
 28. Heiss WD, Grond M, Thiel A, et al. Tissue at risk of infarction rescued by early reperfusion: a positron emission tomography study in systemic recombinant tissue plasminogen activator thrombolysis of acute stroke. J Cereb Blood Flow Metab 1998 Dec;18(12):1298-307.
 29. Heiss WD, Thiel A, Grond M, et al. Which targets are relevant for therapy of acute ischemic stroke? Stroke 1999 Jul;30(7):1486-9.
 30. Davis SM, Donnan GA. Advances in Penumbra Imaging with MR. Cerebrovasc Dis 2004;17 Suppl 3:23-7.:23-7.
 31. Baird AE, Warach S. Magnetic resonance imaging of acute stroke. J Cereb Blood Flow Metab 1998

- Jun;18(6):583-609.
32. Kidwell CS, Alger JR, Saver JL. Beyond mismatch: evolving paradigms in imaging the ischemic penumbra with multimodal magnetic resonance imaging. *Stroke* 2003 Nov;34(11):2729-35.
 33. Toni D, Chamorro A, Kaste M, et al. Acute treatment of ischaemic stroke. European Stroke Initiative. *Cerebrovasc Dis* 2004;17 Suppl 2:30-46.:30-46.
 34. Hack W, Kaste M, Bogousslavsky J, et al. European Stroke Initiative Recommendations for Stroke Management-update 2003. *Cerebrovasc Dis* 2003;16(4):311-37.
 35. Lee RG, Hill TC, Holman BL, et al. Predictive value of perfusion defect size using N-isopropyl-(I-123)-p-iodoamphetamine emission tomography in acute stroke. *J Neurosurg* 1984 Sep;61(3):449-52.
 36. Chambers BR, Norris JW, Shurvell BL, et al. Prognosis of acute stroke. *Neurology* 1987 Feb;37(2):221-5.
 37. Adams HP, Jr., Davis PH, Leira EC, et al. Baseline NIH Stroke Scale score strongly predicts outcome after stroke: A report of the Trial of Org 10172 in Acute Stroke Treatment (TOAST). *Neurology* 1999 Jul 13;53(1):126-31.
 38. Schwamm LH, Koroshetz WJ, Sorensen AG, et al. Time course of lesion development in patients with acute stroke: serial diffusion- and hemodynamic-weighted magnetic resonance imaging. *Stroke* 1998 Nov;29(11):2268-76.
 39. Baird AE, Dambrosia J, Janket S, et al. A three-item scale for the early prediction of stroke recovery. *Lancet* 2001 Jun 30;357(9274):2095-9.
 40. Rosen BR, Belliveau JW, Chien D. Perfusion imaging by nuclear magnetic resonance. *Magn Reson Med* 1989;5:263-81.
 41. Yoshiura T, Wu O, Sorensen AG. Advanced MR techniques: diffusion MR imaging, perfusion MR imaging, and spectroscopy. *Neuroimaging Clin N Am* 1999 Aug;9(3):439-53.
 42. Baird AE, Benfield A, Schlaug G, et al. Enlargement of human cerebral ischemic lesion volumes measured by diffusion-weighted magnetic resonance imaging. *Ann Neurol* 1997 May;41(5):581-9.
 43. Rordorf G, Koroshetz WJ, Copen WA, et al. Regional ischemia and ischemic injury in patients with acute middle cerebral artery stroke as defined by early diffusion-weighted and perfusion-weighted MRI. *Stroke* 1998 May;29(5):939-43.
 44. Warach S. Measurement of the ischemic penumbra with MRI: it's about time. *Stroke* 2003 Oct;34(10):2533-4.
 45. Kluytmans M, van Everdingen KJ, Kappelle LJ, et al. Prognostic value of perfusion- and diffusion-weighted MR imaging in first 3 days of stroke. *Eur Radiol* 2000;10(9):1434-41.
 46. Wu RH, Bruening R, Berchtenbreiter C, et al. MRI assessment of cerebral blood volume in patients

- with brain infarcts. *Neuroradiology* 1998 Aug;40(8):496-502.
47. Smith AM, Grandin CB, Duprez T, et al. Whole brain quantitative CBF, CBV, and MTT measurements using MRI bolus tracking: implementation and application to data acquired from hyperacute stroke patients. *J Magn Reson Imaging* 2000 Sep;12(3):400-10.
 48. Schaefer PW, Ozsunar Y, He J, et al. Assessing tissue viability with MR diffusion and perfusion imaging. *AJNR Am J Neuroradiol* 2003 Mar;24(3):436-43.
 49. Brott T, Adams HP, Jr., Olinger CP, et al. Measurements of acute cerebral infarction: a clinical examination scale. *Stroke* 1989 Jul;20(7):864-70.
 50. the Internet Stroke Center. NIH Stroke Scale (NIHSS). 2004.
Ref Type: Internet Communication
 51. Rankin J. Cerebral vascular accidents in patients over the age of 60. *Scott Med* 1957;2:200-15.
 52. Bonita R, Beaglehole R. Modification of Rankin Scale: Recovery of motor function after stroke. *Stroke* 1988 Dec;19(12):1497-500.
 53. Roberts TP, Rowley HA. Diffusion weighted magnetic resonance imaging in stroke. *Eur J Radiol* 2003 Mar;45(3):185-94.
 54. Moseley ME, Kucharczyk J, Mintorovitch J, et al. Diffusion-weighted MR imaging of acute stroke: correlation with T2-weighted and magnetic susceptibilityenhanced MR imaging in cats. *AJNR, Am J Neuroradiol* 1990;11:423-9.
 55. Roether J, de Crespigny AJ, D'Arceuil H, et al. MR detection of cortical spreading depression immediately after focal ischemia in the rat. *J Cereb Blood Flow Metab* 1996;16(2):214-20.
 56. Stejskal EO, Tanner JE. Spin diffusion measurements: spin echoes in the presence of a time-dependent field gradient. *J Chem Phys* 1965;42:288-92.
 57. Davis D, Ulatowski J, Eleff S, et al. Rapid monitoring of changes in water diffusion coefficients during reversible ischemia in cat and rat brain. *Magn Reson Med* 1994;31:454-60.
 58. Le Bihan D. Molecular diffusion nuclear magnetic resonance imaging. *Magn Reson* 1991;7:1-30.
 59. S.Heiland. Diffusion- and Perfusion-Weighted MR Imaging in Acute Stroke: Principles, Methods, and Applications. *IMAGING DECISIONS* 2003;4:4-12.
 60. Bruning R, Wu RH, Deimling M, et al. Diffusion measurements in the ischemic human brain with a steady-state sequence. *Invest Radiol* 1996 Nov;31(11):709-15.
 61. Burdette JH, Elster AD, Ricci PE. Acute cerebral infarction: quantification of spin-density and T2 shine-through phenomena on diffusion-weighted MR images. *Radiology* 1999 Aug;212(2):333-9.
 62. Gonzalez RG, Schaefer PW, Buonanno FS, et al. Diffusion-weighted MR imaging: diagnostic accuracy in patients imaged within 6 hours of stroke symptom onset. *Radiology* 1999 Jan;210(1):155-62.

63. Marks MP, de Crespigny A, Lentz D, et al. Acute and chronic stroke: navigated spin-echo diffusion-weighted MR imaging. *Radiology* 1996 May;199(2):403-8.
64. Lovblad KO, Laubach HJ, Baird AE, et al. Clinical experience with diffusion-weighted MR in patients with acute stroke. *AJNR Am J Neuroradiol* 1998 Jun;19(6):1061-6.
65. Le Bihan D, Douek P, Argyropoulou M, et al. Diffusion and perfusion magnetic resonance imaging in brain tumors. *Top Magn Reson Imaging* 1993;5(1):25-31.
66. Parsons MW, Yang Q, Barber PA, et al. Perfusion magnetic resonance imaging maps in hyperacute stroke: relative cerebral blood flow most accurately identifies tissue destined to infarct. *Stroke* 2001 Jul;32(7):1581-7.
67. Schaefer PW, Romero JM, Grant PE, et al. Perfusion magnetic resonance imaging of acute ischemic stroke. *Semin Roentgenol* 2002 Jul;37(3):230-6.
68. Hillis AE, Wityk RJ, Beauchamp NJ, et al. Perfusion-weighted MRI as a marker of response to treatment in acute and subacute stroke. *Neuroradiology* 2004 Jan;.
69. Markus HS. Cerebral perfusion and stroke. *J Neurol Neurosurg Psychiatry* 2004 Mar;75(3):353-61.
70. Villringer A, Rosen BR, Belliveau JW, et al. Dynamic imaging with lanthanide chelates in normal brain: contrast due to magnetic susceptibility effects. *Magn Reson Med* 1988;6:164-74.
71. Bruening R, Berchtenbreiter C, Holzknecht N, et al. Effects of three different doses of a bolus injection of gadodiamide: assessment of regional cerebral blood volume maps in a blinded reader study. *AJNR Am J Neuroradiol* 2000 Oct;21(9):1603-10.
72. Hacklander T, Reichenbach JR, Hofer M, et al. Measurement of cerebral blood volume via the relaxing effect of low-dose gadopentetate dimeglumine during bolus transit. *AJNR Am J Neuroradiol* 1996 May;17(5):821-30.
73. Axel L. Cerebral blood flow determination by rapid-sequence computed tomography. *Radiology* 1980;137:679-86.
74. Davis PL, Wolf GL, Gillen JS. Indicator dilution time-activity curves demonstrated by rapid magnetic resonance imaging techniques and paramagnetic contrast agent. *Invest Radiol* 1989 May;24(5):400-6.
75. Rosen BR, Belliveau JW, Vevea JM, et al. Perfusion imaging with NMR contrast agents. *Magn Reson Med* 1990;14:249-65.
76. Benner T, Heiland S., Erb G, et al. Accuracy of gamma-variate fits to concentration-time curve from dynamic susceptibility-contrast enhanced MRI: influence of time resolution, maximal signal drop and signal-to-noise. *Magn Reson Imaging* 1997;15:307-17.
77. Weisskoff RM, Chesler D, Boxerman JL, et al. Pitfalls in MR measurement of tissue blood flow with intravascular tracers: which mean transit time? *Magn Reson Med* 1993 Apr;29(4):553-8.
78. Rempp KA, Brix G, Wenz F, et al. Quantification of regional cerebral blood flow and volume with

- dynamic susceptibility contrast-enhanced MR imaging. *Radiology* 1994 Dec;193(3):637-41.
79. Ostergaard L, Weisskoff RM, Chesler DA, et al. High resolution measurement of cerebral blood flow using intravascular tracer bolus passages. Part I: Mathematical approach and statistical analysis. *Magn Reson Med* 1996;36:715-25.
 80. Ostergaard L, Sorensen AG, Kwong KK, et al. High resolution measurement of cerebral blood flow using intravascular tracer bolus passages. Part II: Experimental comparison and preliminary results. *Magn Reson Med* 1996;36:726-36.
 81. Ringelstein EB, Biniek R, Weiller C, et al. Type and extent of hemispheric brain infarctions and clinical outcome in early and delayed middle cerebral artery recanalization. *Neurology* 1992 Feb;42(2):289-98.
 82. Reith J, Jorgensen HS, Pedersen PM, et al. Body temperature in acute stroke: relation to stroke severity, infarct size, mortality, and outcome. *Lancet* 1996 Feb 17;347(8999):422-5.
 83. Baird AE, Donnan GA, Austin MC, et al. Reperfusion after thrombolytic therapy in ischemic stroke measured by single-photon emission computed tomography. *Stroke* 1994 Jan;25(1):79-85.
 84. Baird AE, Austin MC, McKay WJ, et al. Changes in cerebral tissue perfusion during the first 48 hours of ischaemic stroke: relation to clinical outcome. *J Neurol Neurosurg Psychiatry* 1996 Jul;61(1):26-9.
 85. Boysen G, Pessin MS. Thrombolytic Therapy. In: Ginsberg MD, Bogousslavsky J, editors. *Cerebrovascular Disease: Pathophysiology, Diagnosis, and Management*. Blackwell Science; 1998. p. 1887-900.
 86. Hacke W. Thrombolysis: Stroke Subtype and Embolus Type. In: Zoppo GJ, Mori E, Hacke W, editors. *Thrombolytic Therapy in Acute Ischemic Stroke II*. Springer-Verlag; 1993.
 87. Barber PA, Davis SM, Infeld B, et al. Spontaneous reperfusion after ischemic stroke is associated with improved outcome. *Stroke* 1998 Dec;29(12):2522-8.
 88. Ryu YH, Chung TS, Yoon PH, et al. Evaluation of reperfusion and recovery of brain function before and after intracarotid arterial urokinase therapy in acute cerebral infarction with brain SPECT. *Clin Nucl Med* 1999 Aug;24(8):566-71.
 89. Marks MP, Tong DC, Beaulieu C, et al. Evaluation of early reperfusion and i.v. tPA therapy using diffusion- and perfusion-weighted MRI. *Neurology* 1999 Jun 10;52(9):1792-8.
 90. Barber PA, Parsons MW, Desmond PM, et al. The use of PWI and DWI measures in the design of "proof-of-concept" stroke trials. *J Neuroimaging* 2004 Apr;14(2):123-32.
 91. Neumann-Haefelin T, Wittsack HJ, Wenserski F, et al. Diffusion- and perfusion-weighted MRI. The DWI/PWI mismatch region in acute stroke. *Stroke* 1999 Aug;30(8):1591-7.
 92. Grandin CB, Duprez TP, Smith AM, et al. Which MR-derived perfusion parameters are the best predictors of infarct growth in hyperacute stroke? Comparative study between relative and quantitative measurements. *Radiology* 2002 May;223(2):361-70.

93. Lovblad KO, Baird AE, Schlaug G, et al. Ischemic lesion volumes in acute stroke by diffusion-weighted magnetic resonance imaging correlate with clinical outcome. *Ann Neurol* 1997 Aug;42(2):164-70.
94. Beaulieu C, de Crespigny A, Tong DC, et al. Longitudinal magnetic resonance imaging study of perfusion and diffusion in stroke: evolution of lesion volume and correlation with clinical outcome. *Ann Neurol* 1999 Oct;46(4):568-78.
95. Lev MH, Segal AZ, Farkas J, et al. Utility of perfusion-weighted CT imaging in acute middle cerebral artery stroke treated with intra-arterial thrombolysis: prediction of final infarct volume and clinical outcome. *Stroke* 2001 Sep;32(9):2021-8.
96. Tong DC, Yenari MA, Albers GW, et al. Correlation of perfusion- and diffusion-weighted MRI with NIHSS score in acute (<6.5 hour) ischemic stroke. *Neurology* 1998 Apr;50(4):864-70.
97. Schellinger PD, Fiebach JB, Jansen O, et al. Stroke MRI within 6h after onset of hyperacute cerebral ischemia. *Ann Neurol* 2001;49:460-9.
98. Flacke S, Keller E, Hartmann A, et al. Verbesserte Diagnostik des frühen Hirninfarktes durch den kombinierten Einsatz von Diffusions- und Perfusions-Bildgebung. *Fortschr Roentgenstr* 1998;168:493-501.
99. Tsuchida C, Yamada H, Maeda M, et al. Evaluation of peri-infarcted hypoperfusion with T2*-weighted dynamic MRI. *J Magn Reson Imaging* 1997 May;7(3):518-22.
100. Butcher K, Parsons M, Baird T, et al. Perfusion thresholds in acute stroke thrombolysis. *Stroke* 2003 Sep;34(9):2159-64.
101. Fiehler J, von Bezold M, Kucinski T, et al. Cerebral blood flow predicts lesion growth in acute stroke patients. *Stroke* 2002 Oct;33(10):2421-5.
102. Seidel G, Meyer-Wiethe K, Berdien G, et al. Ultrasound perfusion imaging in acute middle cerebral artery infarction predicts outcome. *Stroke* 2004 May;35(5):1107-11.
103. Warach S, Dashe JF, Edelman RR. Clinical outcome in ischemic stroke predicted by early diffusion-weighted and perfusion magnetic resonance imaging: a preliminary analysis. *J Cereb Blood Flow Metab* 1996 Jan;16(1):53-9.
104. Uno M, Harada M, Yoneda K, et al. Can diffusion- and perfusion-weighted magnetic resonance imaging evaluate the efficacy of acute thrombolysis in patients with internal carotid artery or middle cerebral artery occlusion? *Neurosurgery* 2002 Jan;50(1):28-34.
105. Fisher M. Characterizing the target of acute stroke therapy. *Stroke* 1997 Apr;28(4):866-72.
106. Baron JC. Perfusion thresholds in human cerebral ischemia: historical perspective and therapeutic implications. *Cerebrovasc Dis* 2001;11 Suppl 1:2-8.:2-8.
107. Lees KR. Advances in neuroprotection trials. *Eur Neurol* 2001;45(1):6-10.

108. Hakim AM. Ischemic penumbra: the therapeutic window. *Neurology* 1998 Sep;51(3 Suppl 3):S44-S46.
109. Hakim AM. The cerebral ischemic penumbra. *Can J Neurol Sci* 1987 Nov;14(4):557-9.
110. Stroke Therapy Academic Industry Roundtable II (STAIR-II). Recommendations for clinical trial evaluation of acute stroke therapies. *Stroke* 2001 Jul;32(7):1598-606.
111. Heiss WD, Rosner G. Functional recovery of cortical neurons as related to degree and duration of ischemia. *Ann Neurol* 1983 Sep;14(3):294-301.
112. Baron JC, Boussier MG, Rey A, et al. Reversal of focal "misery-perfusion syndrome" by extra-intracranial arterial bypass in hemodynamic cerebral ischemia. A case study with 15O positron emission tomography. *Stroke* 1981 Jul;12(4):454-9.
113. Fiehler J, Fiebich JB, Gass A, et al. Diffusion-weighted imaging in acute stroke--a tool of uncertain value? *Cerebrovasc Dis* 2002;14(3-4):187-96.
114. Fiehler J, Foth M, Kucinski T, et al. Severe ADC decreases do not predict irreversible tissue damage in humans. *Stroke* 2002 Jan;33(1):79-86.
115. Kidwell CS, Saver JL, Mattiello J, et al. Diffusion-perfusion MRI characterization of post-recanalization hyperperfusion in humans. *Neurology* 2001 Dec 11;57(11):2015-21.
116. Minematsu K, Li L, Sotak CH, et al. Reversible focal ischemic injury demonstrated by diffusion-weighted magnetic resonance imaging in rats. *Stroke* 1992 Sep;23(9):1304-10.
117. Ueda T, Yuh WT, Maley JE, et al. Outcome of acute ischemic lesions evaluated by diffusion and perfusion MR imaging. *AJNR Am J Neuroradiol* 1999 Jun;20(6):983-9.
118. von Kummer R, Nolte PN, Schnittger H, et al. Detectability of cerebral hemisphere ischaemic infarcts by CT within 6 h of stroke. *Neuroradiology* 1996 Jan;38(1):31-3.
119. von Kummer R, Holle R, Gizyska U, et al. Interobserver agreement in assessing early CT signs of middle cerebral artery infarction. *AJNR Am J Neuroradiol* 1996 Oct;17(9):1743-8.
120. Dippel DW, Du Ry van Beest Holle, van Kooten F, et al. The validity and reliability of signs of early infarction on CT in acute ischaemic stroke. *Neuroradiology* 2000 Sep;42(9):629-33.
121. Kalafut MA, Schriger DL, Saver JL, et al. Detection of early CT signs of >1/3 middle cerebral artery infarctions : interrater reliability and sensitivity of CT interpretation by physicians involved in acute stroke care. *Stroke* 2000 Jul;31(7):1667-71.
122. Lev MH, Farkas J, Rodriguez VR, et al. CT angiography in the rapid triage of patients with hyperacute stroke to intraarterial thrombolysis: accuracy in the detection of large vessel thrombus. *J Comput Assist Tomogr* 2001 Jul;25(4):520-8.
123. Verro P, Tanenbaum LN, Borden NM, et al. CT angiography in acute ischemic stroke: preliminary results. *Stroke* 2002 Jan;33(1):276-8.

124. Koenig M, Kraus M, Theek C, et al. Quantitative assessment of the ischemic brain by means of perfusion-related parameters derived from perfusion CT. *Stroke* 2001 Feb;32(2):431-7.
125. Koenig M, Klotz E, Luka B, et al. Perfusion CT of the brain: diagnostic approach for early detection of ischemic stroke. *Radiology* 1998 Oct;209(1):85-93.
126. Lee KH, Cho SJ, Byun HS, et al. Triphasic perfusion computed tomography in acute middle cerebral artery stroke: a correlation with angiographic findings. *Arch Neurol* 2000 Jul;57(7):990-9.
127. Eastwood JD, Lev MH, Azhari T, et al. CT perfusion scanning with deconvolution analysis: pilot study in patients with acute middle cerebral artery stroke. *Radiology* 2002 Jan;222(1):227-36.
128. Michael F.Hartshorne. Positron Emission Tomography in the Central Nervous System. In: William W.Orrison J, editor. *Neuroimaging*. 1st ed. W.B. Saunders Company; 2000. p. 87-122.
129. Michael F.Hartshorne. Single-Photon Emission Computed Tomography of the Central Nervous System. In: William W.Orrison J, editor. *Neuroimaging*. 1st ed. W.B. Saunders Company; 2000. p. 123-70.
130. Marchal G, Beaudouin V, Rioux P, et al. Prolonged persistence of substantial volumes of potentially viable brain tissue after stroke: a correlative PET-CT study with voxel-based data analysis. *Stroke* 1996 Apr;27(4):599-606.
131. Tsuchida C, Kimura H, Sadato N, et al. Evaluation of brain metabolism in steno-occlusive carotid artery disease by proton MR spectroscopy: a correlative study with oxygen metabolism by PET. *J Nucl Med* 2000 Aug;41(8):1357-62.
132. Davis SM, Donnan GA. Ischemic penumbra: MRI or PET. *Stroke* 2003 Oct;34(10):2536.
133. Karonen JO, Vanninen RL, Liu Y, et al. Combined diffusion and perfusion MRI with correlation to single-photon emission CT in acute ischemic stroke. Ischemic penumbra predicts infarct growth. *Stroke* 1999 Aug;30(8):1583-90.
134. Karonen JO, Ostergaard L, Vainio P, et al. Diffusion and perfusion MR imaging in acute ischemic stroke: a comparison to SPECT. *Comput Methods Programs Biomed* 2001 Jul;66(1):125-8.
135. Wolpert SM, Caplan LR. Current role of cerebral angiography in the diagnosis of cerebrovascular diseases. *AJR Am J Roentgenol* 1992 Jul;159(1):191-7.
136. Kidwell CS, Villablanca JP, Saver JL. Advances in neuroimaging of acute stroke. *Curr Atheroscler Rep* 2000 Mar;2(2):126-35.
137. Ferro JM. Brain embolism - Answers to practical questions. *J Neurol* 2003 Feb;250(2):139-47.
138. Baumgartner RW, Ringelstein EB. [Cerebrovascular ultrasound diagnosis]. *Ther Umsch* 1996 Jul;53(7):528-34.
139. Seidel G, Meyer K. [Harmonic imaging. A new method of ultrasound imaging of brain perfusion]. *Nervenarzt* 2001 Aug;72(8):600-9.

140. Eyding J, Wilkening W, Postert T. Brain perfusion and ultrasonic imaging techniques. *Eur J Ultrasound* 2002 Nov;16(1-2):91-104.

9 CURRICULUM VITAE

Family name	Ma	
First name	Jun	
Date of birth	14.08.1961	
Place of birth	Anshan, Liaoning, P. R. of China	
Home address	Pfingstrosenstr. 60, 0-135 81377, München	
Office address	Abteilung für Neuroradiologie Klinikum der Universität München Marchioninstr. 15 81377 München	
Telephone	(089)-7095-3254	
Fax	(089)-7095-2509	
E-mail	jun.ma@med.uni-muenchen.de	
Primary and high school	1968-1974 1974-1980	Shisan Tiao Primary school, Beijing, China No. 1 High school in Anshan, Anshan, China
Medical education	1980-1986 1986-1989	China Medical University, Shenyang, China, Bachelor degree of Science Dalian Medical University, Dalian, China, M.Sc in Neuroradiology
Professional experience	08.1989-05.1998 05.1998-05.1999 06.1999-07.2002 08. 2002-present	Resident, Attending Physician, Dept. of Radiology, First Affiliated Hospital of Dalian Medical University, Dalian, Liaoning, P. R. of China Visiting Doctor. Department of Radiology, Mount Sinai Medical Center, New York, USA Attending Physician. Dept. of Radiology, First Affiliated Hospital of Dalian Medical University, Dalian, Liaoning, P. R. of China Abteilung für Neuroradiologie Klinikum Großhadern, LMU, München, Deutschland Director: Prof. Dr. med. H. Brückmann

10 ACKNOWLEDGEMENTS

I am indebted to Prof. Dr. Hartmut Brückmann for giving me the opportunity to realize this work and for his encouragement and suggestions.

I would like to thank PD Dr. Roland Brüning, for his two years of guidance and inspiration. He has constantly taken care of the project, patiently and carefully read the thesis. His generous help and creative ideas give this thesis *the soul*.

I am grateful to Prof. Dr. Hamann Gerhard for his supervision to this work and critical advice.

I would also like to thank OA Dr. Klaus Seelos for his encouragement and his attention to the work.

Many thanks to Dipl.-Inf. Rainer Kopietz who has been ready to help when I had encounter difficulties with the computer network. I would like to thank Dr. Dominik Morhard and Dr. Markus Holtmannspötter for the help given to me at various stages of this work.

I wish to especially thank my wife Xiaotao Wang and my daughter Zhitong Ma, for their love and support. I am in debt to them since I was not with them when they needed me.